2018-12-06

Cranial Anatomy and Ontogeny of Gorgosaurus libratus (Tyrannosauridae: Albertosau

Voris, Jared Thomas

UNIVERSITY OF CALGARY

Cranial Anatomy and Ontogeny of *Gorgosaurus libratus* (Tyrannosauridae: Albertosaurinae)

By

Jared Thomas Voris

A THESIS

SUBMITTED TO THE FACULTY OF GRADUATE STUDIES

IN PARTIAL FULFILLMENT OF THE REQUIREMENTS FOR THE

DEGREE OF MASTER OF SCIENCE

GRADUATE PROGRAM IN GEOLOGY AND GEOPHYSICS

CALGARY, ALBERTA

DECEMBER, 2018

ABSTRACT

Tyrannosauridae is a diverse clade of Late Cretaceous theropod dinosaurs that exhibit significant changes in skull morphology through ontogeny. Whereas mature individuals of distinct tyrannosaurid taxa are morphologically disparate, immature individuals have been regarded as morphologically conservative between taxa. An analysis of newly discovered juvenile material for the sympatric tyrannosaurids *Gorgosaurus libratus* and *Daspletosaurus torosus* from the Dinosaur Park Formation, including two complete skulls of *Gorgosaurus* and an isolated postorbital of *Daspletosaurus*, reveals new information on the anatomy and ontogeny of tyrannosaurids. Although these two taxa were previously considered to be morphologically similar at juvenile stages, this study reveals that some taxonomically diagnostic characteristics are present at early ontogenetic stages and can be used to distinguish these taxa. In light of these diagnostic characteristics, it is discovered that a specimen previously identified as a juvenile *Daspletosaurus*, TMP 1994.143.1, is in fact assignable to the albertosaurine *Gorgosaurus*. An in-depth examination of the skull of juvenile *Gorgosaurus* specimens reveals that the ontogeny of this taxon is generally consistent with that of other tyrannosaurids, exhibiting such changes as an increase in cranium depth, development of cranial ornamentation, and widening of teeth. Furthermore, features considered autapomorphies for *Gorgosaurus* (e.g., curling of the postorbital cornual process) and of synapomorphies for the more inclusive clade of Albertosaurinae (*Gorgosaurus* and *Albertosaurus*) are also shown to be ontogenetically variable.

This thesis is original, unpublished, independent work by the author, J. T. Voris

Acknowledgements

First and foremost, I would like to thank my supervisor, Dr. Darla Zelenitsky, as well as Dr. François Therrien of the Royal Tyrrell Museum, who provided me with an amazing opportunity to study tyrannosaurid anatomy during my master's program. Their assistance has been in no short supply, and I can think of no one who deserves more gratitude than they do. I would also like to acknowledge Dr. Larry Witmer and Ryan Ridgely, who provided me with insight into the biology and anatomy of the specimens that formed the basis of this project and for their assistance in CT data segmentation and digital model reconstruction. I am grateful to Dr. Thomas Carr for his insight into tyrannosaur anatomy and ontogeny and for providing helpful feedback on project ideas. For access and assistance in museum collections, I thank Brandon Strilisky, Becky Bavington-Sanchez, Tom Courtenay, Rhian Russell, Heather Feeney, Carl Mehling, Adrienne Stroup, William Simpson, Amanda Millhouse, Kieran Shepherd, Margaret Currie, Jordan Mallon, Kevin Seymour, David Evans, John Scannella, Amy Atwater, and Nicole Ridgwell. Darren Tanke, Dawna MacLeod, and Amy Kowalchuk are graciously acknowledged for their skillful preparation of the specimens. I would also like to extend my gratitude to members of my defense committee, Dr. Susanne Cote and Dr. Annie Quinney, as well as to Dr. Jessica Theodor from whom I gained additional knowledge via coursework.

I am indebted to my undergraduate advisor, Dr. Andrew Heckert, for teaching me the ins-and-outs of vertebrate paleontology, as well as for supporting and assisting me in my many undergraduate research projects. I would never have made it to graduate school without his assistance. My middle and high school teachers and mentors, Ms. Sara Cathey, Mrs. Maura Goodrich-Brouwer, Mr. Scott Strickler, Mrs. Ronda Seay, Mrs. Carolyn Smith, and Mr. Hank

Gauthier were instrumental in fostering my interest in science. I also thank my closest friends, Seth Jenks, Amanda Hendrix, Matt Kondakor, Rachel Nottrodt, and Eamon Drysdale, for supporting me throughout my graduate program, for putting up with many of my thesis/research-induced rants, and in some cases for proof-reading parts of my thesis. Last, but certainly not least, I thank my parents (Jimmy and Fawn Voris), siblings (Jacob, Jacey, and Joshua), grandparents (James and Sherry Voris, Bonnie-Jean Eplee, Cara and Buddy Weaver), aunts and uncles (Kelly, Bubba, and Eric), and to all of the rest of my family for supporting me in my pursuit of a career in paleontology, I love you guys!

This project was supported by funding from the Roger Soderstrom Scholarship, the Department of Geoscience (via teaching assistantships), and by research grants from the Dinosaur Research Institute, the Royal Tyrrell Museum of Palaeontology Cooperating Society, and an NSERC Discovery Grant (to my supervisor).

Dedication

This thesis is dedicated to my late Papa, Frank “Buddy” Weaver, who always pushed me to follow my dreams of becoming a paleontologist and who was always wanting to “pick my brain”. Thank you, Papa.

Table of Contents

List of Figures and Illustrations

List of Tables

List of Institutional Abbreviations

AMNH	American Museum of Natural History
CMN	Canadian Museum of Nature
CMNH	Cleveland Museum of Natural History
FMNH	Field Museum of Natural History
MOR	Museum of the Rockies
MPC	Mongolian Paleontological Center
ROM	Royal Ontario Museum
TMP	Royal Tyrrell Museum of Palaeontology
UALVP	University of Alberta Vertebrate Paleontology Collections
USNM	Smithsonian Museum of Natural History

CHAPTER 1: INTRODUCTION

Tyrannosaurids were the dominant predators during the Late Cretaceous of North America. In the province of Alberta, tyrannosaurids are known from a high diversity of species and a high abundance of specimens (Currie, 2003a; Loewen et al., 2013; Brusatte and Carr, 2016). The discovery of several relatively complete specimens has provided significant insight into the anatomy of tyrannosaurids (e.g. Carr, 1999 Currie, 2003a; Brusatte and Carr, 2016, Carr et al., 2017), although this is biased primarily towards larger individuals in most taxa as smaller, juvenile individuals are scarce or often incomplete (Carr, 1999; Currie, 2003a). In recent years, however, well preserved juvenile individuals have been discovered from Alberta. In this thesis, I describe juvenile remains of two North American taxa, *Gorgosaurus* and *Daspletosaurus*, in order to shed light on the anatomy, ontogeny and taxonomy of these dinosaurs.

1.1 LITERATURE REVIEW

Review of tyrannosaurid taxa—Tyrannosauridae is a latest Cretaceous group of gigantic-sized theropods, defined as the group containing the most recent common ancestor of *Albertosaurus sarcophagus* and *Tyrannosaurus rex* (Osborn, 1906; Sereno, 2005; Sereno et al., 2005). Tyrannosauridae is subdivided into two clades, Albertosaurinae and Tyrannosaurinae, the latter of which contains a clade of longirostrine tyrannosaurids, Alioramini (Holtz, 2001; Currie et al, 2003; Lu et al., 2014).

Albertosaurinae is geographically restricted, with skeletal remains of the clade found only in Alberta, Saskatchewan, and Montana. Albertosaurinae contains only two taxa, *Albertosaurus sarcophagus* and *Gorgosaurus libratus*, the latter of which is sometimes regarded as congeneric

with the senior *Albertosaurus* (e.g. Carr, 1999; Carr and Williamson, 2004; Carr et al., 2017). Adult albertosaurines are generally smaller than their tyrannosaurine counterparts and more gracile in build, even at similar body sizes. To this extent, the metatarsals and pedal phalanges of albertosaurines are relatively longer than those of the more robust tyrannosaurines (Currie, 2003b). In addition, albertosaurines possess shorter ilia and shallower skulls than similar-sized individuals of non-alioramine tyrannosaurines (Currie et al., 2003). From cranial elements, albertosaurines can often be diagnosed by possessing prominent apices of the lacrimal cornual process, nasals that are unconstricted mediolaterally across their entire length (regardless of individual size), a small postorbital cornual processes limited in position to the caudodorsal corner of orbit, and a low sagittal crest on the frontals (Currie, 2003c; Brusatte and Carr, 2016).

The more speciose of the two major subgroups, Tyrannosaurinae contains several genera from both Asia and North America. In contrast to albertosaurines, tyrannosaurines are generally larger and more robust, although some species exhibit dwarfism due to hypothesized ecological restrictions (e.g. members Alioramini and *Nanuqsaurus hoglundi*; Brusatte et al., 2011; Fiorillo and Tykoski, 2014; Lu et al., 2014). At the opposite end of the size spectrum, Tyrannosaurinae also contains the largest members of Tyrannosauroidea, such as *Tyrannosaurus rex* and *Tarbosaurus bataar* (Brochu, 2003; Hurum and Sabath, 2003). Tyrannosaurines are differentiated from albertosaurines and more basal tyrannosauroids by a deep palatal process of the maxilla that obscures the tooth root bulges, an expanded maxillary ramus of the jugal (resulting in a shallow suborbital region), a convex dorsotemporal fossa of the squamosal, a deep quadratojugal process of the squamosal with a square tip, a shallow subcondylar recess, and a round pneumatopore on the ectopterygoid (Carr et al., 2017). The rostrum of most tyrannosaurines is deeper than that of albertosaurines (Currie, 2003c) and is exaggerated in the

largest specimens of *Tarbosaurus* and *Tyrannosaurus*, with rostral depth likely correlating with increased bite force (Brusatte and Carr, 2016).

Alioramini is the basal-most, and perhaps most unique, clade of the tyrannosaurines. They are relatively small, gracile in build, and possess an extremely elongated and dorsoventrally shallow rostrum (Kurzanov, 1976; Currie, 2003a; Brusatte et al., 2009, 2012; Lu et al., 2014). In addition to the elongated rostrum (and related characters), alioramines are unique among tyrannosaurids in the possession of a number of distinct tuberosities on the vaulted region of the nasal, an extremely reduced premaxilla, and 18 or more dentary teeth (Lu et al., 2014). The clade is represented by two genera and three species: *Qianzhousaurus sinensis*, *Alioramus remotus*, and *A. altai* (Kurzanov, 1976; Brusatte et al., 2009, 2012; Lu et al., 2014). Both species of *Alioramus* co-occur with the larger *Tarbosaurus bataar* (Kurzanov, 1976; Brusatte et al., 2009), suggesting ecological niche differentiation within Tyrannosauridae (Kurzanov, 1976; Brusatte et al., 2009).

The more derived tyrannosaurines consist of the taxa *Lythronax argestes*, *Dynamoterror dynastes*, *Teratophoneus curriei*, *Nanuqsaurus hoglundi*, *Daspletosaurus torosus*, *D. horneri*, *Zuchengtyrannus magnus*, *Tarbosaurus bataar*, and *Tyrannosaurus rex* (Brusatte and Carr, 2016; McDonald et al., 2018). Most derived tyrannosaurines are extremely large, with the exception of two smaller taxa, *Teratophoneus* and *Nanuqsaurus*. The holotype and only published specimen of *Teratophoneus* is small but was identified as a sub-adult individual by Carr et al. (2011) and would likely have attained a larger body size upon reaching maturity. The type and only documented specimen of the polar tyrannosaurid from Alaska, *Nanuqsaurus*, is among the smallest alleged adult tyrannosaurids documented (Fiorillo and Tykoski, 2014). The

small size of this taxon was hypothesized to be an adaption to the resource constraints of a higher latitude ecosystem (Fiorillo and Tykoski, 2014).

The largest of the derived tyrannosaurines (sensu Carr et al., 2017), including *Lythronax*, *Daspletosaurus*, *Tarbosaurus*, and *Tyrannosaurus*, share several cranial features that are proposed to allow for higher bite forces (Brusatte and Carr, 2016). First, the surface of the coronoid process of the surangular is more laterally inclined than in more primitive tyrannosaurids and would have provided more surface area for attachment of the adductor mandibulae muscles (Brusatte and Carr, 2016). Second, the nasals are mediolaterally constricted between the lacrimals, which may have served to distribute the stresses experienced during biting between the adductor chamber and rostrum (Brusatte and Carr, 2016). *Lythronax* is the most basal tyrannosaurid to possess constricted nasals but constriction is more extreme in the more derived taxa *Daspletosaurus*, *Tarbosaurus*, and *Tyrannosaurus* (Loewen et al., 2013; see Carr and Williamson, 2004). Third, in the clade formed by *Daspletosaurus*, *Tarbosaurus*, and *Tyrannosaurus*, the nasomaxillary suture is comprised of a series of tongue-in-groove structures that reinforce this joint surface (Brusatte and Carr, 2016). Finally, in the clade formed by *Tarbosaurus* and *Tyrannosaurus*, the teeth become approximately equal in mesiodistal and linguolabial lengths, differing from other tyrannosaurids, which possess labiolingually narrower teeth (Brusatte and Carr, 2016).

Prior studies of tyrannosaurid ontogeny—Ontogenetic changes in the skulls of tyrannosaurids have been documented primarily for better known taxa, such as *Gorgosaurus* (Carr, 1999; Currie, 2003a, b), *Daspletosaurus* (Currie, 2003a; Carr et al., 2017), *Tarbosaurus* (Rozhdestvensky, 1965; Tsuihiji et al., 2011), and *Tyrannosaurus* (Carr, 1999; Carr and

Williamson, 2004). In general, the skull of juvenile tyrannosaurids is shallow and narrow, either lacks or possesses nascent cranial ornamentation, and possesses ziphodont (i.e., laterally compressed) teeth (Carr, 1999; Currie, 2003a; Carr and Williamson, 2004; Tsuihiji et al., 2011). In contrast, the skull of larger and more mature individuals is deep and wide, possesses prominent ornamentation and sculpturing on the nasal, maxilla, lacrimal, jugal, and postorbital bones, and possesses pachydont (i.e., subconical) teeth (Carr, 1999; Currie, 2003a; Carr and Williamson, 2004; Tsuihiji et al., 2011). Many ontogenetic changes are consistent among tyrannosaurid species, which has led some authors to suggest that cranial morphology of juveniles is conservative within Tyrannosauridae (Currie, 2003a, b). While this generally holds true, some juvenile specimens have been identified for various tyrannosauroid species based on taxonomically diagnostic features that are present early in ontogeny (e.g. *Bistahieversor* [Carr and Williamson, 2004], *Gorgosaurus* [Carr, 1999; Currie, 2003a], *Albertosaurus* [Currie, 2003a; Carr, 2010], *Tarbosaurus* [Rozhdestvensky, 1965; Tsuihiji et al., 2011], *Tyrannosaurus* [Carr, 1999; Currie, 2003a; Carr and Williamson, 2004]).

Gorgosaurus is represented by one of the most complete ontogenetic series among tyrannosaurids and has served as the basis for several studies on the ontogenetic changes in tyrannosaurids (Carr, 1999; Currie, 2003ab; Erickson et al., 2004; Bradley, 2015; Bradley et al., 2015). Carr (1999) assigned known *Gorgosaurus* specimens to one of three growth stages, stage 1 juveniles through stage 3 large adults, using the presence of immature cortical bone and skull size as indicators. Stage 1 was subdivided into “small” and “large” categories to differentiate the smallest specimens of *Gorgosaurus*, which were only known from incomplete and disarticulated cranial elements (Carr, 1999), from slightly larger and more complete specimens. However, while Carr (1999) described these ontogenetic changes in detail, there is some debate as to the

validity of some of the characters he described. As Currie (2003a: p. 192) stated: “Many of the described differences in proportions and shapes are undoubtedly size (but not necessarily age) dependent.” Suffice to say, many of the features Carr (1999) regarded as ontogenetic and taxonomically informative for *Gorgosaurus* have been contentious, as they were also observed in another juvenile individual identified as *Daspletosaurus* (TMP 1994.143.1; Currie, 2003a). Because of these similarities observed between juveniles of two sympatric tyrannosaurid taxa, Currie (2003a) suggested that many of the taxonomic features identified by Carr (1999) were merely-size related characteristics that many tyrannosaurids, if not all, exhibited at some point during growth.

1.2. THESIS OBJECTIVES

In this thesis, I describe recently discovered juvenile specimens of *Gorgosaurus* and *Daspletosaurus* in order to document the ontogenetic changes of tyrannosaurid theropods. In Chapter 2, I reassess the taxonomic affinity of the tyrannosaurid specimen TMP 1994.143.1, previously identified as a juvenile *Daspletosaurus* (Currie, 2003a). Based on diagnostic features preserved in the skull and in light of a newly described postorbital of a juvenile *Daspletosaurus*, TMP 1994.143.1 is reassigned to the albertosaurine *Gorgosaurus*. In Chapter 3, two nearly complete skulls of juvenile *Gorgosaurus* individuals are described in an ontogenetic context, with comparisons to larger *Gorgosaurus* individuals (including TMP 1994.143.1) and other tyrannosaurids. This detailed investigation reveals several ontogenetic changes in the skull that are unique to *Gorgosaurus*, in particular, and to albertosaurines, in general, and provides further evidence that taxonomically diagnostic features are present even in immature tyrannosaurid individuals.

CHAPTER 2: REASSESSMENT OF PURPORTED *DASPLETOSAURUS* SKULL TMP 1994.143.1

2.1 INTRODUCTION

Among the best-known tyrannosaurid species from Alberta are the albertosaurine *Gorgosaurus libratus* Lambe, 1914 and the tyrannosaurine D*aspletosaurus torosus* Russell 1970 from the upper Campanian Oldman and Dinosaur Park formations. Mature individuals of *Daspletosaurus* and *Gorgosaurus* can be readily differentiated (Russell, 1970; Currie, 2003a; Carr et al., 2017), but morphological similarities between juvenile tyrannosaurids of different taxa can complicate their taxonomic identification (Currie, 2003a, Tsuihiji et al., 2011). However, recognition of the persistence of taxonomically diagnostic features through ontogeny in various tyrannosauroid species (e.g. *Bistahieversor sealyi*, *Gorgosaurus libratus*, *Albertosaurus sarcophagus*, *Tarbosaurus bataar*, *Tyrannosaurus rex*; Carr, 1999; Currie, 2003a; Carr and Williamson, 2004; Carr and Williamson, 2010; Tsuihiji et al., 2011) suggests that juveniles of some species can be identified. Although a few immature specimens of *Gorgosaurus* have been discovered, only a single skull, TMP 1994.143.1, has been described as an immature (juvenile) *Daspletosaurus* (Currie, 2003a; Hone and Tanke, 2015). This specimen has not only been crucial for ontogenetic studies of the taxon but also has been used widely to establish and code characters for phylogenetic analyses of tyrannosaurs (Currie et al., 2003; Carr and Williamson, 2004, 2005, 2010; Brusatte et al., 2009; Loewen et al., 2013; Brusatte and Carr, 2016; Carr et al., 2017). In light of several recent discoveries of tyrannosaurid specimens from Alberta, including an isolated juvenile *Daspletosaurus* postorbital and two

articulated juvenile *Gorgosaurus* skulls, I reassess the taxonomic affinity of TMP 1994.143.1 in this chapter and demonstrate that it belongs to *Gorgosaurus* rather than to *Daspletosaurus*.

2.2 MATERIALS AND METHODS

Tyrannosaurid specimens from upper Campanian and lower Maastrichtian deposits of Alberta and Montana were examined and measured using digital calipers for comparison with the tyrannosaurid specimen TMP 1994.143.1, previously identified as a juvenile *Daspletosaurus* sp. (Currie, 2003a). Comparative material included juvenile to adult tyrannosaurid specimens of the taxa *Gorgosaurus libratus*, *Albertosaurus sarcophagus*, *Daspletosaurus* spp., and *Tyrannosaurus rex* (Table 2.1).

To assess the taxonomic affinity of TMP 1994.143.1, I focus on comparative work of the morphology of the postorbital, which exhibits several features considered taxonomically informative in tyrannosaurids (e.g. Loewen et al., 2013; Brusatte and Carr, 2016; Carr et al., 2017), and on recently proposed cranial synapomorphies and autapomorphies of various tyrannosaurid taxa (Carr et al., 2017) recovered using the software TNT v1.5. Specifically, I examine 11 synapomorphies of the genus *Daspletosaurus*, five autapomorphies of *Daspletosaurus torosus*, nine unambiguous synapomorphies of Albertosaurinae, two autapomorphies of *Gorgosaurus libratus*, and several synapomorphies for more inclusive clades within Tyrannosaurinae. A phylogenetic analysis was not conducted on TMP 1994.143.1 since juvenile tyrannosaurids have been demonstrated to consistently place basal to adult conspecifics (Sereno et al, 2009; Tsuihiji et al., 2011) due to the delayed and often gradual ontogenetic acquisition of characters during growth (e.g., cranial ornamentation; Carr, 1999; Tsuihiji et al., 2011). Furthermore, given that characters previously coded for *Daspletosaurus* are also based on

TMP 1994.143.1, revision to the taxonomic status of the latter may impact some of these codings.

2.3 RESULTS

Identity of TMP 2013.18.11—TMP 2013.18.11 is an isolated, small tyrannosaurid postorbital from the Dinosaur Park Formation of Alberta (Fig. 2.1). The specimen can be unambiguously identified as *Daspletosaurus* based on the presence of a single synapomorphy: the dorsal squamosal articular surface extends to a point caudal to the rostral margin of the laterotemporal fenestra (Carr et al., 2017). Other characteristics can also be used to identify the specimen as belonging to a tyrannosaurine, of which *Daspletosaurus* is the only known representative in the Dinosaur Park Formation. Such characters include: the cornual process is prominent and C-shaped in lateral view and is separated from the orbital margin by a smooth bone surface (sensu Currie, 2003a), The ventral ramus is vertical and is narrow upon bifurcating from the dorsal bar, and the frontal articular surface is sloped caudoventrally (this study).

General skull remarks for TMP 1994.143.1—The skull is of a previously described (Currie, 2003a; Hone and Tanke, 2015), largely complete specimen that preserves all bones except the vomer, right quadratojugal, laterosphenoid, pterygoid, and left mandible (Currie, 2003a: fig. 18–36). Although most of the skull is disarticulated, the rostrum (including both premaxillae, maxillae, nasal, right jugal, and right lacrimal) is articulated and was found preserved upside down. The rostrum is dorsoventrally compressed and somewhat splayed laterally. With an estimated length of 620 mm (Currie, 2003a), TMP 1994.143.1, here considered a large Stage 1 individual (sensu Carr, 1999a), falls between the smallest known juvenile specimens of

Gorgosaurus (TMP 1986.144.1, TMP 2009.12.14, TMP 2016.14.1; ~500 mm,) and a larger juvenile individual (TMP 1991.36.500; 637 mm).

Description and comparison of postorbital in TMP 1994.143.1—The postorbital of tyrannosaurids is a useful element for determining taxonomic identity as it possesses a suite of morphological features diagnostic to the genus and, in some cases, species level (sensu. Carr et al., 2017). Both postorbitals are present in TMP 1994.143.1. The left element is relatively undeformed, whereas the right has a laterally sheared rostral ramus. The left and right postorbitals are both 138 mm long when measured along the length of the dorsal bar, and are slightly larger than those of small stage 1 individuals (e.g. TMP 1986.144.1, TMP 2009.12.14, TMP 2016.14.1) but slightly smaller than that of the large stage 1 individual TMP 1991.36.500. An isolated postorbital, TMP 2013.18.11, here identified as belonging to a juvenile *Daspletosaurus*, is comparable in size to that of small stage 1 individuals of *Gorgosaurus*.

Although the shape of the rostral ramus of the postorbital differs between the left and right element in TMP 1994.143.1, they are both more similar to that of albertosaurines than to *Daspletosaurus*. The rostral ramus of the right postorbital is long and shallow, as in juveniles of *Gorgosaurus*, whereas the rostral ramus of the left postorbital appears short and deep, more similar to adult *Gorgosaurus* and *Albertosaurus* (Fig. 2.2). In contrast, the rostral ramus of the juvenile *Daspletosaurus* postorbital (TMP 2013.18.11) is long, proximally deep and considerably more robust than that of TMP 1994.143.1 and of similar-sized juvenile *Gorgosaurus* (i.e., TMP 1986.144.1, TMP 2009.12.14. TMP 2016.14.1). The rostral ramus of adult *Daspletosaurus* specimens is extremely robust and deep due to the presence of the swollen and laterally extensive cornual process, such that the ramus appears truncated in lateral view (Fig. 2.3; Currie, 2003; Brusatte and Carr, 2016; Carr et al., 2017).

In both albertosaurines and TMP 1994.143.1, the dorsal margin of the frontal articular surface is horizontal in medial view and deflects ventrally at nearly a right angle towards the laterosphenoid articular surface. In contrast to the condition observed in TMP 1994.143.1 and albertosaurines, the dorsal margin of the frontal articular surface in both juvenile and adult *Daspletosaurus* slopes caudoventrally such that the angle between the frontal and laterosphenoid articular surfaces is obtuse.

The rostral extremity of the frontal sutural surface of the postorbital is shallow in TMP 1994.143.1. This condition is similar to that of albertosaurines, except that its rostral extremity is deeper in large individuals. In juvenile *Daspletosaurus* (TMP 2013.18.11), the rostral-most margin of the frontal sutural surface is shallow, whereas it is extremely deep in adult individuals (more so than in adult albertosaurines).

In the postorbitals of small juvenile *Gorgosaurus* specimens and in the right postorbital of TMP 1994.143.1, the dorsal margin is distinctly sinusoidal in lateral view, with a deeply concave rostral ramus that transitions into a convex region above the caudal ramus. In large albertosaurines, the dorsal margin is only weakly sinusoidal, as the extremity of the rostral ramus is either gently concave (e.g. AMNH 5336) or flat (e.g. TMP 1995.12.115), and the mid-region and caudal process are strongly convex, surpassing the height of the rostral ramus (Fig. 2.2). The dorsal margin of the left postorbital in TMP 1994.143.1 is intermediate in shape between those of juvenile and large albertosaurines, as it is moderately sinusoidal in lateral view and possesses a short concave region near the extremity of the rostral ramus and a strongly convex mid-region. The sinusoidal shape of the dorsal margin of the postorbital in TMP 1994.143.1 and albertosaurines differs considerably from the condition of *Daspletosaurus*. In adult *Daspletosaurus* specimens, the entire dorsal margin of the postorbital is strongly convex, lacking

a concave region of the rostral ramus, due to the extensive and dorsally expanded cornual process characteristic of the genus. In comparison, the dorsal margin of the juvenile *Daspletosaurus* postorbital (TMP 2013.18.11) appears straight in lateral view, with a shallowly concave region at the approximate midpoint of the dorsal bar (Fig. 2.3).

In TMP 1994.143.1, the cornual process is located directly adjacent to the caudodorsal margin of the orbit and extends only a short distance onto the rostral ramus. The degree of development of the cornual process differs between the left and right postorbital. Whereas it is a poorly-developed, rectangular, and textured region on the left element, it is expressed as a small, caudally-curling, semicircular lip on the right element. Despite these differences, the morphology of the cornual process is nearly identical to those observed in *Gorgosaurus*, where the left cornual process is more similar to that of juvenile individuals and the right cornual process is similar to that of subadults and adults (Fig. 2.2). Unlike TMP 1994.143.1 and albertosaurines, the cornual process in *Daspletosaurus* is separated from the caudodorsal margin of the orbit by a smooth bone surface (Currie, 2003; Carr et al., 2017). In large *Daspletosaurus* individuals, the cornual process is much larger and more extensive than in albertosaurines, forming a rugose C-shaped ridge that occupies most of the rostral ramus and lateral surface of the dorsal mid-region, rises above the dorsal surface of the postorbital, and extends caudally to approach the rostral margin of the laterotemporal fenestra. As in larger *Daspletosaurus*, the cornual process of the small *Daspletosaurus* postorbital (TMP 2013.18.11) is also a prominent and C-shaped ridge. However, the cornual process in this specimen differs from those of larger *Daspletosaurus* in that: it is less expansive along the dorsal bar, its surface is smooth and porous rather than rugose, it does not rise above the dorsal surface of the postorbital, and its caudal margin does not approach the laterotemporal fenestra (Fig. 2.3).

The caudal ramus of the postorbital in TMP 1994.143.1 is short relative to the length of the dorsal bar and terminates rostral to the caudodorsal corner of the laterotemporal fenestra. The dorsal articular surface for the squamosal (DASS) slopes ventrolaterally, such that it is visible in lateral view, and terminates as a shallow notch rostral to the rostral margin of the laterotemporal fenestra. The morphology of the DASS and of the caudal ramus in TMP 1994.143.1 is nearly identical to those of albertosaurines (Brusatte and Carr, 2016; Carr et al., 2017), except that the depth of the notch at the rostral extremity of the DASS is intermediate between the condition found in juvenile (absence of a notch in TMP 1986.144.1 and TMP 2009.12.14) and adult individuals (deep notch in ROM 1422). Contrary to TMP 1994.143.1 and albertosaurines, the caudal ramus of large *Daspletosaurus* individuals is long and terminates caudal to the caudodorsal margin of the laterotemporal fenestra, although the condition in the juvenile is unknown because the distal portion of the caudal ramus is broken in TMP 2013.18.11. Furthermore, the DASS in both juvenile (i.e., TMP 2013.18.11) and most adult *Daspletosaurus* (e.g. TMP 2001.36.1) terminates caudal to the rostral margin of the laterotemporal fenestra (Carr et al., 2017) and its rostral extremity smoothly transitions to the exposed dorsal margin of the postorbital to form an uninterrupted and dorsally convex arc, similar to young juvenile *Gorgosaurus*, but in contrast to TMP 1994.143.1 and adult albertosaurines (Carr and Williamson, 2010; Carr et al., 2017).

The ventral ramus of the postorbital in TMP 1994.143.1 is wide proximal to the dorsal bar and tapers ventrally until it reaches the caudal-most extent of the orbit, below which it retains a relatively constant width. A subtle inflection on the caudal margin of the ventral ramus, located dorsal to the caudal-most extent of the orbit, marks the dorsal reach of the contact with the jugal. The distal extremity of the ventral ramus widens to form the suborbital process, a right-angled

blade that expands rostrally into the orbital fenestra and gives the latter a distinctive "comma" shape (Fig. 2.4). The ventral ramus is strongly curved between the rostral extremity of the dorsal bar and the suborbital process, such that the orbital margin between these features is nearly semicircular (Fig. 2.3). The morphology of the ventral ramus and orbital fenestra in TMP 1994.143.1 is consistent with that of *Gorgosaurus* but differs significantly from that of *Daspletosaurus*. In both juvenile and adult *Daspletosaurus*, the ventral ramus is nearly vertical and straight. The width of the ventral ramus is nearly constant between the dorsal bar and caudal-most extent of the orbit in large *Daspletosaurus* but is slightly tapered in the juvenile individual (TMP 2013.18.11). Below the caudal-most extent of the orbit, the ventral ramus of large *Daspletosaurus* is tapered and the suborbital process is either absent or weakly-developed, resulting in an oval-shaped orbital fenestra (Fig. 2.3, 2.3). The suborbital process is broken in TMP 2013.18.11, thus the juvenile *Daspletosaurus* condition is unknown.

Examination of tyrannosaurid synapomorphies in TMP 1994.143.1—Examination of tyrannosaurid cranial characters identified by Carr et al. (2017) as diagnostic for albertosaurines (including *Gorgosaurus*) or *Daspletosaurus* reveals that the cranial morphology of TMP 1994.143.1 is more similar to that of both juvenile and adult *G. libratus* than to any specimen of *Daspletosaurus* (Table 2.2). Of the eight recognized synapomorphies for Albertosaurinae that can be assessed in TMP 1994.143.1, five are definitively exhibit present and three are ambiguous due to ontogenetic differences between juvenile and adult *Gorgosaurus*. These ambiguous characters observed in TMP 1994.143.1 include: the ventral contact between the jugal and quadratojugal (Carr et al., 2017: character 106), the depth of the notch at the rostral tip of the DASS (Carr et al., 2017: character 114), and the inclination of the vomeropterygoid neck (Carr et

al., 2017: character 180), First, the ventral contact between the jugal and quadratojugal in TMP 1994.143.1 possesses a shallow rostrodorsal inflection, a condition intermediate to the steep rostrodorsally inclined (~45°) inflection diagnostic of adult albertosaurines (Carr et al., 2017: character 106) and the horizontal (rostrocaudal) contact of small juvenile albertosaurines (e.g., TMP 2016.14.1) and of tyrannosaurines. Secondly, TMP 1994.143.1 possesses a shallow notch at the rostral tip of the DASS rather than the deep notch diagnostic of albertosaurines (Carr et al., 2017: character 114). However, this character is observed to be ontogenetically variable among albertosaurines: whereas small Stage 1 juveniles (e.g. TMP 1986.144.1, TMP 2009.12.14) lack any significant concavity, large Stage 1 individuals (e.g. TMP 1991.36.500 and TMP 1994.143.1) possess a shallow notch, and the largest individuals (Stage 2 and 3) possess the diagnostic deep notch (e.g. TMP 1981.10.1, TMP 1995.12.116). Finally for the third character, TMP 1994.143.1 displays both the albertosaurine and tyrannosaurine condition with respect to the inclination of the vomeropterygoid neck, where the left palatine displays the tyrannosaurine condition (rostrodorsal inclination) and the right palatine displays the albertosaurine condition (dorsal inclination; Carr et al., 2017: character 180). This presence of both conditions may reflect the transitional ontogenetic stage of the TMP 1994.143.1, intermediate between small Stage 1 juvenile *Gorgosaurus* specimens exhibiting the tyrannosaurine condition in both palatines (e.g., TMP 2009.12.14, TMP 2016.14.1), and large Stage 1 individuals displaying the albertosaurine condition (e.g., TMP 1986.144.1, TMP 1991.36.500). Given that these three albertosaurine synapomorphies are shown here to be acquired gradually during ontogeny, their absence in TMP 1994.143.1 does not necessarily reflect a tyrannosaurine affinity for the specimen but rather its young ontogenetic status.

Examination of the optimized synapomorphies of several tyrannosaurine clades further support the non-tyrannosaurine affinity of TMP 1994.143.1 (Table 1). The specimen exhibits only three of the 26 synapomorphies of all tyrannosaurine clades that include *Daspletosaurus*, all of which are due to either taphonomic deformation (n=1) or individual variation (n=2). First, the subnarial process of TMP 1994.143.1 is horizontal and mostly concealed in lateral view, which would be considered a tyrannosaurine synapomophy (Carr et al., 2017: character 14), but this condition is likely due to the fact that the rostrum is dorsoventrally compressed. Second, although the ridge delimiting the lateral margin of the supratemporal fossa on the dorsal surface of the squamosal in TMP 1994.143.1 is partially divided by a median groove, a condition that approaches the tyrannosaurine synapomorphy of having a complete division of the ridge (Carr et al., 2014: character 122), it is only observed on the right element and is undivided in the left element. Because division of the ridge is only partial and occurs only on the right side, it likely represents individual variation rather than the tyrannosaurine condition. Thirdly, although the sagittal crest on the frontal is slightly taller in TMP 1994.143.1 than is typical for albertosaurines, a tyrannosaurine characteristic (Carr et al., 2017: character 157), it is similar in proportions to that of another smaller, immature *Gorgosaurus*, TMP 2009.12.14. Consequently, the prominence of the crest in both specimens may simply be due to individual variation or, alternatively, to taphonomic deformation as the frontals of both specimens are laterally compressed.

TMP 1994.143.1 could be argued to exhibit three of the 10 assessable synapomorphies of the genus *Daspletosaurus* (Table 2.2; Carr et al., 2017: sup. info), but one of these features is inconsistent with the typical morphology of the genus and the other two features are also present in *Gorgosaurus* (contra Carr et al., 2017). First, although TMP 1994.143.1 and *Daspletosaurus*

both possess a distinct ridge dorsal to the epipterygoid fossa on the laterosphenoid (Carr et al., 2017: character 219), this ridge is rostrocaudally short and does not extend onto the capitate process in TMP 1994.143.1, unlike in *Daspletosaurus*. Due to these differences, the presence of this feature in TMP 1994.143.1 is regarded as individual variation rather than a *Daspletosaurus* synapomorphy. Second, whereas TMP 1994.143.1 exhibits a rostrocaudally-oriented ridge on the nasal process of the frontal, a feature identified as a *Daspletosaurus* synapomorphy (Carr et al., 2017: character 154), this ridge also occurs in *Albertosaurus* (e.g. TMP 1981.9.1), and in some specimens of *Gorgosaurus* (e.g. TMP 2009.12.14), indicating that this character may not be diagnostic. Finally, whereas the primary palatine pneumatopore in both TMP 1994.143.1 and *Daspletosaurus* is located caudal to the rostral margin of the vomeropterygoid neck (Carr et al., 2017: character 184), it is located far more rostral in TMP 1994.143.1. Given that the location of the primary palatine pneumatopore in juvenile *Gorgosaurus* individuals (TMP 2009.12.14) is nearly identical to that of TMP 1994.143.1 and expands to become rostral to the neck only in larger individuals (see Carr, 2010), this feature is regarded as an ontogenetic variation rather than a taxonomic indicator for TMP 1994.143.1.

2.4. DISCUSSION

Specimen TMP 1994.143.1 was identified originally as *Daspletosaurus* sp. by Currie (2003a), although the criteria supporting this taxonomic assignment were not explicitly discussed. Very few features were noted to be exclusive to this specimen and adult *Daspletosaurus*, but many similarities were noted between it and albertosaurines (including *Gorgosaurus*) of various growth stages (e.g. supranarial processes of premaxilla separated by forked medial process of nasal; Currie, 2003a: 196). Most subsequent authors also assumed a

Daspletosaurus identity for TMP 1994.143.1 without elaborating on the justification for its taxonomic assignment (Brusatte et al., 2011; Bever et al., 2013; Loewen et al., 2013; Brusatte and Carr, 2016; Carr et al., 2017).

Hone and Tanke (2015) were the first (and only) to explicitly describe characteristics of TMP 1994.143.1 attributing it to *Daspletosaurus*. These characteristics include: 1) mesial carinae extending to the base of the crown on maxillary and dentary teeth, 2) high number of dentary teeth (n=18); 3) subnarial processes of the premaxilla and nasal are separated below the external nares; 4) cornual process of the lacrimal is positioned dorsal to the ventral ramus; 5) dorsal bar of the lacrimal is inflated; and 6) maxillary fenestra contacts the ventral margin of the antorbital fossa. After careful review of these characteristics in the context of the present study, these features are found to be either taxonomically non-diagnostic or the result of taphonomic deformation. First, mesial carinae extending to the base of the crown are only observed in a few teeth in the rostral-most alveoli (i.e., LM4, RD4, RD6, RD7) in TMP 1994.143.1 and that characteristic is also observed in some *Gorgosaurus* specimens (e.g., TMP 1986.144.1, TMP 1983.36.100), suggesting it may not be a diagnostic feature of *Daspletosaurus*. Second, the high number of dentary teeth found in TMP 1994.143.1 is only one more tooth than the number of teeth typically found in *Daspletosaurus* and in some *Gorgosaurus* individuals (e.g., TMP 1986.144.1, TMP 1991.36.500: Carr and Williamson, 2000) and is therefore not taxonomically diagnostic. Third, the separation of the subnarial processes of the premaxilla and nasal below the external nares has been shown by Currie (2003) to not be a diagnostic feature of *Daspletosaurus*; in fact, these processes are in contact in all tyrannosaurids, including TMP 1994.143.1 (contra Hone and Tanke, 2015). Fourth, whereas the cornual process of the crushed right lacrimal appears to be positioned dorsal to the ventral ramus, this is the result of deformation and the

cornual process of the undeformed left lacrimal is situated rostral to the ventral ramus and also rostral to the primary pneumatopore, as in albertosaurines. Fifth, whereas the dorsal bar of the lacrimal appears to be inflated on the right lacrimal, this is again a result of dorsoventral compression and the undistorted left element is uninflated. Finally, whereas the maxillary fenestra contacts the ventral margin of the antorbital fossa in the left maxilla, this is also an artifact of taphonomic deformation, as the maxilla is dorsoventrally compressed and the antorbital fossa below the fenestra is flattened to the level of the subcutaneous surface. The maxillary fenestra of the right maxilla in TMP 1994.143.1 is separated from the subcutaneous surface by the antorbital fossa, as in *Gorgosaurus*.

In the context of new fossil discoveries, examination of previously known specimens, and recent anatomical descriptions (Brusatte and Carr, 2016; Carr et al., 2017), we here re-identify the juvenile tyrannosaurid TMP 1994.143.1 as *Gorgosaurus libratus* rather than the sympatric tyrannosaurid *Daspletosaurus*. The specimen possesses two autapomorphies of *Gorgosaurus* (Carr et al. 2017: character 161) and all but three of the assessable synapomorphies of Albertosaurinae (Table 2.2); the three absent features are due to the early ontogenetic stage of the specimen (see Examination of tyrannosaurid synapomorphies present in TMP 1994.143.1 above). On the other hand, TMP 1994.143.1 lacks all three autapomorphies of *Daspletosaurus torosus* (Carr et al., 2017: characters 74, 77, 244), and possesses very few synapomorphies of the genus *Daspletosaurus* or of more inclusive tyrannosaurine clades containing *Daspletosaurus* (Table 2.2). Most of the similarities with *Daspletosaurus* are the result of ontogenetic variation, individual variation, or taphonomic deformation (see Examination of tyrannosaurid synapomorphies present in TMP 1994.143.1 above). If TMP 1994.143.1 was a juvenile *Daspletosaurus*, one would expect it to exhibit several tyrannosaurine synapomorphies and lack

albertosaurine synapomorphies. Consequently, the identification of TMP 1994.143.1 as *Gorgosaurus* is the most parsimonious interpretation.

In addition to synapomorphies, other features of the skull, particularly of the postorbital, are also exclusively shared between TMP 1994.143.1 and *Gorgosaurus* and differentiate them from *Daspletosaurus*. Whereas TMP 1994.143.1 and *Gorgosaurus* possess a cornual process that does not extend far onto a shallow rostral ramus, a sinusoidal dorsal margin of the postorbital (more pronounced in juveniles), and a ventrally tapering ventral ramus, *Daspletosaurus* possesses a cornual process that extends further onto the rostral ramus than albertosaurines, a convex dorsal margin of the postorbital, a deep rostral ramus (in adult specimens), and a ventral ramus of relatively constant width (in adult specimens).

The taxonomic reassignment of TMP 1994.143.1 improves our understanding of the ontogeny of *Gorgosaurus* as it is intermediate in size between small juvenile and subadult specimens (i.e., TMP 2009.12.14 and TMP 1991.36.500, respectively). This more complete growth series for the taxon reveals that some diagnostic features are acquired gradually during ontogeny, with some synapomorphies appearing only in later growth stages. Also, osteological features, diagnostic or not, acquired during growth do not necessarily form synchronously among individuals of similar size or even between left and right elements of a single individual. While taxonomically diagnostic characters are present in juveniles of *Gorgosaurus* and other tyrannosaurids, tyrannosaurids still undergo generally similar ontogenetic patterns of change (Carr, 1999; Currie, 2003a, b). However, it is possible that some of the similarities in the ontogenetic patterns between *Gorgosaurus* and *Daspletosaurus* (sensu Currie, 2003a) may be due to the prior attribution of TMP 1994.143.1 to *Daspletosaurus* rather than *Gorgosaurus*.

The taxonomic reassignment of TMP 1994.143.1 leaves a gap in our understanding of *Daspletosaurus* ontogeny by removing the only known juvenile individual with a relatively complete skull from the growth series. However, a recently discovered postorbital (TMP 2013.18.11) represents the remains of the smallest known *Daspletosaurus* individual and provides insight into the ontogeny of this taxon. This postorbital is similar in size to that of the three smallest known (small Stage 1 juvenile) *Gorgosaurus* skulls (~500 mm in length), but is considerably more robust. The well-developed cornual process of TMP 2013.18.11 is more developed than in any other similar-sized tyrannosaurid, even larger individuals of *Tyrannosaurus rex* (e.g. CMN 7541: skull length 572 mm; Bakker et al., 1988). This observation suggests that the cornual process develops at an earlier ontogenetic stage in *Daspletosaurus* than in other tyrannosaurids, an interpretation consistent with the fact that *Daspletosaurus* possesses the largest and most extensive cornual process of all tyrannosaurids (Carr et al., 2017). Furthermore, this specimen reveals that the cornual process changes dramatically in size and rugosity during *Daspletosaurus* ontogeny, as it is small and smooth in TMP 2013.18.11 and becomes highly rugose and expanded to cover most of the dorsal bar in large *Daspletosaurus* individuals (Currie, 2003; Brusatte and Carr, 2016; Carr et al., 2017). The expansion of the cornual process also appears to be associated with other ontogenetic changes in the postorbital, such as the extreme deepening of the rostral ramus (resulting in an apparent shortening of the ramus) and the increased convexity of the dorsal margin. In contrast, several features of the *Daspletosaurus* postorbital, such as the rostral extent of the DASS and the caudoventral slope of the supratemporal fossa along the frontal articulating surface, do not change through ontogeny.

The results of this study may have implications for phylogenetic analyses of tyannosaurids. Given that TMP 1994.143.1 has been utilized for character construction in several

phylogenetic analyses (Currie et al., 2003; Carr and Williamson, 2004; Carr et al., 2005; Carr and Williamson, 2010; Brusatte et al., 2010; Loewen et al., 2013; Brusatte and Carr, 2016; Carr et al., 2017), many of these characters may need to be reevaluated and possibly modified in light of the revised taxonomic affinity of the specimen. Specifically, characters referring to the juvenile morphology of tyrannosaurid taxa (e.g. Carr et al., 2017: characters 25, 108) or characters which used TMP 1994.143.1 to establish character states in *Daspletosaurus* may need revision. Such revisions may affect the character coding for *Daspletosaurus* and alter its position in phylogenetic reconstructions.

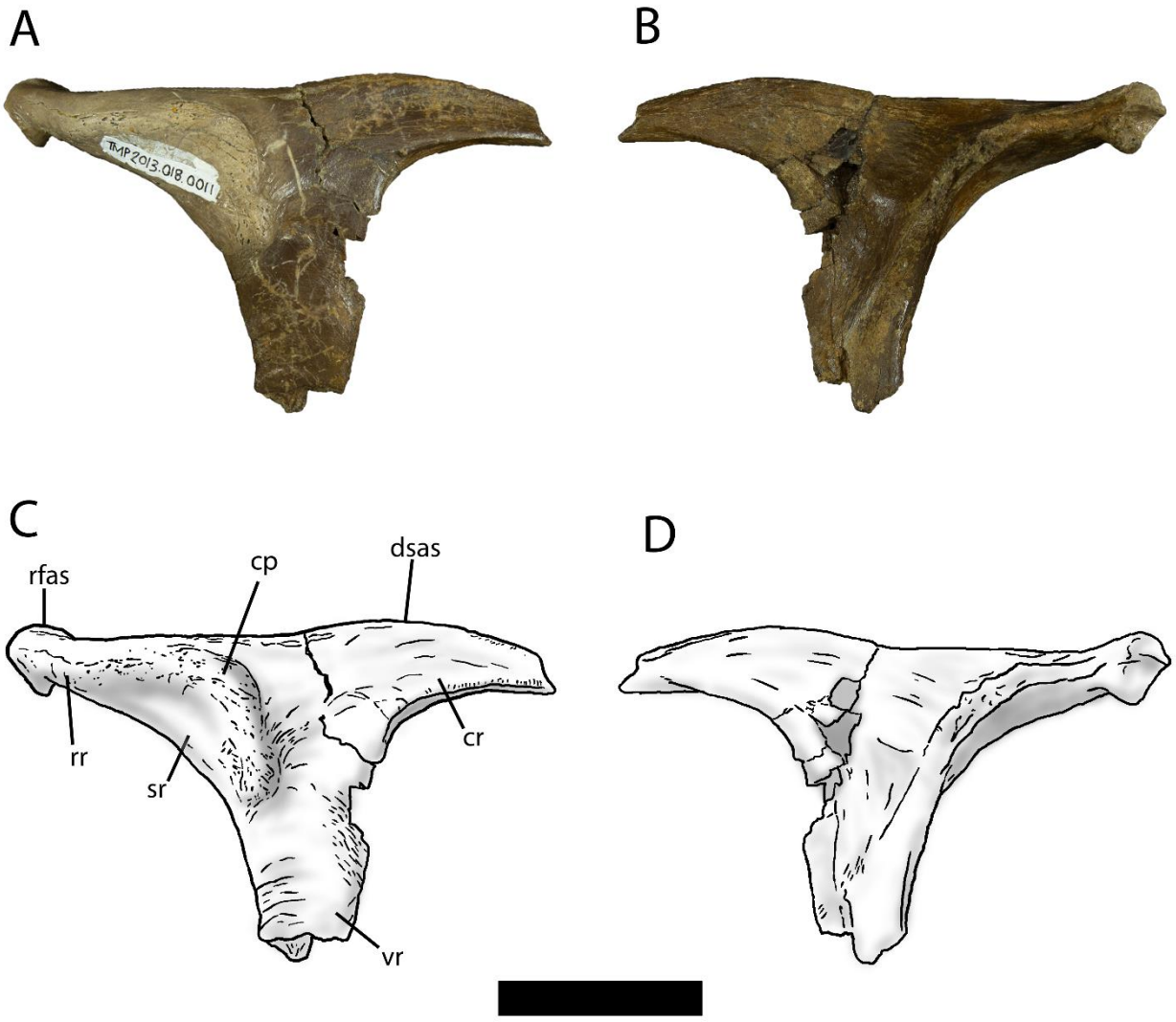

Figure 2.1. Juvenile *Daspletosaurus* postorbital in lateral (A, C) and medial views (B, D). Abbreviations as follows: cp: cornual process; cr, caudal ramus; dsas, rostral end of dorsal squamosal articular surface; rfas, rostral expansion of frontal articular surface; rr, rostral ramus; sr, smooth region separating cornual process from orbital margin; vr, ventral ramus.


A.
B.
sop
C.
fas
dass
rr
cp
cr
vr

Figure 2.2. Comparison of *Gorgosaurus* postorbitals through ontogeny in dorsal and lateral view: (A) juvenile individual, TMP 2009.12.14, right postorbital (reversed); (B) large juvenile individual TMP 1994.143.1, left postorbital; (C) adult individual, TMP 1995.12.116, left postorbital (distal portion of ventral ramus is missing). Abbreviations are as follows: cp, cornual process; cr, caudal ramus; dass, dorsal articular surface for squamosal; fas, frontal articular surface; rr, rostral ramus; sop, suborbital process; vr, ventral ramus. Scale bar equals 50 mm.

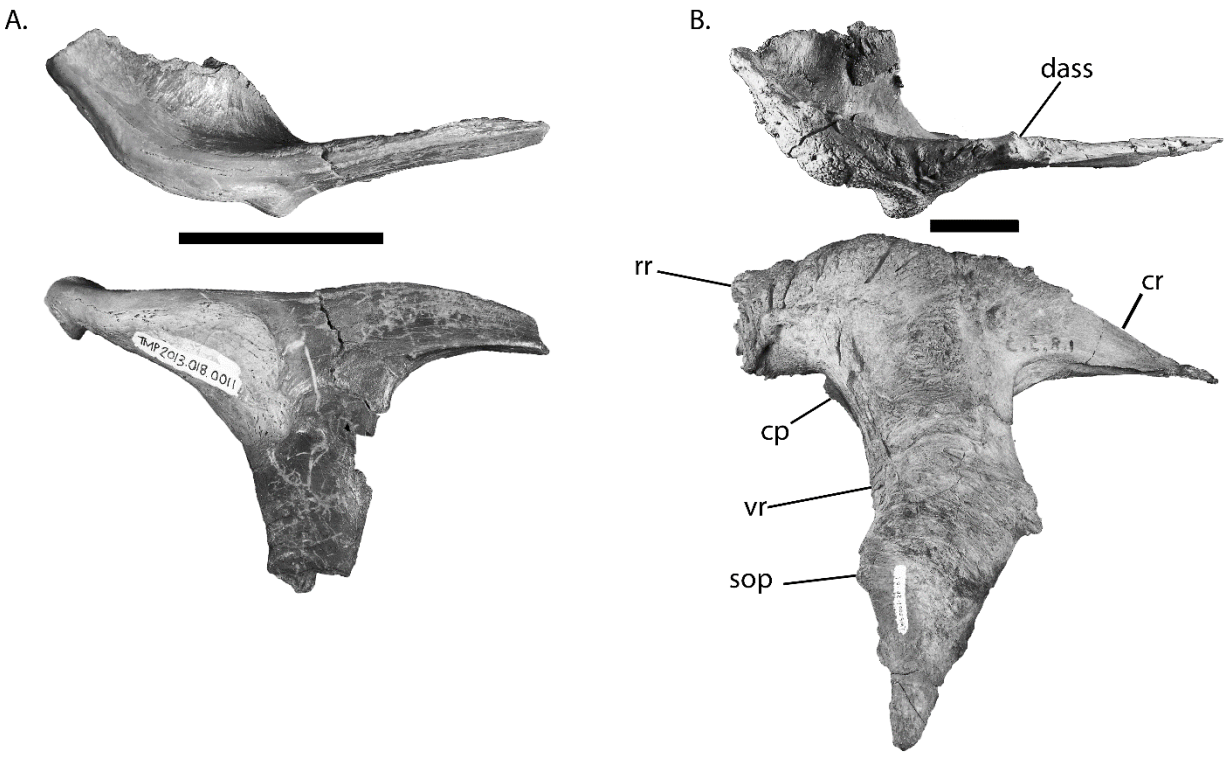

Figure 2.3. Comparison of *Daspletosaurus* postorbitals through ontogeny in dorsal and ventral views: (A) juvenile individual, TMP 2013.18.11, left postorbital; (B) adult individual, TMP 2001.36.1, right postorbital (image reversed). Abbreviations are same as Fig. 2.2. Scale bars equal 50 mm.

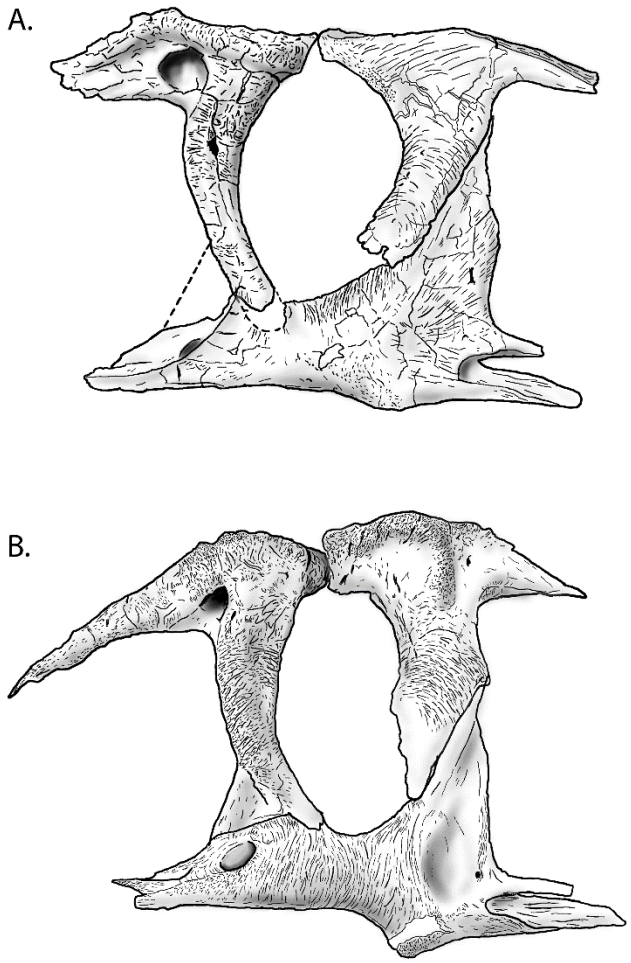

Figure 2.4. Orbital forming elements of (A) the large juvenile *Gorgosaurus* individual, TMP 1994.143.1, and (B) the adult *Daspletosaurus* individual, TMP 2001.36.1.

Table 2.1. List of specimens that were observed for comparison in the current study.

Taxon	Specimen Number	Formation	Material	Specimen Age
Gorgosaurus libratus	AMNH FARB 5336	DPFm	Skull	adult
	AMNH FARB 5432	DPFm	l.maxilla & partial l.jugal	adult
	AMNH FARB 5458	DPFm	Skull and skeleton	adult
	AMNH FARB 5664	DPFm	Skull and skeleton	juvenile
	CMN 2120	DPFm	Holotype skull	large adult
	CMN 11841	DPFm	Partial Braincase	subadult
	CMN 12603	DPFm	Maxilla	subadult
	FMNH PR 2212	DPFm	partial skull and skeleton	juvenile
	ROM 683	DPFm	Maxillae	subadult
	ROM 1247	DPFm	Skull	subadult
	ROM 1422	DPFm	Partial Skull	subadult
	TMP 1986.144.1	DPFm	Skull and skeleton	juvenile
	TMP 1991.36.500	DPFm	Skull and skeleton	juvenile
	TMP 1991.153.1	DPFm	skull and partial skeleton	juvenile
	TMP 1994.12.602	DPFm	Partial skull	adult
	TMP 1993.36.539	DPFm	partial maxilla	small juv.
	TMP 1994.143.1	DPFm	Skull and skeleton	juvenile
	TMP 1995.12.116	DPFm	postorbital	adult
	TMP 1996.12.430	DPFm	frontal	juvenile
	TMP 1997.12.223	DPFm	maxilla	large adult
	TMP 1999.33.1	DPFm	skull and skeleton	subadult
	TMP 2000.12.11	DPFm	Partial Skull	large adult
	TMP 2009.12.14	DPFm	skull and skeleton	juvenile
	TMP 2008.12.61	DPFm	frontal	juvenile
	TMP 2015.12.70	DPFm	ectopterygoid	adult
	TMP 2016.14.1	DPFm	skull and skeleton	juvenile
	UALVP 10	DPFm	skull	adult
	USNM V12814	DPFm	skull and skeleton	adult
Albertosaurus sarcophagus	AMNH 5222	HSCFm	skull	adult
	CMN 5600	HSCFm	Holotype skull	adult
	CMN 5601	HSCFm	Paratype skull	adult
	CMN 11315	HSCFm	partial skull and skeleton	subadult

	TMP 1981.9.1	HSCFm	frontoparietal	huge adult
	TMP 1981.10.1	HSCFm	partial skull and skeleton	adult
	TMP 1985.98.1	HSCFm	skull and skeleton	adult
	TMP 1986.64.1	HSCFm	skull and skeleton	subadult
	TMP 1997.58.1	HSCFm	dentaries and partial tail	adult
	TMP 1998.63.88	HSCFm	maxilla	adult
	TMP 1999.50.57	HSCFm	lacrimal	subadult
	TMP 1999.50.140	HSCFm	maxilla	juvenile
	TMP 2000.45.26	HSCFm	lacrimal	subadult
	TMP 2000.45.27	HSCFm	spenial	subadult
Daspletosaurus torosus	AMNH 5346		Maxilla	adult
	AMNH 21809		Caudal portion of nasal	adult
	CMN 350		Postorbital and nasal	adult
	CMN 8506		Holotype skull and skeleton	adult
	CMN 11594		Partial skull	Subadult
	CMN 57108		Nasal	adult
	FMNH PR 308	DPFm	Skull	adult
	FMNH PR 864		Dentary	adult
	FMNH PR 1196		Dentary	adult
	FMNH PR 2007		Maxilla	adult
	TMP 1985.62.1	DPFm	skull and skeleton	large adult
	TMP 1999.55.170	DPFm	dentary	subadult
	TMP 2001.36.1	Oldman	skull and skeleton	large adult
	TMP 2003.10.3	Oldman	partial skull	adult
	TMP 2013.18.11	DPFm	postorbital	juvenile
	TMP Jugal	DPFm	jugal	adult
D. horneri	AMNH FARB 5477	???	maxilla	subadult
	MOR 590	TMFm	skull	l. subadult
	MOR 1130	TMFm	skull and partial skeleton	adult
	TMP 2016.XX.YY	Bearpaw	partial skull	l. adult
Tyrannosaurus rex	AMNH FARB 5029	Hell Creek	braincase	adult
	AMNH FARB 5117	Hell Creek	braincase and postorbital	adult
	BHI 3033	Hell Creek	skull and skeleton	adult
	BMRP 2002.4.1	Hell Creek	skull	juvenile
	CM 9380	Hell Creek	partial skull and skeleton	adult
	CMNH 7541	Hell Creek	skull	juvenile
	FMNH PR 2081	Hell Creek	skull and skeleton	l. adult
	MOR 555	Hell Creek	skull and skeleton	adult
	MOR 1125	Hell Creek	skull+?	l. adult

	TMP 1981.6.1	Willow Creek	partial skull and skeleton	subadult
	TMP 1981.12.1	Scollard	postorbital and partial skele.	adult

Table 2.2. List of synapomorphies for several tyrannosaurid clades and the conditions for *Daspletosaurus*, adult *Gorgosaurus*, juvenile *Gorgosaurus*, and TMP 1994.143. Synapomorphies recovered from the dataset of Carr et al. (2017).

	Character	*Daspletosaurus*	*Gorgosaurus*	*juv. Gorgo*	TMP 1994.143.1
Albertosaurinae	**Lacrimal**, Form of the joint surface for the frontal in medial view (Character 86)	Medially deflected conical projection that also tapers caudally	Medial surface is flat; tapers caudally in TMP 1994.12.602	Medial surface is flat	Medial surface is flat; left element tapers caudally
	Jugal, Angle of the caudal margin of the suture with lacrimal in lateral view (Character 96)	Shallow in *D. torosus*; Steep in *D. horneri*	Steep	Steep	Steep
	Jugal, Slope of the ventral margin of quadratojugal joint surface angle in lateral view (Character 106)	Approximately rostrocaudal; nearly straight	Prominent rostrodorsal inflection of approximately 45°	Nearly straight or shallow rostrodorsal inflection	Shallow rostrodorsal inflection
	Postorbital, form of the caudodorsal margin of the squamosal ramus in lateral view (Character 114)	Shallow concave notch or uninterrupted convex arc	Emarginated by squamosal (discrete notch within margin)	shallow concave notch	Shallow to deep concave notch
	Postorbital, Extent of the squamosal ramus relative to caudodorsal margin of lateral temporal fenestra (Character 115)	Reaches or extends caudal to margin	Terminates rostral to margin	Terminates rostral to margin	Terminates rostral to margin
	Quadrate, Orientation of the medial margin of the quadratojugal articular surface where the quadratojugal wraps around the quadrate lateral condyle (Character 147)	vertical or dorsomedial	dorsolateral	dorsolateral	dorsolateral
	Palatine, Orientation of the neck of the vomeropterygoid process in lateral view (Character 180)	inclined rostrodorsally	Vertical	rostrodorsally inclined in some (e.g. TMP 2009.12.14 and TMP 2016.14.1); vertical in others (e.g. TMP 1986.144.1)	left element is rostrodorsally inclined; right element is approximately vertical

	Basisphenoid, Inflation of the ceiling of the basisphenoid recess in ventral view (Character 210)	Present	Absent	Absent	Absent
Gorgosaurus libratus	**Frontal**, Shape of the frontal in mediolateral cross section ahead of dorsotemporal fossa	Slope towards interfrontal suture; concave	Slope away from interfrontal suture; convex	slope away from interfrontal suture; convex	slope away from interfrontal suture; convex
	Jugal, Rostrocaudal length of the basal postorbital process relative to the dorsoventral depth of the suborbital region	Postorbital process rostrocaudally longer than suborbital depth	Postorbital process shorter than suborbital depth	Postorbital process shorter than suborbital depth	Postorbital process length slightly shorter than suborbital depth
Daspletosaurus spp.	**Maxilla**, Form of the subcutaneous surface texture in lateral view (character 43).	Extremely coarse; deep sulci rostral of antorbital fossa	Random foramina and shallow grooves and ridges	Smooth or random foramina and shallow grooves and ridges	Random foramina and shallow grooves and ridges
	Lacrimal, Presence of an accessory caudally extending cornual process on the lateral surface between the cornual process and the supraorbital ramus (Character 72)	present	absent	absent	absent
	Lacrimal, Exposure of the maxillary process of rostral ramus in lateral view (Character 89).	Only ventral margin visible	both dorsal and ventral margins visible	both dorsal and ventral margins visible	both dorsal and ventral margins visible
	Postorbital, cornual process, position relative to laterotemporal fenestra, lateral view (Character 113)	Approaches fenestra	Does not approach fenestra	Does not approach fenestra	Does not approach fenestra
	Squamosal, Position of the rostral tip of the dorsal postorbital process (Character 130)	Caudal to rostral margin of lateral temporal fenestra	Level with or rostral to rostral margin of laterotemporal fenestra	Level with or rostral to rostral margin of laterotemporal fenestra	Rostral to rostral margin of laterotemporal fenestra

	Frontal, nasal process, ridge that extends rostrocaudally along the process, presence, dorsal view (Character 154).	Present	mostly absent; present in some e.g. TMP 1994.12.602	present in some e.g. TMP 2009.12.14	present
	Vomer, Presence of deep keel below stem	Present	Present in some (e.g. TMP 2000.13.11)	present in some (TMP 2009.12.14)	?
	Palatine, primary opening of palatine recess, location of rostral margin, lateral view (Character 184).	Level with or caudal to recess	Rostral to recess	Caudal to recess	Caudal to recess
	Laterosphenoid, mediolaterally oriented ridge on dorsolateral surface that extends laterally to the edge of the dorsotemporal fenestra (Character 219).	Present extends onto capitate process	Absent	Absent	Present; does not extend onto capitate process
	Dentary, position of the transition point between the ventral and rostral margins of the bone, lateral view (Character 229).	Below alveoli 1-3	Below the fourth alveolus	Below the fourth alveolus	Below the fourth alveolus
	Maxillary teeth, number of teeth (Character 261).	15-17	13-15	13-14	13
D. torosus	**Lacrimal**, rostral ramus, length relative to the ventral ramus (Character 74)	Longer than ventral ramus	shorter than ventral ramus	longer than the ventral ramus	Approximately equal
	Lacrimal, transition between antorbital fossa and the subcutaneous surface of the ventral ramus, form, lateral view (Character 77).	Variable: fossa is continuous (e.g. TMP 2001.36.1) or deeply inset ()	Fossa is deeply inset forming a ridge along subcutaneous surface	Fossa is deeply inset forming a ridge along subcutaneous surface	Fossa is deeply inset forming a ridge along subcutaneous surface
	Surangular, adductor muscle attachment site dorsal to surangular shelf, orientation, lateral and dorsal views (Character 244)	Faces almost equally dorsally and laterally	Faces almost equally dorsally and laterally	Faces almost equally dorsally and laterally	Faces almost equally dorsally and laterally
Tyrannosaurina	**Premaxilla**, Orientation of the subnarial (maxillary) processes of the premaxilla (Character 14)	Dorsal; processes mostly obscured in lateral view	Dorsolateral	Dorsolateral; most juvenile skulls are laterally compressed	Dorsal-dorsolateral; specimen is dorsoventrally compressed however

	Maxilla, Depth of the joint surface for the palatine (Character 40)	Deep; conceals tooth root bulges in medial view	Shallow, tooth root bulges visible in medial view	Shallow, tooth root bulges visible in medial view	?
	Nasal, extent of premaxillary process apposition (Character 54)	Separated for most of their length	Apposed for most of their length; abruptly separate at tip	Apposed for most of their length; abruptly separate at tip	Apposed for most of their length; abruptly separate at tip
	Lacrimal, extent of rostrodorsal process (Character 81)	Long	Generally short	generally short	short on left; long on right (length comparable to *Gorgosaurus* TMP 1994.12.602)
	Squamosal, morphology of the surface of the dorsotemporal fossa (Character 123)	Convex	Flat or concave	flat	flat
	Squamosal, morphology of the rostral tip of the quadratojugal process (Character 125)	Squared off	Tapered	Tapered	Tapered
	Squamosal, presence of a pneumatic recess in ventral view (Character 131)	Recess present; edges are undercut	Fossa instead of recess; edges are not undercut	Fossa instead of recess; edges not undercut	Fossa instead of recess; edges not undercut
	Ectopterygoid, inflation of the ectopterygoid body and pterygoid process (Character 174)	Inflated	Uninflated	Uninflated	Uninflated
	Ectopterygoid, shape of the pneumatopore in ventral view (Character 177)	Large and round or triangular	Thin and narrow slit	Thin and narrow slit	Thin and narrow slit
	Ectopterygoid, surface morphology of floor immediately adjacent to pneumatopore (Character 178)	Pneumatopore and floor separated by a shelf	Flat	Flat	Flat

	Palatine, presence of brace in the rostroventral corner of the jugal articulation (Character 188)	Present	Absent; maxilla contacts rostroventral corner of jugal contact	Absent; maxilla contacts rostroventral corner of jugal contact	Absent; maxilla contacts rostroventral corner of jugal contact
	Laterosphenoid, morphology of the antotic crest, rostral to the epipterygoid fossa in rostral and lateral views (Character 216)	Robust and rugose	Indistinct	Indistinct	Indistinct
Derived Tyrannosaurines	**Postorbital**, position of the cornual process relative to the orbital margin (Character 112)	Caudodorsal; Separated from orbital margin by smooth region of bone	Adjacent to orbit	Adjacent to orbit	Adjacent to orbit
	Squamosal, morphology of the ridge delimiting the lateral margin of the dorsotemporal fossa (Character 122)	Divided into pair of ridges	Undivided	Undivided	Left is undivided; right is partially divided by a short and shallow groove
	Quadratojugal, extent of the dorsal quadratojugal process of jugal relative to base of the quadratojugal stem in the caudoventral corner of the laterotemporal fenestra (Character 134)	Approaches quadratojugal stem	Does not approach stem	Does not approach stem	Does not approach stem
	Quadratojugal, shape of the rostral tip of the jugal process (Character 135)	Squared off	Rounded	Tapered	Rounded
	Frontal, morphology of the sagittal crest (Character 135)	Dorsoventrally tall and unpaired	present as a slight midline bulge; variable	present as a slight midline bulge; variable; moderately tall in TMP 2009.12.14	Moderately tall
	Frontal, rostrocaudal length of the sagittal crest relative to the entire length of the frontal (Character 158)	>25%	<15%	Much less than 15%	<15%
	Dentary, Angle between the rostral margin versus the dorsal margin (Character 237)	Approximately 90°	Approximately 45° or less	Less than 45°	Approximately 45°

	Surangular, morphology of the surangular shelf over the caudoventral foramen (Character 241)	Shelf projects ventrolaterally and overhangs foramen	Dorsal margin of foramen is in contact with shelf but shelf projects laterally and does not overhang	Dorsal margin of foramen is in contact with shelf but shelf projects laterally and does not overhang	Dorsal margin of foramen is in contact with shelf but shelf projects laterally and does not overhang
	Angular, morphology of the ventral margin (Character 248)	Rostral region flexed at caudal dentary contact such that there is distinct angle	Smoothly convex	Smoothly convex	Smoothly convex
	Maxilla, exposure of the promaxillary fenestra in lateral view (Character 20)	Concealed by lateral lamina in lateral view	Visible	Visible	?
Daspletosaurus+Tyrannosaurini	**Maxilla**, rotrocaudal length of maxillary fenestra relative to the maximum length of the antorbital fossa ahead of the rostral-most point of the antorbital fenestra (Character 24)	Greater than 50% and also greater than 50% the length of the eyeball-bearing portion of the orbit	Less than 50%	Less than 50%	Less than 50%
	Maxilla, morphology of nasal contact in subadult-adult specimens* (Character 42)	Deeply scalloped with several interlocking tongue-and-groove joints	Weakly scalloped	Weakly scalloped	Weakly scalloped (where visible); no interlocking tongue-and-groove joints

	Nasal, constriction of frontal ramus (Character 59)	Constricted to less than half the width of the widest point of the nasal	Unconstricted	Unconstricted	Unconstricted; greater than 50% maximum width of nasal; nasal dorsoventrally compressed and flaired laterally
	Jugal, caudal extent of the antorbital fossa on the maxillary ramus (Character 91)	Does not extend past the jugal pneumatopore	Undercuts and extends behind pneumatopore, caudodorsal margin may be resorbed	Undercuts pneumatopore and extends behind pneumatopore to tip of rostral ascending process	Undercuts pneumatopore and extends behind pneumatopore to tip of rostral ascending process
	Jugal, orientation of the long axis of the jugal pneumatopore (Character 93)	Nearly horizontal	Rostrocaudally inclined at nearly 45° from horizontal	Rostrocaudally inclined at nearly 45° from horizontal	Rostrocaudally inclined at nearly 45° from horizontal
	Jugal, morphology of the fossa located at the base of the postorbital ramus (Character 97)	Deep	Shallow	flat; fossa absent or undeveloped	flat

CHAPTER 3: DESCRIPTION OF JUVENILE *GORGOSAURUS* SPECIMENS PROVIDES NEW INSIGHT INTO ALBERTOSAURINE ONTOGENY

3.1 INTRODUCTION

With a nearly complete growth series, several studies have reported on the osteological ontogeny and growth patterns within *Gorgosaurus libratus* (Carr, 1999; Currie, 2003a, b; Erickson et al., 2004; Bradley, 2015; Bradley et al., 2015). In particular, Carr (1999) provided an in-depth analysis into the ontogenetic changes of the individual cranial bones in *Gorgosaurus* and concluded these trends to be uniform across Tyrannosauridae. In his study, Carr (1999) assigned known *Gorgosaurus* specimens to one of three growth stages (stage 1 juveniles through stage 3 large adults) using the presence of immature cortical bone and size as indicators. Stage 1 was subdivided into "small" and "large" categories to differentiate the smallest specimens of *G. libratus*, which are only known from isolated elements (Carr, 1999), from slightly larger and more complete specimens. Later, Currie (2003a) provided a thorough description of anatomical characteristics of various North American tyrannosaurid taxa, which also included features related to ontogenetic stage. However, due to the incomplete nature of the small juvenile specimens known at the time, the documentation of the ontogenetic changes in *Gorgosaurus* was limited in both studies. The recent discovery of two complete and small juvenile *Gorgosaurus* specimens offers new insight into tyrannosaurid ontogeny allowing for the documentation of previously unknown growth-related changes of the skull.

3.2 MATERIALS AND METHODS

The skulls of two juvenile *Gorgosaurus* individuals, TMP 2009.12.14 and TMP 2016.14.1, are described in detail and compared with several other *Gorgosaurus* and other North American tyrannosaurid specimens (Table 2.1). TMP 2009.12.14 consists of an articulated skeleton preserving a complete dorsal vertebral series (including most ribs), sacrum, scapular and pectoral girdles, fore- and hindlimbs, and proximal caudal vertebrae (Ca1 and Ca2). The skeleton lacks many cervical vertebrae and post-Ca2 caudal vertebrae. TMP 2016.14.1 consists of a largely complete and articulated skeleton preserving a complete cervical and thoracic vertebral series, pelvis, proximal caudals, and hindlimbs. Measurements of the skull elements of TMP 2009.12.14 and TMP 2016.14.1 are listed in Table 3.1.

The skull of TMP 2009.12.14 was CT (computed tomography) scanned with a hospital-grade scanner located at the University of Calgary. The skull was scanned longitudinally at a slice thickness of 0.5 mm. The skull and various individual skull bones were segmented in Amira 5.3.3, which was used to generate isosurface and volren models of the specimen. Several other specimens were also CT scanned for comparison (Table 3.2).

3.3 DESCRIPTION AND ONTOGENETIC PATTERNS IN *GORGOSAURUS*

General Skull Morphology

The skulls of TMP 2009.12.14 and TMP 2016.14.1 are slightly compressed laterally, but otherwise well-preserved. The skull length is 497 mm and 515 mm, respectively, measured from the rostral margin of the premaxilla to the caudal-most point of quadratojugal (Fig. 3.1), making the skulls of these individuals approximately 50% the skull length of the largest known specimens of *Gorgosaurus*. The skull length from the premaxilla to occipital condyle is 501 mm from in TMP 2009.12.14 but is unmeasurable in TMP 2016.14.1 due to articulation of the skull

and cervical vertebrae. The cranium is shallow relative to more mature *Gorgosaurus*, possessing a length to depth ratio of 3.9 and 4.1 in TMP 2009.12.14 and TMP 2016.14.1, respectively, in contrast with a length to depth of approximately 3.4 in the adult UALVP 10 (depth=maximum skull depth at rostral margin of antorbital fenestra). With a femur length of 543 mm and 555 mm, respectively, the femur:skull length ratio is approximately 1.09 and 1.08, which is consistent with measurements of other non-alioramine tyrannosaurids (Currie, 2003b; Brusatte et al., 2012; Lu et al., 2014).

All the cranial bones on the left side of TMP 2009.12.14 are preserved in articulation (Fig. 3.3), whereas the right side is missing the articular, epipterygoid, ethmoid, jugal, lacrimal, orbitosphenoid, prearticular, quadrate, quadratojugal, squamosal, surangular, and prearticular. The right angular and ectopterygoid were found disarticulated near the skull. The right postorbital had fallen into the orbit, indicating that some elements were exposed and transported during the Cretaceous. Because many cranial elements are either missing or disarticulated, the braincase is exposed in right lateral view.

The left side of the skull of TMP 2016.14.1 is articulated with all elements present, but the right side lacks the quadrate, and quadratojugal. In contrast to TMP 2009.12.14, in which the upper and lower jaws are in occlusion, the mandible of TMP 2016.14.1 is depressed. Because the skull is in articulation with the rest of the body, the supporting jacket cannot be flipped and the right side of the skull TMP 2016.14.1 could not be examined in the context of this project.

Dermatocranium

Premaxilla—The body of the premaxilla in TMP 2009.12.14 and TMP 2016.14.1 is shallow, with depth-to-length ratios of 1.01 and 0.89, respectively (Fig. 3.4), similar to that of other immature tyrannosaurids (Carpenter, 1992; Carr, 1999; Tsuihiji et al., 2011). This condition is

distinct from that of adults, where the premaxilla is much deeper (e.g., depth to length ratio is 1.39 in TMP 1986.36.116; Currie, 2003a; Rauhut et al., 2010; Xu et al., 2012).

The supranarial and subnarial processes branch from the body of the premaxilla dorsally and caudally, respectively, forming most of the rostrodorsal and ventral boundaries of the external nares. The subnarial process slopes ventrolaterally and is visible in lateral view across its entire extent (Fig. 3.4; Carr et al., 2017). The supranarial process (ascending premaxillary process of Brochu, 2003; nasal process of Currie, 2003a) extends dorsally above the body of the premaxilla for approximately 10 mm in TMP 2009.12.14 and 17 mm in TMP 2016.14.1 before arcing dorsocaudally to form the dorsal margin of the external nares in conjunction with the nasal (Fig. 3.4). The supranarial process is received caudolaterally and caudoventrally by the nasal at just over half the length of the external nares.

Maxilla—The maxilla of TMP 2009.12.14 and TMP 2016.14.1 is long and low, with a length to depth ratio of 0.34 and 0.33 (Fig. 3.5a), respectively, comparable to the ratio of immature non-alioramine tyrannosaurids (Carr, 1999; Currie, 2003b; Brusatte et al., 2012: table 2), but larger *Gorgosaurus* specimens have a higher length to depth ratio (0.41 for TMP 1986.36.96, and 0.43 for TMP 1994.12.602), corresponding to a dorsoventrally deeper maxilla (Fig. 3.5b). The difference in maxilla depth between juvenile and adult *Gorgosaurus* is consistent with reports of other tyrannosaurids and is associated with an overall increase in cranium depth with increasing body size (Carr, 1999; Currie, 2003a, Tsuihiji et al., 2011; Brusatte et al., 2012).

The texture of the subcutaneous surface of the maxilla differs between TMP 2009.12.14 and TMP 2016.14.1. The subcutaneous surface of TMP 2016.14.1 and smaller *Gorgosaurus* individuals (e.g. TMP 1993.36.539) is smooth, except for a weakly textured region adjacent to the rostral and rostroventral margins of the antorbital fossa (Fig. 3.4b). In contrast, the

subcutaneous surface of the maxilla of TMP 2009.12.14 is weakly rugose, characterized by shallow ridges and grooves situated along the rostroventral alveolar margin that are roughly aligned with small neurovascular foramina and associated nerve grooves (Fig. 3.4a). As such, the ridges and grooves have a rostroventral orientation rostral to the fourth alveolus, a caudoventral to caudal orientation caudal to the sixth alveolus, and no discernible pattern of orientation between the fourth and sixth alveoli where the neurovascular foramina in this region usually open ventrally. In large *Gorgosaurus* individuals (e.g. TMP 1994.12.602, TMP 1997.12.223), the subcutaneous surface is more rugose, with larger foramina and deeper and more randomly oriented ridges and grooves (Fig. 3.5b). The differences in subcutaneous texture of the maxilla between individuals of different sizes suggests that it develops through ontogeny (Carr, 1999). The maxilla texturing of albertosaurines is more similar to that of teratophonines and alioramines than to the more rugose maxillae of derived tyrannosaurines (i.e. *Lythronax*, *Tarbosaurus*, *Tyrannosaurus*, and *Zhuchengtyrannus*; Hone et al., 2011; Brusatte and Carr, 2016; Carr et al., 2017). Subcutaneous sculpturing in *Daspletosaurus* is extreme, with a network of deeply-incised and ventrally elongated sulci rostral to the antorbital fossa, prominent ridges, and large neurovascular foramina (Brusatte and Carr, 2016; Carr et al., 2017).

The subcutaneous surface of the maxilla forms a rugose and stepped rim around the antorbital fossa in tyrannosaurids. In TMP 2009.12.14, the ventral margin of this rim transitions caudally from a step to a flange that is separated from the antorbital fossa by a rostrocaudally-oriented channel. This channel is not present in other *Gorgosaurus* specimens (e.g. TMP 2016.14.1, TMP 1985.11.3). Rostroventral to the maxillary fenestra, the roots of the maxillary teeth create a swelling within the antorbital fossa, causing the fossa to grade into the subcutaneous surface in this region in juvenile specimens (Fig. 3.6). In large albertosaurines (e.g.

TMP 1994.12.602, TMP 1981.10.1), there is no swelling of antorbital fossa due to maxillary teeth (Fig. 3.5b).

Because the skulls of TMP 2009.12.14 and TMP 2016.14.1 are articulated, the palatal shelf, situated on the medial surface of the maxilla, could only be observed via CT scans in the former specimen. As in other tyrannosaurids, the palatal shelf extends along the medial surface of the maxilla from the approximate level of the jugal contact to that of the premaxillary process. The palatal shelf is relatively straight and terminates rostrally as a weakly downturned rostromedial process. In comparison, the rostromedial process is nearly straight in smaller *Gorgosaurus* individuals (TMP 1985.11.3) and in *Alioramus* (Brusatte et al., 2011) whereas it is strongly downturned in larger *Gorgosaurus* individuals (e.g. TMP 1994.12.602, TMP 1997.12.223) and other tyrannosaurids (e.g. *Daspletosaurus* TMP 2001.36.1, *Tyrannosaurus* CM 9380). More caudally along the palatal shelf, the palatine articular surface juts medially as a shallow and wide flange with a dorsally concave medial margin in *Gorgosaurus* (e.g. TMP 2009.12.14 and TMP 1997.12.223) and most other tyrannosaurids. In *Daspletosaurus*, the palatine articular surface tightly abutts the body of the maxilla, such that the flange is largely absent and the palatine contact is deep and relatively straight.

Nasal—The nasals of TMP 2009.12.14 and TMP 2016.14.1 are co-ossified into a single element, as in other tyrannosaurids (Currie, 2003a). The midline suture between the left and right nasals is unfused at the rostral and caudal ends, forming short fissures. These fissures are more extensive across the dorsal surface of the nasal in TMP 2009.12.14 and TMP 2016.14.1, 43% and 50% of total nasal length, respectively, than in adult individuals (33% of total nasal length in TMP 2000.12.11). This observation suggests that fusion of the nasals continued throughout ontogeny,

presumably in association with the increasing bite force (Rayfield, 2004, 2005; Snively et al., 2006).

In albertosaurines, long, paired, and appressed midline prongs of the nasal separate the caudal ends of the left and right supranarial processes of the premaxilla (Fig. 3.7; prongs are unpaired and unilateral in some specimens, e.g. ROM 1247). These prongs terminate rostrally at or close to the level of the lateral premaxillary processes, such that premaxillary ramus of the nasal is trident-shaped in dorsal and ventral views. Although similar midline prongs have also been documented in *Bistahieversor* and in some specimens of *Daspletosaurus* and *Tarbosaurus*, they are significantly shorter and less distinct than those of albertosaurines, resulting in a premaxillary ramus that is forked rather than trident-shaped (Currie, 2003a; Carr et al., 2017). Consequently, the presence of such prominent midline prongs of the nasal is unique to Albertosaurinae.

Tyrannosaurid nasals are divided into two regions: a rostral, vaulted region, and a caudal, smooth and flat region located between the lacrimals. In TMP 2009.12.14 and TMP 2016.14.1, the dorsal surface of the vaulted region is ornamented by a few low bosses but is otherwise texturally smooth. In comparison, the nasal of some subadult individuals (e.g. TMP 1999.33.1) is ornamented by several prominent bosses, but these are reduced in larger adults, a pattern also noted in *Tyrannosaurus* by Carr and Williamson (2004; also see Carr et al., 2017). In terms of rugosity, the vaulted region of adult *Gorgosaurus* nasals is extremely rugose relative to juveniles and subadults and is characterized by a network of distinct and randomly oriented grooves and ridges (e.g. TMP 2000.12.11).

The width of the nasal is relatively consistent between the vaulted and flattened regions (~33 mm) in both TMP 2009.12.14 and TMP 2016.14.1, with the nasal being only slightly wider

immediately behind the external nares (35.9 mm) in TMP 2009.12.14 (Fig. 3.7a). The nasal width is also consistent across the vaulted and flattened regions in more mature *Gorgosaurus* and *Albertosaurus* individuals (Fig. 3.7b), as well as in *Qianzhousaurus* (Lü et al., 2014). Some large *Gorgosaurus* specimens (e.g. TMP 2000.12.11) exhibit minor mediolateral constriction in the middle of the vaulted region, as also observed in *Alioramus altai* (Brusatte et al., 2011: fig. 10). In contrast, the nasals of derived tyrannosaurines (e.g. *Daspletosaurus*, *Tyrannosaurus*, *Tarbosaurus*) exhibit a narrowed frontal ramus, located in the flattened region between the lacrimals, such that the width of the nasal is tapered and constricted caudally (Currie, 2003a; Loewen et al., 2013). Constriction of the frontal ramus is more extreme in *Tyrannosaurus* and *Tarbosaurus* than in *Daspletosaurus* (Brochu, 2003; Carr and Williamson, 2004; Tsuihiji et al., 2011). In *Lythronax*, the nasal is constricted in the region of rostral ramus of the lacrimal (see below) but the frontal ramus of the nasal is laterally expanded (Loewen et al., 2013). Constriction of the nasal appears to be closely linked to inflation of the lacrimal sinus in large tyrannosaurines, as nasal constriction is less dramatic in juvenile individuals and nearly absent in albertosaurines, both of which lack extensive inflation of the lacrimal (see Carr and Williamson, 2004).

The nasomaxillary suture behind the external nares is relatively straight in TMP 2009.12.14 and TMP 1986.144.1, which is also the case in most non-albertosaurine tyrannosaurids (Fig. 3.1a, 3.2). In contrast, a prominent and ventrally convex tongue of the nasal overlaps the dorsolateral margin of the maxilla, just rostral to the maxillary flange (sensu Carr and Williamson, 2004) in TMP 2016.14.1 (Fig. 3.1b), other albertosaurines, and even in some *Daspletosaurus* specimens (e.g. CMN 350, TMP 1998.48.1). In many isolated maxillae of the aforementioned taxa, a shallow concavity/depression in the dorsal margin of the bone is present

where this tongue of the nasal would have been located. Basal theropods, proceratosaurids, and many non-tyrannosaurid tyrannosauroids have a deeper and more distinct depression at the caudal margin of the external nares (Brusatte et al., 2010: character 30; Brusatte and Carr, 2016: character 30; Carr et al., 2017: character 41), but this depression does not relate to the form of nasal articulation.

Lacrimal—The T-shaped lacrimal is longer than tall in TMP 2009.12.14 and TMP 2016.14.1, with a length-to-depth ratio of 1.44 and 1.35, respectively, and is deeper in more mature individuals (e.g. ratio of 1.14 in ROM 1247). The lateral surface of the lacrimal is perforated by a large pneumatopore, which is the primary opening of the lacrimal diverticulum of the antorbital sinus, at the convergence of the rostral and ventral rami (Fig. 3.8). Despite the large size of the primary pneumatopore, the lacrimal diverticulum of *Gorgosaurus* is uninflated relative to that of large tyrannosaurines (e.g. *Daspletosaurus*, *Tarbosaurus*, *Tyrannosaurus*; Carr, 1999; Currie, 2003a; Carr and Williamson, 2004; Carr and Williamson, 2010; Brusatte et al., 2010; Brusatte and Carr, 2016; Carr et al., 2017).

The rostral ramus of the lacrimal is forked distally into a medial and lateral lamina in TMP 2009.12.14 and TMP 2016.14.1. The medial lamina is fully exposed ventral to the lateral lamina and tapers rostrally to form a scarf joint with the maxilla. Two struts connect the lateral and medial laminae, forming a smaller secondary lacrimal pneumatopore at the mid-region of the rostral ramus (Fig. 3.8a). The rostral strut, located at the rostral end of the lacrimal, expands from mid-height of the medial lamina to the medial underside of the lateral lamina. The caudal strut extends from the ventral margin of the medial lamina to the ventral margin of the lateral lamina and also forms the rostral margin of the primary lacrimal pneumatopore. In larger *Gorgosaurus* specimens, the lateral lamina extends further ventrally, forming a curtain-like structure that

conceals most of the medial lamina and rostral ramus component of the antorbital fossa in lateral view (Fig. 3.8b, c; Carr, 1999); however, the rostral end of the medial lamina is visible in lateral view in all albertosaurines (sensu Carr et al., 2017). The two struts connecting the medial and lateral laminae are horizontally oriented in adult *Gorgosaurus*, which likely occurs due to thickening of the lateral lamina through ontogeny.

The lateral lamina is forked at the rostral end to receive a small (8.2 mm long) finger-like nasal process in a tongue-and-groove joint in TMP 2009.12.14 (Fig. 3.8a). The nasal process is absent in TMP 2016.14.1 and in TMP 1986.144.1 (Carr, 1999), but is elongated and robust in adult specimens, suggesting the feature is acquired through ontogeny. The presence of the nasal process is variable in other derived tyrannosaurids: it is absent in *Alioramus altai* (Brusatte et al., 2011) and *Lythronax* (Loewen et al., 2013:fig. 2), short in juvenile *Tarbosaurus* individuals but absent in adults (Hurum and Sabath, 2003; Currie et al., 2003; Tsuihiji et al., 2011), generally absent in *Daspletosaurus* (Carr, 1999; Currie, 2003a) but short in some specimens (e.g., CMN 8506), and elongated in *Bistahieversor* (Carr and Williamson, 2010), *Albertosaurus*, and *Tyrannosaurus* (Brochu, 2003; Brusatte et al., 2011).

A discrete, cornual process of approximately 12 mm in height is present on the lacrimal of TMP 2009.12.14, whereas TMP 2016.14.1 and other immature *Gorgosaurus* individuals possess a less prominent cornual process (Carr, 1999). The dorsal prominence and position of this projection in TMP 2009.12.14 is most similar to those of mature individuals of *Albertosaurus sarcophagus*, in which the apex is pronounced more dorsally than laterally and is located above the primary pneumatopore (e.g. TMP 1981.10.1, TMP 2000.45.26; Carr, 2010), but may be result of lateral deformation of the skull. In TMP 2016.14.1, the cornual process projects dorsolaterally and is positioned rostral to the primary pneumatopore, being similar to, but less

prominent than in mature *Gorgosaurus libratus* (e.g. ROM 1247, TMP 1994.12.602). The dorsal surface of the cornual process is not markedly rugose in either TMP 2009.12.14 or TMP 2016.14.1, contrary to larger *Gorgosaurus* specimens.

Postorbital—The postorbital of TMP 2009.12.14 and TMP 2016.14.1 is gracile with a slender dorsal bar, as in other immature *Gorgosaurus* specimens (e.g. TMP 1986.144.1, TMP 1994.143.1). In lateral view, the dorsal bar consists of a dorsally convex caudal ramus and a gently concave rostral ramus, such that the entire dorsal margin appears sinusoidal (Fig. 2.2a, b). A sigmoidal dorsal bar of the postorbital is also found in immature individuals of other tyrannosaurids, including *Alioramus altai* (IGM 100/1844; Brusatte et al., 2012) and *Tarbosaurus* (MPC-D 107/7;(Tsuihiji et al., 2011: fig. 8), as well as in some tyrannosauroids (e.g., *Xiongguanlong baimoensis*; see Li et al., 2010: fig. 1). In larger and presumably more mature *Gorgosaurus* specimens (e.g. *Gorgosaurus* TMP 1995.12.116), the dorsal margin of the rostral ramus is either flat or weakly concave and the convex region is more extensive along the dorsal bar (e.g. TMP 1995.12.116: Fig. 2.2c). In large tyrannosaurines, the dorsal margin of the postorbital is convex (see chapter 1).

In albertosaurines, the dorsal margin of the postorbital is emarginated to receive the rostral tip of the dorsal postorbital process of the squamosal (Carr and Williamson, 2010; Brusatte and Carr, 2016; Carr et al., 2017). The degree of emargination varies through ontogeny, with the small juvenile specimens possessing an unemarginated and smoothly convex dorsal margin of the postorbital (e.g. TMP 1986.144.1, TMP 2009.12.14, TMP 2016.14.1), larger juvenile specimens possessing a shallow notch (TMP 1991.36.500, TMP 1994.143.1), and subadult and adult specimens possessing a deep notch (e.g. ROM 1422, UALVP 10). The presence of this feature has been identified as a synapomorphy of Albertosaurinae and an independently acquired

autapomorphy of *Teratophoneus curriei* (Brusatte and Carr, 2016; Carr et al., 2017). In other tyrannosaurids, the the rostral extremity of the dorsal articular surface for the smoothly transitions to the exposed dorsal margin of the postorbital (Brusatte and Carr, 2016; Carr et al., 2017), as in juvenile *Gorgosaurus*.

A rugose protuberance, referred to as the postorbital cornual process by Carr (1999), ornaments the lateral surface of the postorbital in the caudodorsal corner of the orbit in most specimens of *Gorgosaurus* (Fig. 2.2). In both TMP 2009.12.14 and TMP 2016.14.1, this process is poorly developed, being limited to a slightly raised and textured region adjacent to the caudodorsal margin of the orbit. In larger *Gorgosaurus*, the process curls backwards to form a lip-like structure and appears as a rugose semicircle or crescent shape in lateral view (Carr et al., 2017), a morphology also seen in *Teratophoneus* (Loewen et al., 2013; see also Zanno et al. 2010). In contrast, the cornual process of *Albertosaurus* extends laterally and does not curl caudally (e.g. TMP 1981.10.1). In all albertosaurines and in *Alioramus altai* (and to a lesser extent in *Teratophoneus*; Zanno et al., 2010: fig. 2a), the cornual process is small, abuts the orbital margin, and does not expand beyond the dorsal margin of the postorbital (Brusatte et al., 2011; Carr and Williamson, 2010; Brusatte and Carr, 2016). The morphology and position of the cornual process is different in derived tyrannosaurines. In *Daspletosaurus*, the cornual process is a large a C-shaped protuberance positioned well behind the orbital margin that covers most of the rostral ramus and dorsal mid-region of the postorbital. A small palpebral ossification caps the lateral surface of the rostral ramus (pers. obs. TMP 2001.36.1). Relative to *Daspletosaurus*, the cornual process of *Tyrannosaurus* and *Tarbosaurus* is less inflated and less expansive, being mostly constricted to the rostral ramus and rostral half of the dorsal mid-region. In the latter two taxa, the palpebral ossification is larger than in *Daspletosaurus*.

The ventral ramus of the postorbital in TMP 2009.12.14 and TMP 2016.14.1 contacts the ascending postorbital process of the jugal for most of its length and tapers ventrally until it reaches the caudal-most margin of the orbit, ventral of which, it is constant in width and terminates as a rounded tip. In another similar sized specimen (TMP 1986.144.1), the end of the ventral ramus is subtly rectangular due to the presence of a weakly-developed suborbital process. In small *Gorgosaurus* specimens, the orbit is nearly equal in length and in height, such that it is sub-circular in shape (Fig. 3.1). In more mature *Gorgosaurus* and most other tyrannosaurids, the ventral ramus of the postorbital possesses a prominent right-angled suborbital process resulting in a distinctly rectangular distal end of the ventral ramus (Fig. 2.2b). Additionally, the suborbital process inflects into the orbit and gives it a distinct comma-shape. In contrast, the morphology of the ventral ramus of *Daspletosaurus* and alioramines differs from that of *Gorgosaurus* and most other tyrannosaurids. In *Daspletosaurus,* the extremity of the ventral ramus tapers to an acute angle and the suborbital process is either absent (e.g. CMN 350) or indistinct (e.g. CMN 8506), resulting in an oval-shaped orbit in all specimens. In alioramines, the ventral ramus is narrow and completely lacks a suborbital process. In *Alioramus altai*, the orbit is circular in shape, but it is an oblique oval in the alioramine *Qianzhousaurus* (Brusatte et al., 2013; Lü et al., 2014).

Jugal—In small, immature specimens of *Gorgosaurus*, such as TMP 2009.12.14, TMP 2016.14.1, and TMP 1986.144.1, the maxillary ramus of the jugal is shallower than its suborbital region, such that the region rostral to the postorbital process tapers rostrally and appears triangular in lateral view (Fig 3.8a–d; Carr, 1999). The minimum depth of the suborbital region in TMP 2009.12.14 is deeper than in other individuals of comparable skull length (TMP 2009.12.14 = 33.3 mm [L]; TMP 1986.144.1 = 21.5 mm [L], 26.1 mm [R]; TMP 2016.14.1= 21.1 mm [L]). In large albertosaurines, the maxillary ramus is nearly equal in depth to that of the

suborbital region, resulting in the region rostral to the postorbital process being trapezoid-shaped (Fig. 3.9e, f). The orbital margin of the jugal in juvenile *Gorgosaurus* individuals is either relatively straight or gently concave. In contrast, the ventral margin of the orbit in large albertosaurines is more distinctly concave. In comparison, the maxillary ramus is generally deep relative to the suborbital region and the ventral orbital margin is more deeply concave in large derived tyrannosaurine individuals (Carr, 1999; Brusatte and Carr, 2016; Carr et al., 2017).

At its rostral extremity, the jugal forms the caudoventral floor of the antorbital fossa and is invaded by a diverticulum of the antorbital sinus (Witmer, 1997). In juvenile *Gorgosaurus* (e.g. TMP 2009.12.14, TMP 2016.14.1), the entire margin of the antorbital fossa on the jugal is a distinct, pronounced ridge (Fig. 3.9a–e). The dorsal margin of the jugal pneumatopore is marked by a shallow secondary fossa that is mostly concealed in lateral view. In the largest albertosaurines (e.g. TMP 2000.12.11, TMP 1982.13.3), the rostral and caudodorsal-most margins of the antorbital fossa are resorbed and the secondary fossa is more widely-exposed in lateral view than in juvenile individuals, such that it appears lens-shaped (Fig. 3.9f). In large tyrannosaurines (e.g. *Daspletosaurus*, *Tarbosaurus*, and *Tyrannosaurus*), the margin of the antorbital fossa is resorbed and the secondary fossa is deeply excavated and more widely-exposed than in adult albertosaurines, such that it appears oval-shaped or circular in lateral view (Brusatte et al., 2011; Brusatte and Carr, 2016; Carr et al., 2017).

The lateral surface of the postorbital ramus of the jugal is flat in TMP 2009.12.14, TMP 2016.14.1, and the left jugal of TMP 1994.143.1, similar to the condition observed in adult *Bistahieversor* and other primitive tyrannosauroids (Brusatte and Carr, 2016; Carr et al., 2017). In the right jugal of TMP 1994.143.1 and larger tyrannosaurids, including adult *Gorgosaurus*,

the lateral surface is raised into a prominent ridge caudal to the postorbital articulation, which braces the postorbital–jugal contact (Carr et al., 2017).

Quadratojugal—Both TMP 2009.12.14 and TMP 2016.14.1 preserve only the left quadratojugal. This bone forms most of the caudal wall (in conjunction with the squamosal) and part of the ventral floor (in conjunction with the jugal) of the lateral temporal fenestra (Fig. 3.10). The dorsal process of the quadratojugal is narrow in TMP 2009.12.14 (Fig. 3.10a), and of similar proportions to that of the subadult TMP 1994.143.1 (Currie, 2003a: fig. 24). In contrast, the dorsal process of TMP 2016.14.1 is broad, as in larger *Gorgosaurus* individuals (Fig. 3.10b).

Squamosal—The caudal process of the squamosal is wedge-like in all *Gorgosaurus* specimens regardless of size, but it is thin and gracile in small individuals (TMP 2009.12.14, TMP 2016.14.1, and TMP 1994.143.1; Fig. 3.11) and robust in larger *Gorgosaurus* specimens (e.g. TMP 1992.36.82). The squamosal sinus is a concave pocket in the ventral surface of the squamosal present in all growth stages of *Gorgosaurus* but it lacks an undercutting rim that would make the sinus more chamber-like like that of large tyrannosaurines (Carr et al., 2017). Despite the robusticity of the caudal process in adult *Gorgosaurus*, no diverticulum of the squamosal sinus invades it, contra large tyrannosaurines (Brusatte and Carr, 2016; Carr et al., 2017).

Palatal Complex

Quadrate— Due to the articulation of the skull bones, the quadrate could not be physically observed in either TMP 2009.12.14 or TMP 2016.14.1. However, it could be described for TMP 2009.12.14 based on reconstructions via CT scans and the description was supplemented by additional scans of TMP 1994.143.1 (Fig. 3.12). Overall, the morphology of the quadrate in TMP 2009.12.14 is largely consistent with that of other tyrannosaurids but differs in that the quadrate

cotylus and mandibular condyles are more gracile than in larger individuals of *Gorgosaurus* and other large tyrannosaurids.

The quadrate is pneumatic in all tyrannosaurids, with the quadrate pneumatopore situated dorsal to the mandibular condyles at the base of the pterygoid ala (Currie, 2003a). In *Gorgosaurus* (TMP 2009.12.14, TMP 1994.143.1, TMP 1992.36.527), the quadrate pneumatopore occupies a relatively consistent position just dorsal to the medial condyle, where it opens rostroventrolaterally as a narrow slit. It is separated from the medial fossa of the pterygoid ala by a relatively thin bone lamina. The quadrate pneumatopore of *Gorgosaurus* opens ventrally onto a discrete triangular fossa on the rostral surface of the medial condyle (Fig. 3.12d). This fossa is bounded both laterally and medially by prominent ridges that intersect ventrally. In other tyrannosaurids, the lateral ridge is either short, as in *Alioramus altai*, or absent, as in *Daspletosaurus*. In *Albertosaurus*, the position of the pneumatopore varies between individuals: whereas the position of the pneumatopore is similar to that of *Gorgosaurus* in one specimen (TMP 1986.64.1), it opens medially from within the medial fossa of the pterygoid ala in another specimen (TMP 81.10.1). It is unclear if this variability observed in *Albertosaurus* is pathological.

Palatine—Only the vomeropterygoid processes of the left palatines are visible in lateral view in both TMP 2009.12.14 and TMP 2016.14.1 (Fig. 3.1). To compensate for the limited visibility of the element, the palatine of TMP 2009.12.14 was digitally rendered from CT scans for additional detail. The palatine of TMP 2009.12.14 is longer relative to height than those of larger albertosaurine individuals (TMP 2009.12.14 height/length ratio =0.35; adult *Albertosaurus* TMP 1981.10.1 = 0.43). The palatine of juvenile *Gorgosaurus* individuals, TMP 2009.12.14 and TMP 2016.14.1, deviate from the typical albertosaurine morphology in possessing a rostrally inclined

vomeropterygoid neck (Fig. 3.13a) rather than the dorsally-projecting neck seen in large albertosaurines and one juvenile *Gorgosaurus* specimen (TMP 1986.144.1; Fig. 3.13c). The palatine of TMP 1994.143.1 is intermediate between the immature and adult morphologies and exhibits a slight rostral inclination in the right palatine (Fig. 3.13b) but a dorsal inclination in the left. Interestingly, the orientation of the vomeropterygoid process in TMP 2009.12.14, TMP 2016.14.1, and TMP 1994.143.1 may represent the ancestral condition as it is present in all non-albertosaurine tyrannosauroids (Brusatte and Carr, 2016; Car ret al., 2017).

The palatines of tyrannosaurids are pneumatic and perforated by two pneumatopores located on the lateral surface of the bone. In TMP 2009.12.14 and other tyrannosaurids, the rostral pneumatopore opens rostrally into a triangular fossa on the maxillary process of the palatine (Fig. 3.13). This fossa is large in albertosaurines of all growth stages, where it extends across most of the maxillary process, but short in tyrannosaurines (e.g. *Daspletosaurus torosus*, TMP 2001.36.1). The caudal pneumatopore is roughly circular to oval in shape and opens laterally directly below the vomeropterygoid process. The caudal pneumatopore is large in albertosaurines of all growth stages, but expands to cover almost half the breadth of the vomeropterygoid neck in large individuals (Fig. 3.13c; Carr, 2010). In tyrannosaurines the caudal pneumatopore is small, occupying a third or less of the basal width of the vomeropterygoid neck (Carr, 2010; Gold et al., 2013).

Vomer—Articulation of the skulls bones prevents observation of the vomer in both TMP 2009.12.14 and TMP 2016.14.1 but it was digitally reconstructed based on CT scans in TMP 2009.12.14 (Fig. 3.14). The vomer of TMP 2009.12.14 possesses a lanceolate rostral process with parallel lateral margins. In adult *Gorgosaurus* (e.g TCM 2001.89.1, TMP 2000.12.11), the rostral process is expanded into a narrow diamond shape in dorsal and ventral views (Larson,

2013: fig. 2.8), supporting a subtle ontogenetic widening of the rostral process. Similar differences are observed between juvenile and adult individuals of *Tyrannosaurus* rex and *Tarbosaurus bataar*, where the rostral process of immature individuals is lanceolate with parallel lateral margins and that of adult individuals is wide and diamond-shaped (Witmer and Ridgely, 2010; Larson, 2013). This difference has been regarded by some as indicative of taxonomic variation between two taxa, i.e. *Nanotyrannus lancensis* and *Tyrannosaurus rex* (Larson, 2013), but are more likely to reflect different ontogenetic stages (sensu Tsuihiji et al., 2011). The difference in rostral process width between *Gorgosaurus* and *Tyrannosaurus*/*Tarbosaurus* may reflect the wider rostrum of the latter.

Previous studies have indicated that the vomer of *Gorgosaurus* was lacking a ventrally projecting keel caudal to the rostral process (Carr et al., 2017). However, the vomer of several specimens of *Gorgosaurus* possess such a keel (e.g. TMP 2009.12.14, TMP 2000.12.11, and TCM 2001.89.1; Fig. 3.14a), whereas only one specimen (ROM 1247) lacks it. Recoding of this feature for *Gorgosaurus* would change its occurrence from being an autapomorphy of *Albertosaurus sarcophagus* to being a synapomorphy of Albertosaurinae.

Pterygoid— In TMP 2009.12.14, the pterygoid is straight and slender between the basipterygoid and palatal articulations, with roughly parallel dorsal and ventral margins (Fig. 3.15). This region exhibits a slight dorsal arc in a subadult *Gorgosaurus* specimen (TMP 1994.143.1) and is unknown in adult *Gorgosaurus* individuals. In large tyrannosaurids (e.g. *Albertosaurus* TMP 1981.10.1 [Currie, 2003: fig. 13], *Daspletosaurus torosus* TMP 2001.36.1), the pterygoid bar is more robust and is strongly bowed between the basipterygoid and palatal articulations.

The quadrate process of the pterygoid in young *Gorgosaurus* (e.g. TMP 2009.12.14, TMP 1994.143.1) is oriented dorsolaterally at almost ninety-degrees to the pterygoid bar (Fig. 3.15b),

as in other tyrannosaurids. However, Currie (2003a) noted a much shallower angle between the quadrate process and pterygoid bar in a large specimen of *Albertosaurus sarcophagus* (TMP 1981.10.1), suggesting this morphology reflected a narrower cranium in albertosaurines than in large tyrannosaurines. Re-examination of this specimen indicates the quadrate ramus was broken from the pterygoid bar and was re-attached during preparation at an incorrect angle (~180° from the pterygoid bar). Because the angle between the quadrate process and pterygoid bar in TMP 2009.12.14 and TMP 1994.143.1 is consistent with that of tyrannosaurines, it is unlikely that this angle has any bearing on the temporal width of the skull in tyrannosaurids.

Ectopterygoid—The jugal ramus of the ectopterygoid is slender and uninflated in TMP 2009.12.14, as occurs in ancestral tyrannosauroids. In larger *Gorgosaurus* (e.g. TMP 2015.12.70), the jugal ramus of the ectopterygoid is slightly swollen due to inflation of the internal ectopterygoid sinus. Inflation of the jugal ramus is exaggerated in large tyrannosaurines, in which swelling of the jugal ramus is apparent (Carr, 1999; Carr et al., 2005, 2017; Currie, 2003a).

Mandible

Due to the articulation of the skull, CT scans were used to reconstruct and describe most of the mandibular elements in TMP 2009.12.14. The lack of CT scans for TMP 2016.14.1, allowed for examination of the exposed left dentary and surangular only. Tyrannosaurid mandibles are comprised of the dentary, supradentary–coronoid, surangular, articular, angular, prearticular, and splenial bones. In general, mandibular bones are conservative in morphology, exhibiting few differences among tyrannosaurid taxa. Because of this, isolated tyrannosaurid mandibular elements from the Dinosaur Park Formation are difficult to assign to a precise taxon, with identifiable bones being primarily the dentary, surangular, angular, and sometimes prearticular.

Combined with the lack of taxonomically diagnostic characteristics, the scarcity of adult tyrannosaurid mandibular material prevents an in-depth comparison of the ontogenetic changes of *Gorgosaurus* mandibles. For this study, the largest definitive and relatively complete *Gorgosaurus* mandible is from the subadult specimen ROM 1247.

Dentary—The dentary of tyrannosaurids undergoes a significant increase in depth relative to length through ontogeny (Carr, 1999; Currie and Zhiming, 2001; Currie, 2003a). In *Gorgosaurus*, the dentary is long and slender in juvenile individuals (e.g. TMP 2009.12.14 and TMP 2016.14.1; Fig. 3.16a) and short and deep in large individuals (e.g. ROM 1247; TMP 1994.12.602; Fig. 3.16b). Measurements of the depth of the mandibular symphysis and length of the alveolar row provide a depth-to-length ratio of 0.18 and 0.20 for TMP 2009.12.14 and TMP 2016.14.1, respectively, whereas the depth-to-length ratio is 0.25 for larger *Gorgosaurus* specimens (TMP 1994.12.602).

Some researchers have argued that the presence of a dentary groove (sensu Schmerge and Rothschild, 2016a,b) can be used for taxonomic identification in tyrannosaurids (Schmerge and Rothschild, 2016a, 2016b; Rothschild and Naples, 2017), whereas others have questioned its taxonomic utility, arguing that the depth of this feature is ontogenetically variable and even variable at an individual level (Brusatte et al., 2016). Examination of several *Gorgosaurus* dentaries in the context of this study confirms that a dentary groove is present in most specimens but that it varies in depth with ontogenetic stage and between individuals. In juvenile individuals, the dentary groove is deep and decreases in depth rostrally (e.g. TMP 2009.12.14, TMP 2016.14.1), is distinct in TMP 1986.144.1, and is absent in TMP 1999.55.170. In large *Gorgosaurus* specimens, the dentary groove is generally shallow (e.g. TMP 1983.36.134) but may be completely absent (e.g. TMP 2000.12.11). Variation in the expression of the dentary

groove is also seen in *Albertosaurus sarcophagus*, where many specimens lack a dentary groove altogether (e.g. TMP 1999.50.40 [juvenile], TMP 2003.45.84 [adult]) but it is present in others (e.g. TMP 1986.64.1 [subadult]). In small tyrannosaurines the dentary groove is typically present and distinct but is indistinct or absent in larger individuals. The highly variable nature of the dentary groove in albertosaurines indicates that it is not phylogenetically informative within Tyrannosauridae, contra Schmerge and Rothschild (2016a, 2016b; also see Rothschild and Naples, 2017), and is instead more closely linked to ontogenetic stage (see Brusatte et al., 2016).

Supradentary-Coronoid—The supradentary and coronoid elements are indistinguishably fused in tyrannosaurids. Subadult or adult *Gorgosaurus* supradentary–coronoid elements could not be examined in the context of this study. The supradentary is a dorsally concave, scimitar-shaped bone that forms the ventromedial brace for the dentary tooth row (Fig. 3.17). The supradentary of TMP 2009.12.14 is shallow relative to that of larger tyrannosaurids (e.g. *Tyrannosaurus rex* [Brochu, 2003], *Daspletosaurus* TMP 2001.36.1), being deepest below the tenth alveolus. The supradentary extends rostrally from the twisted coronoid partition, located medial to the dorsal dentary-surangular articular facet, to the fourth alveolus, whereas in a *Tyrannosaurus* specimen the supradentary extends to the third alveolus (Brochu, 2003).

Surangular— The surangular of TMP 2009.12.14 and TMP 2016.14.1 is shallower than that of larger individuals (Carr, 1999) and deeper than that of smaller individuals (e.g. TMP 1994.12.155 [Currie and Dong, 2001], TMP 2001.12.2; Fig. 3.16). The caudal surangular foramen is small, as in other immature tyrannosaurids (Carr, 1999). At the caudal margin of the surangular foramen, the surangular is perforated by a second, smaller foramen in *Gorgosaurus*, as in *Tyrannosaurus rex* and *Alioramus altai* (Brusatte et al., 2012; Gold et al., 2013).

Articular—The articular was digitally reconstructed for TMP 2009.12.14 based on CT scans (Fig. 3.17). A definitive adult *Gorgosaurus* articular was not available for comparison. Articulation with the more rostral prearticular is mostly obliterated but the two appear to contact each other for most of the dorsoventral depth of the articular. A dorsomedially oriented foramen, the chorda tympani (Currie, 2003a), is located behind the glenoid fossa, as in *Tyrannosaurus* and *Alioramus* (Brochu, 2003; Currie, 2003a; Gold et al., 2014), and connects to a small pneumatic chamber.

Prearticular—Tyrannosaurid prearticulars are U-shaped, flattened at both the caudal and rostral ends, and thickened along the mid-region where it forms the ventral contours of the mandible in tandem with the surangular and angular (Currie, 2003b; Fig. 3.17).

The mid-region of the prearticular in TMP 2009.12.14 is constricted, as in TMP 1986.144.1 (Carr, 1999). This region becomes expanded in larger juvenile individuals (TMP 1994.143.1) and in subadult individuals (ROM 1247).

Angular—The angular of TMP 2009.12.14 is shallow relative to the angular of larger individuals (e.g. TMP 1994.143.1), but tapers rostrally as in other tyrannosaurids (Brochu, 2003; Currie, 2003b). A small, ventrally protruding knob is situated between and marks the the caudal-most points of the dentary and splenial in TMP 2009.12.14 (Fig. 3.17). In contrast, most other tyrannosaurid specimens, including other *Gorgosaurus*, lack such a distinct knob and instead possess a shallow pocket on the lateral surface of the angular. The prominence of this knob in TMP 2009.12.14 likely represents individual variation.

Splenial—The caudal process of the splenial in TMP 2009.12.14 is slightly shallower than that of larger tyrannosaurids. The mylohyoid foramen is completely enclosed with the ventral margin being formed by theconjunction of unfused rostral and caudal processes (Fig. 3.16). Although it

is possible that the closure of this foramen varies with ontogeny, as hypothesized by Currie and Zhiming (2001), more recent findings suggest individual variation may play a more significant role (Tsuihiji et al., 2011).

Braincase and Skull Roof

The absence of the lacrimal, postorbital, quadratojugal, quadrate, jugal, and epipterygoid on the right side of the skull of TMP 2009.12.14 exposes the braincase in lateral view. Due to the complete articulation of the specimen, the braincase of TMP 2016.14.1 is not exposed and only examination of the frontals and parietals is possible. For identification of ontogenetic changes, other *Gorgosaurus* braincases were examined, including: juvenile (TMP 1994.143.1), subadult (ROM 1247), and adult (TMP 1994.12.602) specimens. Some features were also documented using the braincase of an adult *Albertosaurus* specimen, TMP 1981.10.1.

Frontal—The frontal of TMP 2009.12.14 and TMP 2016.14.1 is elongated and triangular in dorsal view, with a length-to-width ratio of 2.33-2.67 (left frontal of TMP 2009.12.14 is slightly mediolaterally compressed) indicating a narrow temporal region of the skull in these specimens (Fig. 3.7a, 3.17a). The frontal has a largely constant width throughout the postorbital articular surface but is marginally widest at its rostral end (Fig. 3.18). In the largest albertosaurines (e.g. TMP 1981.10.1: Fig. 3.18c, d)) as well as in *Teratophoneus* (Loewen et al., 2013: fig. 3), the frontal is significantly wider at the rostral end of the postorbital articular surface than anywhere else. The frontal of large *Gorgosaurus* individuals is wider than that of juvenile individuals, (e.g. TMP 1994.12.602, l:w= 1.85[L], 1.81[R]; Currie, 2003a). These metrics are consistent with an ontogenetic increase in frontal width, which has been noted in previous studies of tyrannosaurid ontogeny, and co-occurs with a wider temporal region (Carr, 1999; Currie, 2003a; Carr and Williamson, 2010; Tsuihiji et al., 2011). In other tyrannosaurids, in contrast, the frontal is either

widest at the caudal end of the postorbital contact (e.g. *Alioramus* [Bever et al., 2013:fig. 2], *Lythronax* [Loewen et al., 2013:fig. 2], *Daspletosaurus* [Carr and Williamson, 2004: fig. 8]) or is of roughly constant width across this contact, such that the postorbital region of the frontal is rectangular in dorsal view (e.g. *Tarbosaurus* [Tsuihiji et al., 2011: fig. 5], *Tyrannosaurus* [Carr and Williamson, 2004: fig. 8]).

Caudomedially, the frontal rises into a sagittal crest that is deep in TMP 2009.12.14 and shallow in TMP 2016.14.1. The height of the sagittal crest in TMP 2009.12.14 and another immature individual, TMP 1994.143.1, is most likely the result of mediolateral compression but may also relate to the individual variation. Ontogenetic variation in the size and even presence of the sagittal crest has been noted previously in other tyrannosaurids, such as in *Tyrannosaurus* and *Tarbosaurus*, where the youngest and smallest specimens lacked a frontal sagittal crest and larger juveniles possessed a shallow crest (Carr, 1999; Currie, 2003a; Carr and Williamson, 2004; Tsuihiji et al., 2011).

The frontal exhibits a distinct supratemporal ridge that extends from the rostral corner of the postorbital contact to the sagittal crest and marks the rostral extent of the supratemporal fossa. In TMP 2009.12.14, TMP 2016.14.1, and other juvenile *Gorgosaurus* individuals, the supratemporal ridge is prominent and extends rostrolaterally to the frontal-postorbital suture (Fig. 3.18a). In larger juvenile and subadult *Gorgosaurus* specimens (e.g. TMP 1994.143.1), the supratemporal ridge is less prominent than in juveniles, extends primarily laterally, and is sigmoidal in dorsal view (Fig. 3.18b–d; also see Tsuihji et al., 2011: fig. 5e, f).

The supratemporal fossa of TMP 2009.12.14 and TMP 2016.14.1 is flat, contrasting with the shallow fossa of larger juvenile individuals (e.g. TMP 1991.36.500, TMP 1994.143.1) and the deep fossa of subadult and adult *Gorgosaurus* (e.g. ROM 1247, TMP 1994.12.602; sensu Carr,

1999). In exceptionally small tyrannosaurids (e.g. *Tarbosaurus*, MPC-D 107/7), the supratemporal fossa is also referred to as being flat (Tsuihiji et al., 2011), but it appears dorsally convex (Tsuihiji et al, 2011: fig. 2a, 10c) which may represent an early ontogenetic feature.

Parietal—The caudal region of the parietal in tyrannosaurids is raised into a distinct, transversally-oriented nuchal crest that perpendicularly intersects the narrow midline sagittal crest (Currie, 2003a). While the nuchal crest of TMP 2016.14.1 is broken, that of TMP 2009.12.14 is low, being only slightly taller than the rostral apex of the sagittal crest, and narrow, and the crest lamina is thin (Fig. 3.7a). The nuchal crest is taller, wider, and thicker in larger albertosaurines (e.g. TMP 1981.10.1). In comparison, the nuchal crest is even more robust in large tyrannosaurines, which possess a tall and thick nuchal crest that extends well beyond the dorsal margin of the skull roof (Currie, 2003a; Tsuihiji et al., 2011; Fig. 3.7b), presumably to facilitate the insertion of larger neck muscles (Tsuihiji et al., 2010).

In TMP 2009.12.14, the frontoparietal suture is mediolaterally-oriented near its lateral margin. Closer to the midline, the suture is rostrocaudally-oriented, with a wide, finger-like process of the parietal that inserts between contralateral sagittal crests of the frontals (observed via CT scans). In larger specimens of *Gorgosaurus* (e.g. ROM 1247, TMP 1994.12.602) and *Albertosaurus* (TMP 1981.10.1), the finger-like process of the parietal is expanded into a wedge that articulates with the frontals along a caudolaterally oriented suture (Fig. 3.7, 3.17). Several juvenile specimens of other tyrannosaurid taxa, including *Alioramus* (IGM 100/1844; Bever et al., 2013) and *Tyrannosaurus* (LACM 28471; Carr and Williamson, 2004), possess a narrow, finger-like rostral process of the parietal but this process is extremely narrow and "mushroom-like" in the youngest tyrannosaurids (e.g. *Tarbosaurus* MPC-D 107/7; Tsuihiji et al., 2011:510). In large specimens of *Daspletosaurus* and *Tyrannosaurus*, the frontoparietal suture is typically

transverse (Carr and Williamson, 2004) and invasion of the parietal between the frontals is minimal.

Prootic—In tyrannosaurids, the rostral and dorsal regions of the prootic form the lateral wall for the rostral tympanic recess (Bever et al., 2013). In TMP 2009.12.14, other juvenile individuals, and subadult *Gorgosaurus* (e.g. ROM 1247; TMP 1994.143.1), the dorsal region of the prootic is slightly convex and the rostral tympanic recess is largely uninflated (Fig. 3.19a–c). In contrast, the dorsal region of the prootic in the large adult specimen TMP 1994.12.602 is convex and swollen due to significant expansion of the rostral tympanic recess, which forms an elongate bulge along the dorsal extent of the prootic (Fig. 3.19d). Similar to the adult *Gorgosaurus*, the dorsal region of the prootic in large *Daspletosaurus* (CMN 8506) and *Tyrannosaurus* (AMNH FARB 5117) is also inflated.

In tyrannosaurids, the superficial lamina of the prootic extends caudoventrally below the tongue-shaped caudal process of the prootic and distally bifurcates into two tapered points (Bever et al., 2013). In TMP 2009.12.14 and other juvenile and subadult specimens (e.g. ROM 1247, TMP 1994.143.1), the superficial lamina sits within a shallow fossa bounded by the weakly convex rostral and dorsal regions (Fig. 3.19a–c). At the extreme rostrodorsal corner of this fossa, the foramina for the maxillomandibular branch of the trigeminal nerve (V_{2-3}) and facial nerve (VII) are located within a small, laterally-directed secondary fossa on the lateral surface of the prootic, a condition also seen in *Alioramus altai* (IGM 100/1844; Bever et al., 2013) and a juvenile *Tarbosaurus bataar* (MPC-D107/7; Tsuihiji et al., 2011). In contrast, in larger *Gorgosaurus* individuals, the superficial lamina is situated within a deep fossa due to extensive inflation of the rostral and dorsal regions of the prootic (Fig. 3.19d). Also due to the swollen nature of these regions, the maxillomandibular and facial nerves are re-directed

caudoventrally and exit through a single large foramen (e.g. TMP 1994.12.602), similar to the condition observed in other large tyrannosaurids (Witmer and Ridgely, 2009; Tsuihiji et al., 2011).

Laterosphenoid—The laterosphenoid exhibits a prominent, laterally protruding capitate process located ventrolateral to the frontoparietal suture. In TMP 2009.12.14, the ventral edge of the capitate process is marked by a pronounced antotic crest, which extends ventrally for a short distance before bifurcating into a dorsal and rostroventral ridge around the shallow, epipterygoid fossa which serves as the articulation site of the epipterygoid (Witmer and Ridgely, 2009; Bever et al., 2013). The rostroventral ridge of the antotic crest is indistinct and the dorsal ridge is pronounced just above the epipterygoid fossa but does not extend caudally onto the prootic as the otosphenoidal crest, as in *Alioramus*, *Daspletosaurus*, and *Tyrannosaurus* (Bever et al., 2013). In larger albertosaurines (e.g. TMP 1994.12.602), the rostroventral ridge of the antotic crest is more distinct, forming a greater separation of the orbital and temporal spaces but the the dorsal ridge and otosphenoidal crest are only subtly prominent (sensu Bever et al., 2013; Fig. 3.19d). The rostroventral branch of the antotic crest is rugose and more distinct in large tyrannosaurines (e.g. *Tyrannosaurus*, *Daspletosaurus*) than in large *Gorgosaurus* (Carr and Williamson, 2010; Brusatte et al., 2010; Bever et al., 2013; Brusatte and Carr, 2016; Carr et al., 2017).

In all specimens of *Gorgosaurus*, the epipterygoid fossa is distinctly D-shaped. In contrast, the epipterygoid fossa is triangular in *Albertosaurus sarcophagus* (TMP 1981.10.1), *Tyrannosaurus* (AMNH FARB 5117), *Daspletosaurus* (CMN 8506) and *Alioramus* (Bever et al., 2013).

Parabasisphenoid—The parabasisphenoid of TMP 2009.12.14 possesses a long and low cultriform process with a shallow ventral curvature (Fig. 3.19a). Comparison of the length (i.e., from the sella turcica to the tip of the cultriform process) and height (i.e., from the sella turcica to

the basipterygoid process) of the element provides a ratio of 0.89 for TMP 2009.12.14 whereas the parabasisphenoid is deeper in larger albertosaurines (0.73 in the larger juvenile *Gorgosaurus* TMP 1994.143.1, and 0.47 in an adult *Albertosaurus sarcophagus* TMP 1981.10.1). As a result of this increased height, the cultriform process is rostrocaudally short and strongly curved along the ventral margin in subadult and adult *Gorgosaurus* individuals (e.g. TMP 1994.143.1, TMP 1994.12.602, TMP 1981.10.1; Fig. 3.19b–d). Similar to juvenile *Gorgosaurus*, the cultriform process of *Alioramus altai* and juvenile *Tyrannosaurus* is also elongated with a shallow ventral curvature (Witmer and Ridgely, 2010; Bever et al., 2013). In large *Tyrannosaurus* specimens, however, the cultriform process is deep with a strongly sweeping ventral curvature (Witmer and Ridgely, 2010).

The preotic pendant (crista prootica of Brochu, 2003) is a caudoventrolaterally-directed wing-like projection that forms the rostroventral wall of the rostral tympanic recess and is the site of origin of the pterygoideus muscle (Holliday and Witmer, 2008; Bever et al., 2013). The preotic pendant of TMP 2009.12.14 is short and crest-like, lacking the ventrally extending "wing" observed in subadult/adult individuals (e.g. TMP 1994.12.602; Fig. 3.19a, d). A similarly shortened preotic pendant was noted in the juvenile *T. rex* CMNH 7541, which reflects the immaturity of the specimen as larger specimens have a deeply extended pendant (Witmer and Ridgley, 2010).

The preotic pendant varies in its bony components among tyrannosaurids, although generally it receives significant contributions from the prootic (see Bever et al., 2013). In *Gorgosaurus* (TMP 2009.12.14, TMP 1994.143.1, TMP 1994.12.602), it is almost completely formed by the parabasisphenoid, receiving only minor contribution from the prootic more dorsally (Currie, 2003a). The suture between the parabasisphenoid and prootic is obvious in juvenile *Gorgosaurus*

TMP 2009.12.14 and TMP 1994.143.1, but it is difficult to discern in the larger adult TMP 1994.12.602 due to a greater degree of fusion among the bones of the braincase.

Supraoccipital—The supraoccipital is an unpaired and narrow element located on the dorsal occipital surface of the skull, where it extends dorsally from the foramen magnum and fuses with the caudal surface of the nuchal crest. In TMP 2009.12.14, the supraoccipital is tall relative to the height of the nuchal crest, extending dorsoventrally for nearly three-quarters of the total height of the crest. This contrasts with the observed condition in most large tyrannosaurid specimens, including subadult and adult *Gorgosaurus* (e.g., ROM 1247), where the supraoccipital is less than half the total height of the nuchal crest (Bever et al., 2013; Fig. 3.20). Similar to TMP 2009.12.14, the supraoccipital of the immature *Alioramus altai* holotype (IGM 100/1844) extends dorsally for more than half the total height of the nuchal crest (Bever et al., 2013). These differences between younger and more mature tyrannosaurids suggest the height of the nuchal crest relative to that of the supraoccipital changes through ontogeny. Ontogenetic change in the size of the nuchal crest may affect the surface area for the attachment of the cranial dorsiflexor muscles, which may have implications for ontogenetic shifts in feeding behavior or neck muscle strength/mobility (Snively and Russell, 2007; Tsuihiji, 2010).

The supraoccipital of *Gorgosaurus* is inflated by a tall diverticulum of the caudal tympanic recess (the supraoccipital pneumatic sinus of Witmer and Ridgely [2009]), which extends much further dorsally than the other diverticula of this recess. In TMP 2009.12.14, inflation of the supraoccipital is minimal as the sinus is narrow. In larger *Gorgosaurus* individuals, the caudal surface of the bone is distinctly swollen and appears as a wide ridge on the caudal surface of the nuchal crest (e.g. TMP 1994.12.602: Fig. 3.20c). The morphology of supraoccipital inflation in *Gorgosaurus* is similar to that of *Alioramus* and *Daspletosaurus* but differs from that of

Tyrannosaurus. In *Tyrannosaurus*, the inflated region of the supraoccipital is shallow at all growth stages. This may be in part due to the unique morphology of the supraoccipital of *Tyrannosaurus* and *Tarbosaurus* (see below; Carr et al., 2017).

A pair of caudally-projecting tabs are present on the caudodorsal margin of the supraoccipital in most tyrannosaurids (Bever et al., 2013), including TMP 2009.12.14. These tabs are prominent, narrow, and separated by a flat region in TMP 2009.12.14. In contrast, in larger *Gorgosaurus* (e.g. TMP 1994.12.602), these tabs are wide and separated by a shallow pocket. Among tyrannosaurines, the tabs are separated by a deep concavity in *Daspletosaurus* (see Tsuihiji, 2010: fig 14c, e), whereas the dorsal region of the supraoccipital is completely bifurcated into two dorsally ascending processes that lack tabs in *Tyrannosaurus* and *Tarbosaurus* (Carr, 1999; Hurum and Sabath, 2003). In *Gorgosaurus*, the flattened dorsal surface of the tabs are perforated by small pneumatic foramina that communicate with the supraoccipital pneumatic sinus. It is unknown if the tabs of other tyrannosaurids possess such foramina.

Otoccipital—The exoccipital and opisthotic elements are indistinguishably fused into the paired otoccipitals, which laterally extend as elongated paroccipital processes in tyrannosaurids (Currie, 1997). In TMP 2009.12.14, the paroccipitals are short in their caudolateral extent, such that ratio of the length of these processes relative to the basioccipital length of the skull is 0.13 (Fig. 3.7a). In contrast, the paroccipital processes of the larger adult *Gorgosaurus* TMP 1994.12.602 are caudolaterally longer (Fig. 3.7b), resulting in a process length-to-skull length ratio of 0.19. The distal end of the paroccipital process in TMP 2009.12.14 exhibits a strong ventral inflection, but lacks the distinct dorsal inflection seen in the fan-shaped distal ends of larger *Gorgosaurus* (e.g. TMP 1994.12.602).

The otoccipital forms most of the margin of the foramen magnum, which also receives minor contributions from the dorsally positioned supraoccipital and, in some cases, the basioccipital (see below). On the occipital condyle, the otoccipital-basioccipital contact can be identified by a laterally sloping scarf joint in all tyrannosaurids (Currie, 2003a). The foramen magnum is oval in TMP 2009.12.14 due to compression but circular in the undeformed and larger individuals TMP 1994.12.602 and ROM 1247. This condition contrasts with that seen in the holotype specimen of *Alioramus altai* (IGM 100/1844) and one specimen of *Tyrannosaurus* (AMNH FARB 5117), which possess a projection into the margin of the foramen magnum (Bever et al., 2013). The absence of this feature in other tyrannosaurids suggests this projection may represent individual variation or taphonomic deformation (Bever et al, 2013; Lu et al., 2014: fig. 2a).

Tyrannosaurid paroccipital processes are highly pneumatic, housing most diverticula of the caudal tympanic recess in addition to a small portion of the rostral tympanic recess (e.g. Witmer and Ridgley, 2009, 2010; Bever et al., 2013). As with the prootic, the lateral and caudal surfaces of the paroccipital processes in TMP 2009.12.14 are not significantly inflated (Fig. 3.19a). This condition contrasts with that of larger *Gorgosaurus* (e.g. TMP 1994.12.602), in which the dorsal two-thirds of the paroccipital process are inflated and the ventral one-third extends rostrocaudally as a distinct ventral flange, a feature also observed in many other large tyrannosaurids (Brochu, 2003; Hurum and Sabath, 2003; Witmer and Ridgely, 2009; Bever et al., 2013; Fig. 3.7b, 3.18d, 3.19c). The absence of both a ventral flange and inflated paroccipital processes in TMP 2009.12.14 and their presence in TMP 1994.12.602 suggests they are acquired through ontogeny and are associated with the expansion of the tympanic sinuses.

Two foramina, corresponding to the canals for the vagus (CN X) and hypoglossal (CN XII) cranial nerves, pierce the caudal surface of the otoccipital between the occipital condyle and

paroccipital processes in a depression referred to as the paracondylar pocket (Bever et al., 2013). In TMP 2009.12.14, the medial-most and circumferentially larger foramen, which opens laterally from the neck of the occipital condyle, is for the hypoglossal nerve whereas the foramen for the vagus nerve is located ventrolateral to the hypoglossal foramen. In the adult *Gorgosaurus* individual TMP 1994.12.602, a caudodorsal shelf directs the opening of the hypoglossal foramen ventrolaterally. The relative positions and sizes of these foramina in *Gorgosaurus* are similar to *Tyrannosaurus rex* (AMNH FARB 5117) but different from those of *Alioramus altai*, in that the vagus foramen is larger and positioned dorsolateral to the hypoglossal foramen (Bever et al., 2013). A third, more ventrally-positioned foramen in TMP 1994.12.602 communicates with the lateral subcondylar recess and is therefore likely a pneumatopore.

Basioccipital—The basioccipital forms most of the occipital condyle and, more ventrally, the medial portion of the basal tubera. On the lateral surface of the basal tubera in TMP 2009.12.14, the basiocciptal contacts the parabasisphenoid and otoccipital to form an open tripartite suture (Fig. 3.19a). This suture appears as a narrow gouge on the ventrolateral surface of the braincase in juvenile and subadult specimens of various Tyrannosauridae (e.g. *Gorgosaurus*: TMP 2009.12.14, TMP 91.36.500, ROM 1247; *Tyrannosaurus*: CMNH 7541). This gouge is closed in adult individuals of *Gorgosaurus* (TMP 94.12.602), *Albertosaurus sarcophagus* (TMP 1981.10.1) and other tyrannosaurids (e.g. *Daspletosaurus torosus* CMN 8506, *Tyrannosaurus* AMNH FR 5117), resulting in an uninterrupted parabolic arc around the basal tubera (Fig. 3.20c). In TMP 2009.12.14, the basioccipital does not contribute to the margin of the foramen magnum due to the complete closure of the left and right otoccipitals on the occipital condyle. In the larger adult individual TMP 1994.12.602, the basioccipital has a narrow contribution to the ventral margin of the foramen magnum because the left and right otoccipitals do not come in

contact on the occipital condyle. The extent of the contribution of the basioccipital to rim of the foramen magnum is largely unknown in other large tyrannosaurids due to fusion of the otoccipital and basioccipital on the occipital condyle.

3.4 DISCUSSION

Ontogenetic changes in skull proportions

The skulls of the two juvenile *Gorgosaurus*, TMP 2009.12.14 and TMP 2016.14.1, are long and shallow relative to that of large individuals, indicating an ontogenetic increase in skull depth in this taxon. This trend is well documented for all tyrannosaurid taxa which possess a growth series (Carr, 1999; Currie, 2003a, b; Carr and Williamson, 2004; Carr and Williamson, 2010; Tsuihiji et al., 2011).

The ontogenetic increase in skull depth is also apparent in the shape changes that occur in the various cranial fenestrae of *Gorgosaurus*. For example, the antorbital fenestra is longer than tall in juvenile individuals (e.g. TMP 2009.12.14 and TMP 2016.14.1) but is nearly equal in proportions in larger individuals (e.g. AMNH 5664; see Carr, 1999). The orbital fenestra of the juveniles is large relative to the skull and circular in shape. In these individuals, the eyeball would have occupied most of the orbit, as in other juvenile tyrannosaurids (Currie, 2003a). In contrast, the orbital fenestra of larger *Gorgosaurus* is small relative to skull size, comma-shaped, and tall (Currie, 2003a, b). The eyeball would have been positioned in the dorsal, semicircular, portion of the orbital fenestra, and bounded ventrally by the suborbital process of the postorbital. Despite the difference in height of the orbital fenestra between juvenile and mature *Gorgosaurus*, the rostrocaudal length of the orbital fenestra in TMP 2009.12.14 and TMP 2016.14.1 is similar to that of the eyeball-bearing portion of the fenestra in more mature individuals (e.g. UA 10).

In addition to increasing in depth, the skull of *Gorgosaurus* also undergoes an ontogenetic increase in width (Currie, 2003a). In juvenile individuals, the frontal bone and rostral ramus of the postorbitals are narrow and broaden in later growth stages, resulting in a wider temporal region (Carr, 1999; Currie, 2003a). This increase in temporal width likely aids in reinforcing the adductor chamber of the skull (in tandem with the increase in cranium depth), thereby allowing for greater bite forces to be achieved by larger individuals than by juveniles (Brusatte and Carr, 2016). An ontogenetic widening of the postorbital is also observed in tyrannosaurines, where the rostral ramus of juvenile *Daspletosaurus* (TMP 2013.18.11) and *Tyrannosaurus* (CMNH 7541) is narrower than that of adults. Also, because the rostral ramus of juvenile tyrannosaurines is wider than that of similar-sized juvenile *Gorgosaurus*, it may indicate that juvenile tyrannosaurines possessed wider skulls than juvenile albertosaurines.

Newly documented morphological changes during ontogeny

In the context of this research, previously unrecognized morphological changes through late stage ontogeny have been documented at the species, genus, subfamily, and family levels. These changes provide new insight into the acquisition of autapomorphic and synapomorphic characters states in tyrannosaurids and may have some bearing on determining the ancestral conditions of such features.

Gorgosaurus libratus—The ontogenetic development of the cornual process on the postorbital in *Gorgosaurus* is distinct from that of other tyrannosaurids (except perhaps from *Teratophoneus*). In juvenile individuals (e.g. TMP 1986.144.1, TMP 2009.12.14, TMP 2016.14.1), the cornual process is a flat or slightly raised, rough region of bone located adjacent to the orbit margin, a morphology similar to that seen in immature individuals of *Alioramus altai* and *Albertosaurus sarcophagus*. In slightly larger individuals (e.g. TMP 1991.36.500, TMP

1994.143.1), the cornual process is raised into a small lip with a weakly-developed caudal curl. Finally, in the largest individuals, the cornual process is large with a more extensive caudal curl that laps onto the smooth lateral surface of the dorsal bar, similar to *Teratophoneus curriei*. In other tyrannosaurids the cornual process undergoes an ontogenetic expansion to cover a larger portion of the dorsal bar but the process either does not curl caudally or migrates further from the orbital margin (e.g. *Daspletosaurus*).

Albertosaurinae—Several synapomorphies of the clade, which contains both *Albertosaurus* and *Gorgosaurus*, are observed to be ontogenetically acquired in *Gorgosaurus*. Although small juvenile specimens are not represented in the growth series of *Albertosaurus*, some ontogenetic differences in these same features are observed between subadult and adult specimens. These unique ontogenetic patterns include features of the skull relating to: 1) the morphology of the orbital slot and postorbital articular surface of the frontal, 2) the jugal-quadratojugal contact, 3) the postorbital-squamosal contact, and 4) the orientation of the vomeropterygoid process of the palatine.

Morphology of the orbital slot and postorbital articular surface of the frontal. The orbital slot of the frontal is long, rostrocaudally-oriented, and curved, and the width of the frontal is constant along the postorbital contact in juvenile albertosaurines (e.g. TMP 2009.12.14). In subadult individuals (e.g. ROM 1247), the orbital slot is slightly arced but mostly transverse in dorsal view and the frontal is slightly wider at the rostral end of the postorbital articular surface than elsewhere along its extent. In the largest albertosaurine individuals (e.g., TMP 1981.9.1), the orbital slot becomes completely transverse in dorsal view and the frontal is much wider at the rostral end of the postorbital articular surface than elsewhere along its length (as also seen in *Teratophoneus* [Loewen et al., 2013: fig. 3]).

Jugal-quadratojugal contact. The ventral margin of the jugal-quadratojugal contact is rostrocaudally oriented and straight in juvenile albertosaurines (e.g. TMP 1986.144.1, TMP 2009.12.14), but transitions to being rostrodorsally inclined at nearly 45° in large individuals (e.g. ROM 1247, TMP 2000.12.11; Carr et al., 2017: character 106).

Postorbital-squamosal contact. The transition between the squamosal-postorbital contact and dorsal margin of the postorbital is an uninterrupted convex arc in small juvenile *Gorgosaurus*, as is the condition of most tyrannosaurines. In slightly larger, juvenile albertosaurines, the rostral end of the squamosal is situated within a shallow emargination. In the largest albertosaurines, this emargination is deep representing the derived condition (also seen in *Teratophoneus*; Carr et al., 2017: character 114).

Orientation of the vomeropterygoid process of the palatine. In small juvenile specimens of *Gorgosaurus*, the vomeropteryogoid neck of the palatine is either rostrodorsally inclined (e.g. TMP 2009.12.14, TMP 2016.14.1), as in all non-albertosaurine tyrannosauroids, or dorsally inclined (e.g. TMP 1986.144.1). Transitional morphologies are observed in slightly larger juvenile specimens, in which one side exhibits a slight rostrodorsal inclination and the other a dorsal inclination (e.g. TMP 1994.143.1). In the largest albertosaurine specimens, the vomeropterygoid neck projects dorsally (e.g. AMNH 5336, TMP 1981.10.1; Carr et al., 2017: character 180).

Although the adult condition observed in the latter three features have been identified as synapomorphies of Albertosaurinae in previous phylogenetic analyses (e.g. Carr et al., 2017), they are here shown to be absent or otherwise variably expressed in immature individuals (e.g. TMP 1986.144.1, TMP 2009.12.14, TMP 2016.14.1) and to be acquired only in later growth stages.

Tyrannosauridae—In addition to those of Albertosaurinae, several synapomorphies of Tyrannosauridae are also absent in immature *Gorgosaurus*.

Lacrimal cornual process morphology. In most small juvenile specimens of *Gorgosaurus* the cornual process of the lacrimal is rounded and lacks a discrete apex (e.g. TMP 1986.144.1, TMP 2016.14.1). In larger individuals the cornual process is raised to a prominent apex (e.g. TMP 1994.143.1, TMP 1991.36.500, ROM 1247).

Postorbital process of jugal. In small juvenile specimens of *Gorgosaurus*, the lateral surface of the postorbital ramus of the jugal is flat. Larger individuals develop a pronounced ridge caudal to the postorbital articular surface which braces the postorbital–jugal contact and prevents overlapping of the two bones. The bracing of this joint increases cranial buttressing perhaps facilitating greater bite forces (Brusatte and Carr, 2016).

Ectopterygoid Inflation. In small juvenile *Gorgosaurus* specimens, the jugal ramus of the ectopterygoid is slender and uninflated (e.g. TMP 1986.144.1, TMP 2009.12.14). In larger individuals, the jugal ramus of the ectopterygoid is swollen due to expansion of the ectopterygoid sinus.

Other Ontogenetic Changes—The frontoparietal suture of the skull of tyrannosaurids is a complex joint that changes considerably through ontogeny and may be closely linked with the evolution of the high bite forces that have been documented in derived taxa (Therrien and Henderson, 2005; Brusatte and Carr, 2016). In very young *Tarbosaurus* (~2 years of age), the frontoparietal suture is mostly transverse except for a narrow, rostrally projecting, mushroom-shaped parietal wedge that inserts between the frontals (Tsuihiji et al., 2011). In addition, the sagittal crest does not extend onto the frontals. A similar morphology of this joint appears in the mid-upper Turonian Bissekty tyrannosauroid (*Timurlengia euotica*?), which appears to possess a

possess a narrow parietal wedge (or lack one altogether) and further lacks a frontal extension of the sagittal crest (Averianov and Sues, 2012: fig. 2). In juvenile tyrannosaurids (e.g. *Gorgosaurus*: TMP 2009.12.14; *Tyrannosaurus*: LACM 28471: Carr and Williamson, 2004), the parietal wedge is a wider finger-like process that is laterally concealed by a shallow sagittal crest of the frontal. In more mature individuals, the parietal wedge widens into a triangle-shape and the sagittal crest of the frontal increases in height. The widening of the parietal wedge may be linked to the development of the frontal sagittal crest, which increases the surface area for the insertion of mandibular adductor muscles.

Most of the differences observed between the braincase of TMP 2009.12.14 and of larger albertosaurines can be attributed to the expansion of various braincase sinuses. One of these changes occurs in the paroccipital process of the prootic and opisthotic bones. The paroccipital process in TMP 2009.12.14 and TMP 1994.143.1 is uninflated, narrow, and lacks a ventral flange (sensu Bever et al., 2013). In contrast, larger *Gorgosaurus* specimens (e.g. TMP 1994.12.602) possess a ventral flange due to the inflation of the dorsal two-thirds of the paroccipital process. A second ontogenetic change is related to the position of the foramina for the maxillomandibular (V_{2-3}) and facial nerves (VII). In juvenile tyrannosaurids (e.g., TMP 2009.12.14), the foramina for the maxillomandibular and facial nerves pierce the braincase laterally from within a shallow fossa. In contrast, inflation of the prootic engulfs the maxillomandibular and facial foramina and redirects them through a single caudoventrally-oriented foramen (Witmer and Ridgely, 2009; Tsuihiji et al., 2011). The ontogenetic transition from two distinct foramina to a single foramen for the maxillomandibular and facial nerves was also noted in *Tarbosaurus* (Tsuihiji et al., 2011), suggesting it may be widespread among tyrannosaurids.

Other ontogenetic changes that occur in the braincase of tyrannosaurids include the elongation of the paroccipital processes. In juvenile specimens, the paroccipital processes are short, and the distal ends are narrow. In larger juvenile and subadult individuals (e.g. ROM 1247, TMP 1994.143.1), the paroccipital processes are longer and the distal ends are expanded into a broad fan-shape. Elongation of the paroccipital processes and expansion of the distal ends is exaggerated in large adult individuals (e.g. TMP 1994.12.602). The increase in paroccipital process length may be associated with the ontogenetic increase in skull width.

Recapitulation of ancestral tyrannosauroid features in juvenile *Gorgosaurus*

The absence of some tyrannosaurid and albertosaurine features in juvenile *Gorgosaurus* and a presence of ancestral characters makes juvenile individuals appear more primitive than conspecific adults. For example, the shallow skull, rounded cornual process of the lacrimal, and absence of a ridge bracing the postorbital contact on the jugal, are features inconsistent with the morphology of mature tyrannosaurids, but typical characteristics of many non-tyrannosaurid tyrannosauroids (e.g. *Appalachiosaurus*). Moreover, the occurrence of these primitive features in large-bodied non-tyrannosaurid tyrannosauroids (e.g. *Appalachiosaurus*, *Bistahieversor*), suggests the ontogenetic acquisition of such characters is not a byproduct of increased body size, but rather a unique and peramorphic transition to the derived robust tyrannosaurid morphology. As many of these characters appear to be linked to increased cranial buttressing and loadbearing (sensu Brusatte and Carr, 2016), conceivably, the transition from a more gracile and primitive juvenile tyrannosaurid skull form reflects a change in ecological niche from predators of smaller and likely faster prey to those of presumably slower and larger prey (i.e. megaherbivores).


A.
5 CM
MUSEUM
B.

Figure 3.1. Skulls of two juvenile *Gorgosaurus* individuals in left lateral view: (A) TMP 2009.12.14; (B) TMP 2016.14.1. Lower scale bar equals 100 mm.

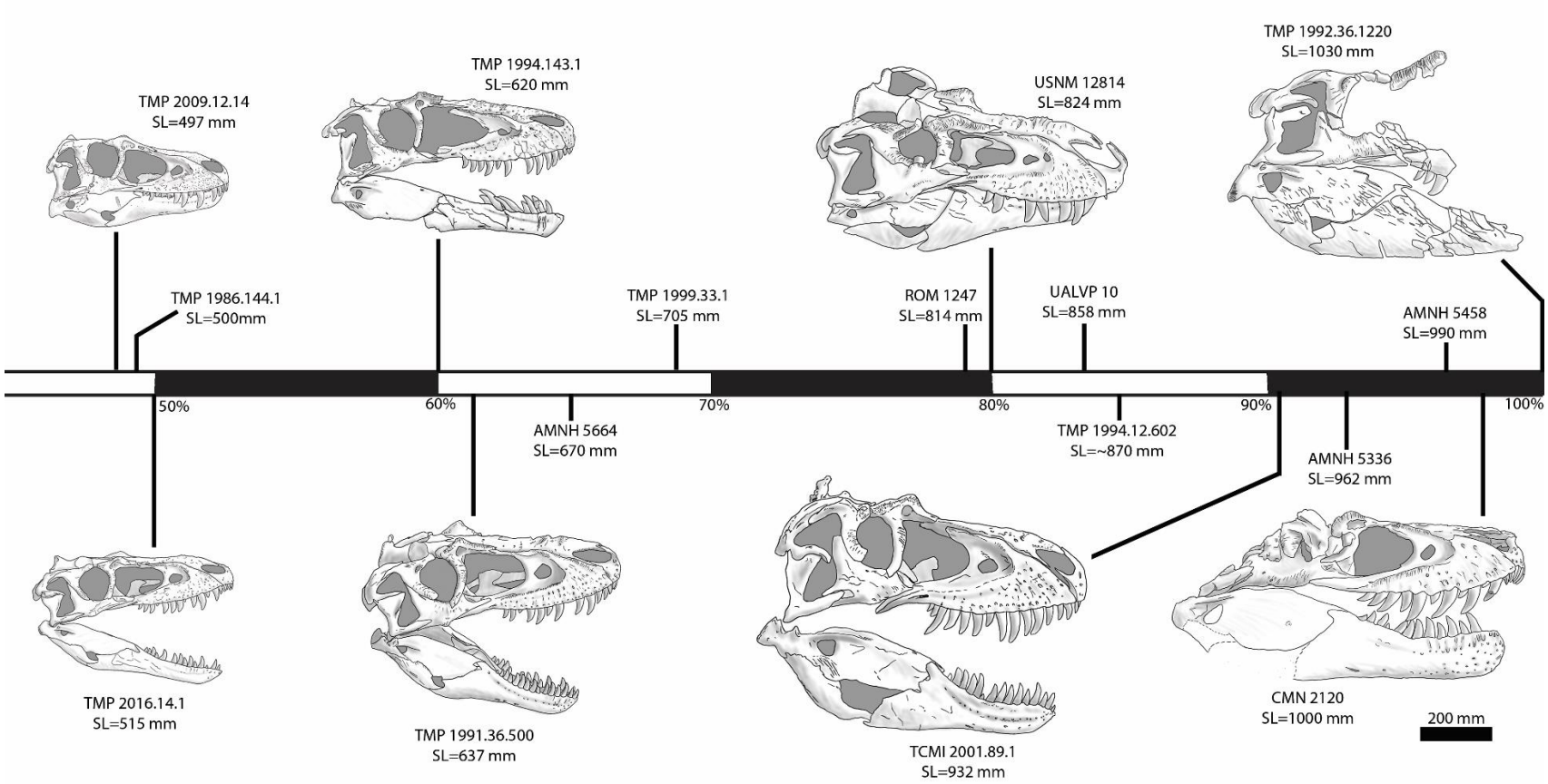

Figure 3.2. Growth series consisting of most complete *Gorgosaurus* skulls. Placement indicates percentage of the skull length of the largest known specimen TMP 1992.36.1220 (SL=1030 mm).

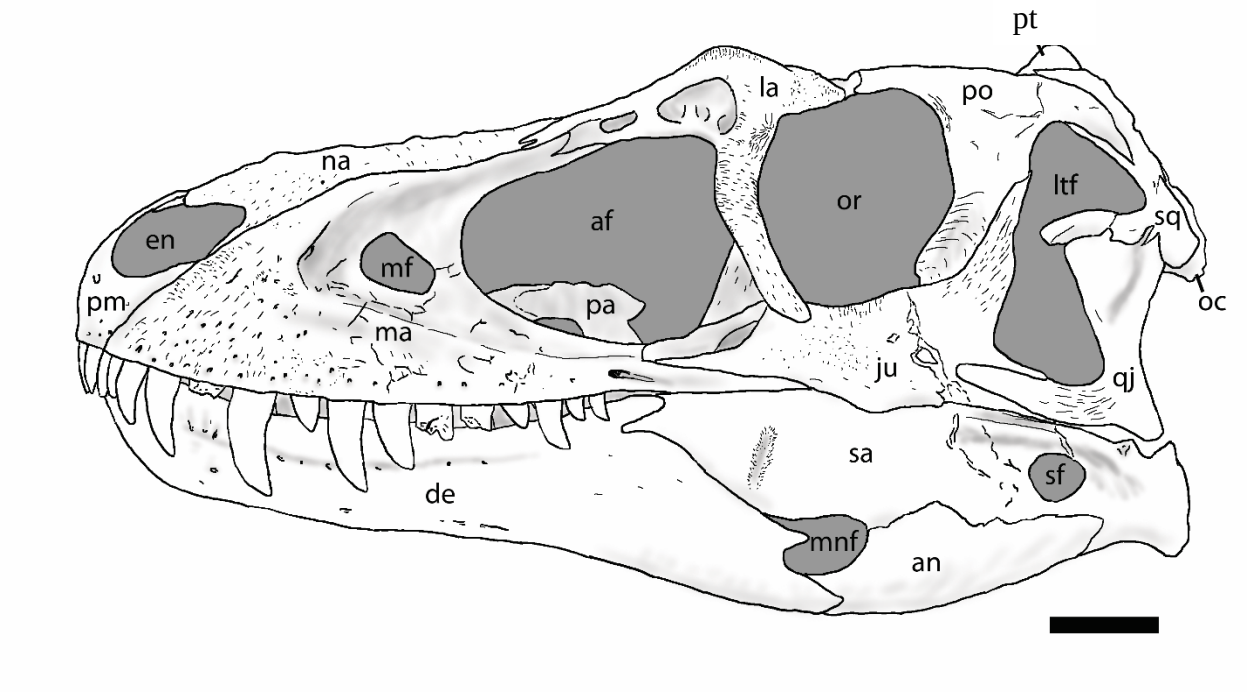

Figure 3.3. Line drawing of skull of TMP 2009.12.14. Abbreviations as follows: af, antorbital fenestra; an, angular; de, dentary; en, external nares; ju, jugal; la, lacrimal; ltf, laterotemporal fenestra; ma, maxilla; mf, maxillary fenestra; mnf, mandibular fenestra; na, nasal; or, orbit; pa, palatine; po, postorbital; pm, premaxilla; pt, parietal; oc, otoccipital; qj, quadratojugal; sa, surangular; sf, surangular foramen; sq, squamosal. Scale bar equals 50 mm.

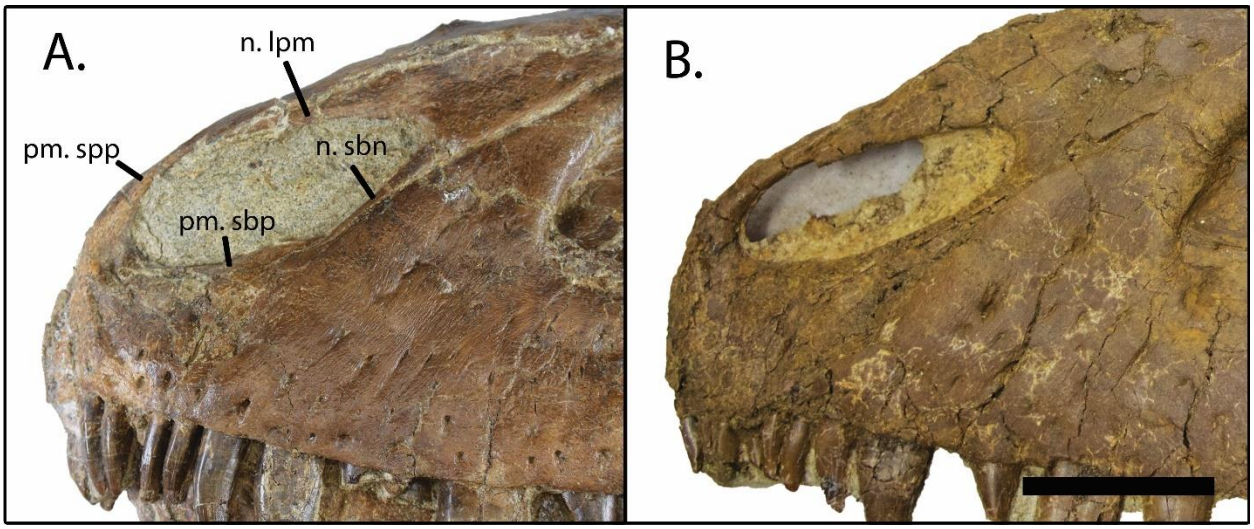

Figure 3.4. Rostral end of snout of juvenile *Gorgosaurus* individuals, (A) TMP 2009.12.14 and (B) TMP 2016.14.1, showing the difference in subcutaneous texture of the maxilla between individuals of similar size. Abbreviations are as follows: n. lpm, lateral premaxillary process of nasal; n. sbn, subnarial process of nasal; pm. sbp, subnarial process of premaxilla; pm. spp, supranarial process of premaxilla. Scale bar equals 50 mm for both.

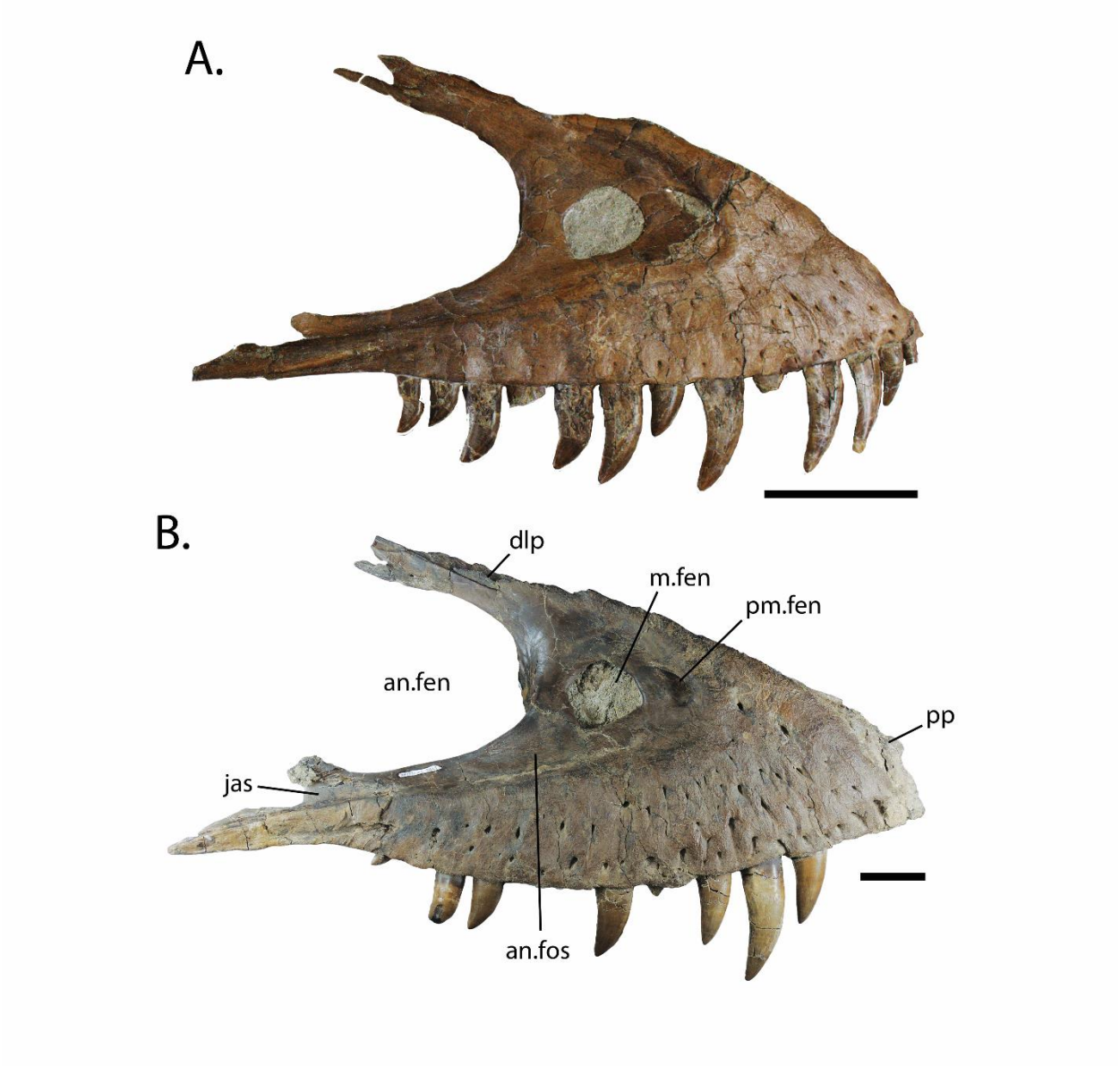

Figure 3.5. Comparison of *Gorgosaurus* maxillae in lateral view: (A) juvenile individual, TMP 2009.12.14) and (B) adult individual, TMP 1997.12.233. Abbreviations are as follows: an. fen., antorbital fenestra; an. fos, antorbital fossa; dlp, dorsolateral process; jas, jugal articular surface; m. fen, maxillary fenestra; pm. fen, promaxillary fenestra; pp, premaxillary process. Scale bar equals 50 mm.

Figure 3.6. Small juvenile *Gorgosaurus* maxilla (TMP 1993.36.539) in lateral view showing the swollen rostroventral corner of the antorbital fossa (saf) resulting in a smooth transition between this fossa and the subcutaneous surface. Scale bar equals 50 mm.

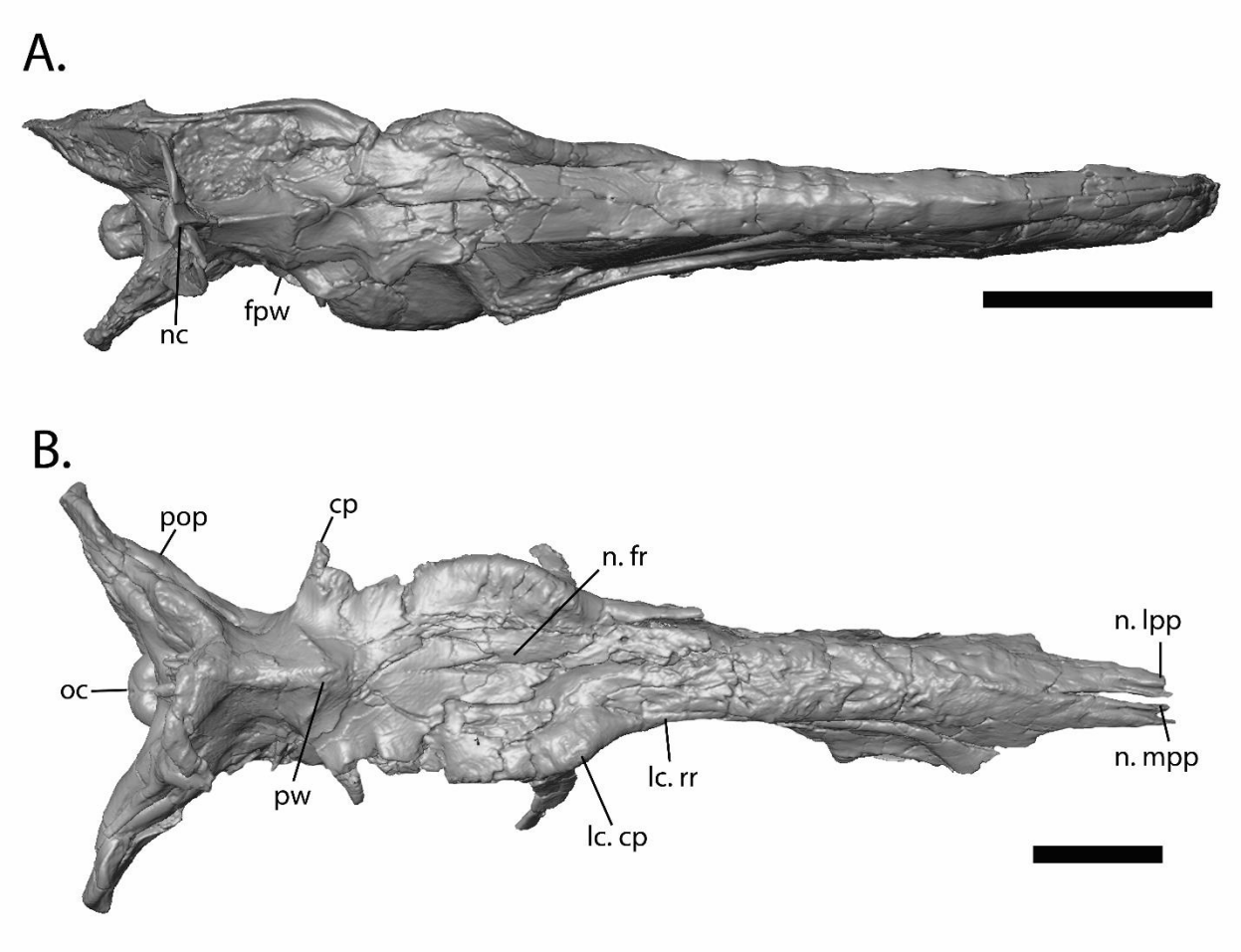

Figure 3.7. Comparison of *Gorgosaurus* skulls in dorsal view:(A) juvenile individual, TMP 2009.12.14 and (B) adult individual, TMP 1994.12.602. Abbreviations are as follows: lc. Cp, lacrimal cornual process; lc. rr, lacrimal rostral ramus; n. fr, frontal ramus of nasal; n. lpp, lateral premaxillary process of nasal; n. mpp, medial premaxillary process of nasal. Scale bar equals 100 mm.

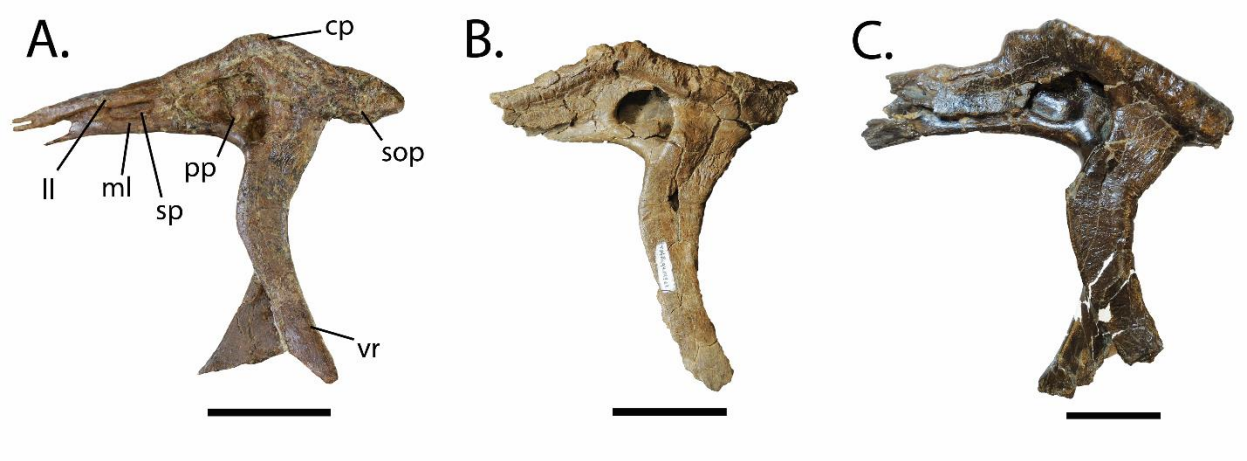

Figure 3.8. Comparison of lacrimals of *Gorgosaurus* specimens: (A) small juvenile individual, TMP 2009.12.14, (B) large juvenile individual, TMP 1994.143.1, and (C) subadult individual, ROM 1247. Abbreviations are as follows: cp, cornual process; ll, lateral lamina; ml, medial lamina; primary pneumatopore; sp, secondary pnuematopore; sop, supraorbital process; vr, ventral ramus. All scale bars equal 50 mm.

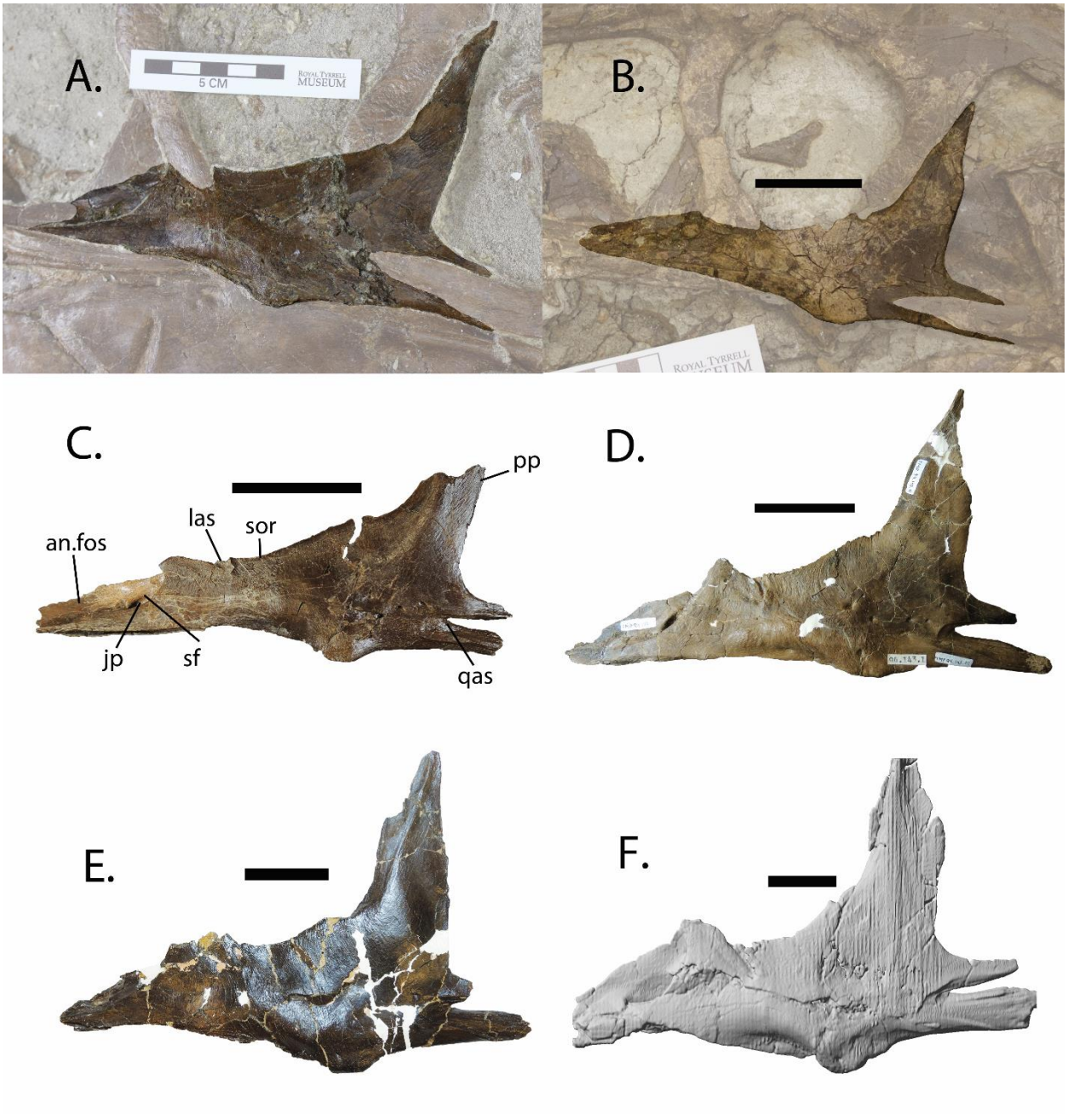

Figure 3.9. Comparison of six *Gorgosaurus* jugals of various growth stages: small juvenile individuals, (A) TMP 2009.12.14, (B) TMP 2016.14.1, (C) TMP 1986.144.1, (D) large juvenile individual, TMP 1994.143.1, (E) subadult individual, ROM 1247, (F) adult individual, TMP 2000.12.11. Abbreviations are as follows: anfos, antorbital fossa; jp, jugal pneumatopore; las,

lacrimal socket; pp, postorbital process; qas, quadratojugal articular surface; sf, secondary fossa; sor, suborbital region. All scale bars equal 50 mm.

Figure 3.10. Juvenile *Gorgosaurus* quadratojugals: (A) TMP 2009.12.14 and (B) TMP 2016.14.1. Scale bars equal 50 mm.

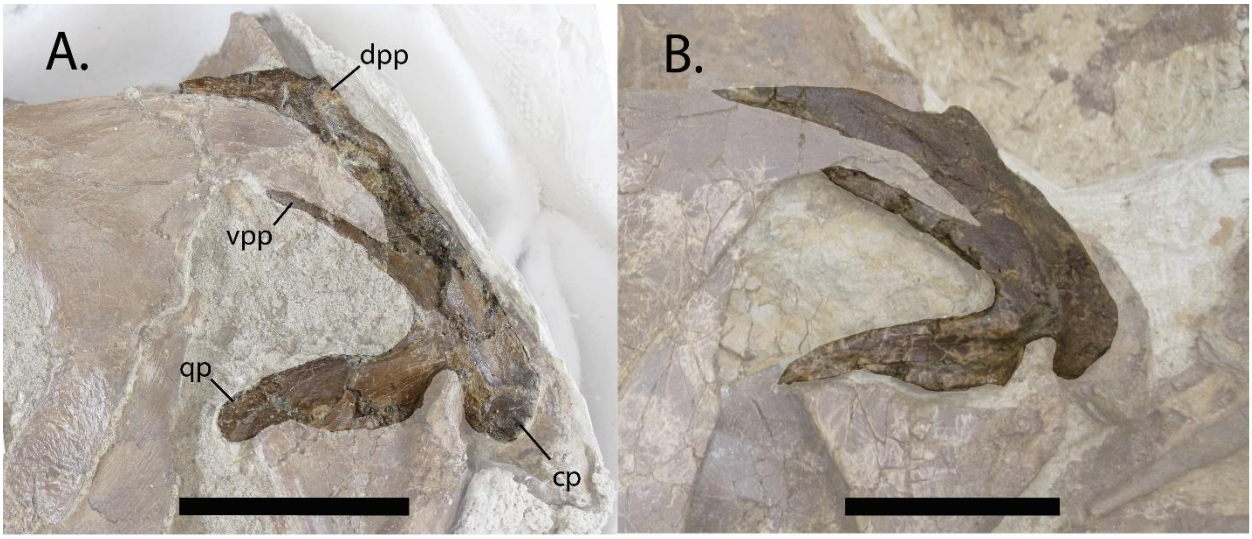

Figure 3.11. Juvenile *Gorgosaurus* squamosals in lateral view: (A) TMP 2009.12.14 and (B) TMP 2016.14.1. Abbreviations are as follows: cp, caudal process; dpp, dorsal postorbital process; qp, quadratojugal process; vpp, ventral postorbital process. Scale bars equal 50 mm.

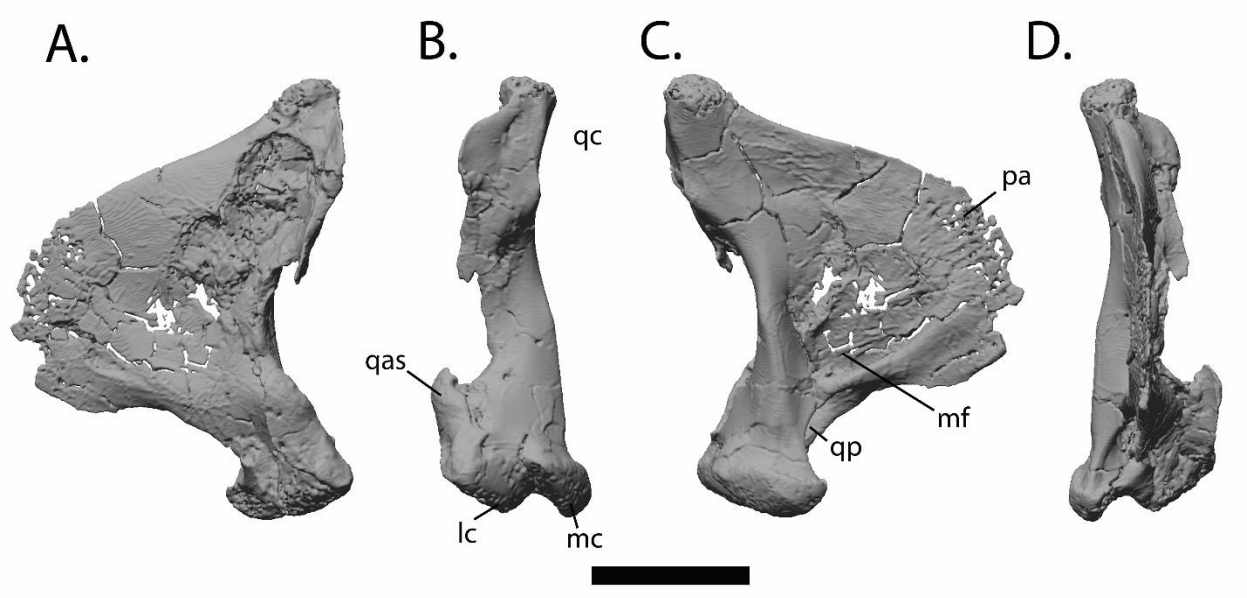

Figure 3.12. Large juvenile *Gorgosaurus* quadrate (TMP 1994.143.1) in (A) lateral, (B) caudal, (C) medial, and (D) rostral views. Abbreviations are as follows: lc, lateral condyle; mc, medial condyle; mf, medial fossa; pterygoid ala; qc, quadrate cotylus; qp, quadrate pneumatopore. Scale bar equals 50 mm.

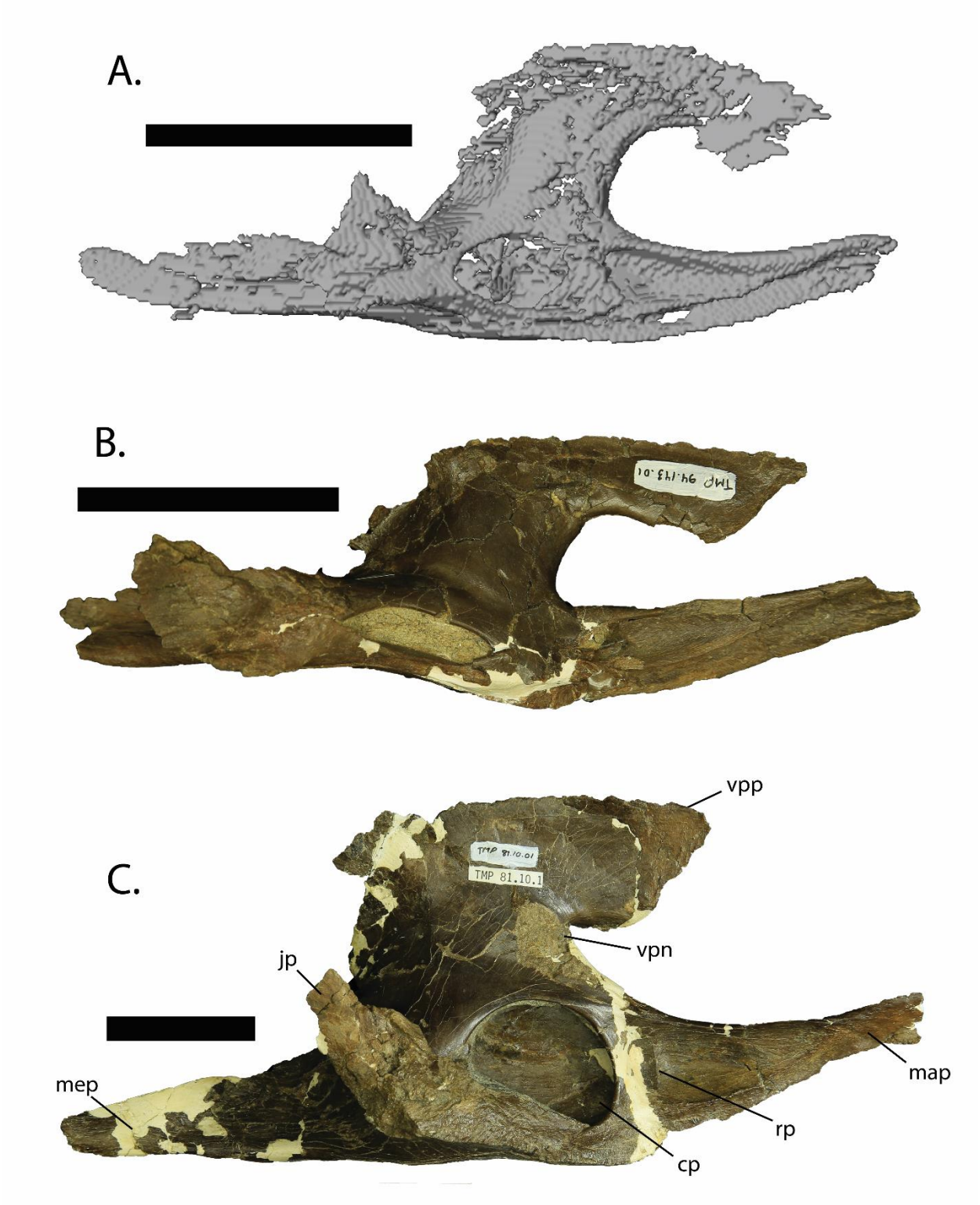

Figure 3.13. Albertosaurine palatines in lateral view:(A) small (TMP 2009.12.14) and (B) large (TMP 1994.143.1) juvenile *Gorgosaurus* individuals and (C) an adult *Albertosaurus*

sarcophagus individual, TMP 1981.10.1. Abbreviations are as follows: cp, caudal pneumatopore; jp, jugal process; map, maxillary process; mep, medial process; rp, rostral pneumatopore; vpn, vomeropterygoid process. Scale bars equal 50 mm.

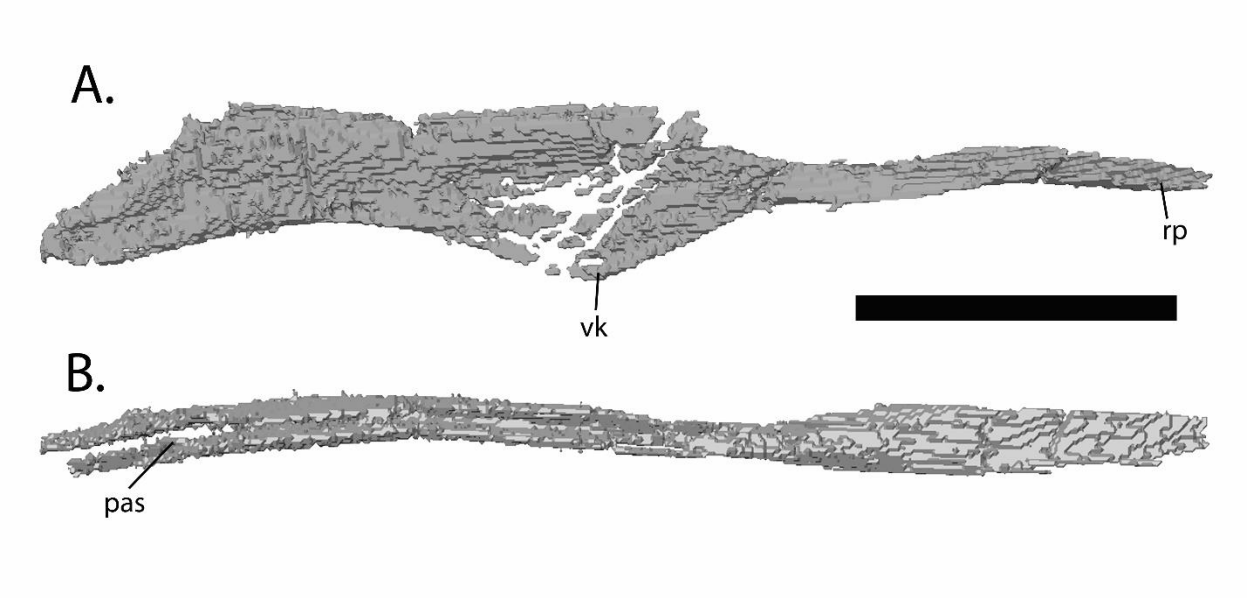

Figure 3.14. CT reconstruction of the vomer of juvenile *Gorgosaurus* individual TMP 2009.12.14 in (A) lateral and (B) dorsal view. Abbreviations are as follows: pas, pterygoid articular surface; rp, rostral process; vk, ventral keel. Scale bar equals 50 mm.

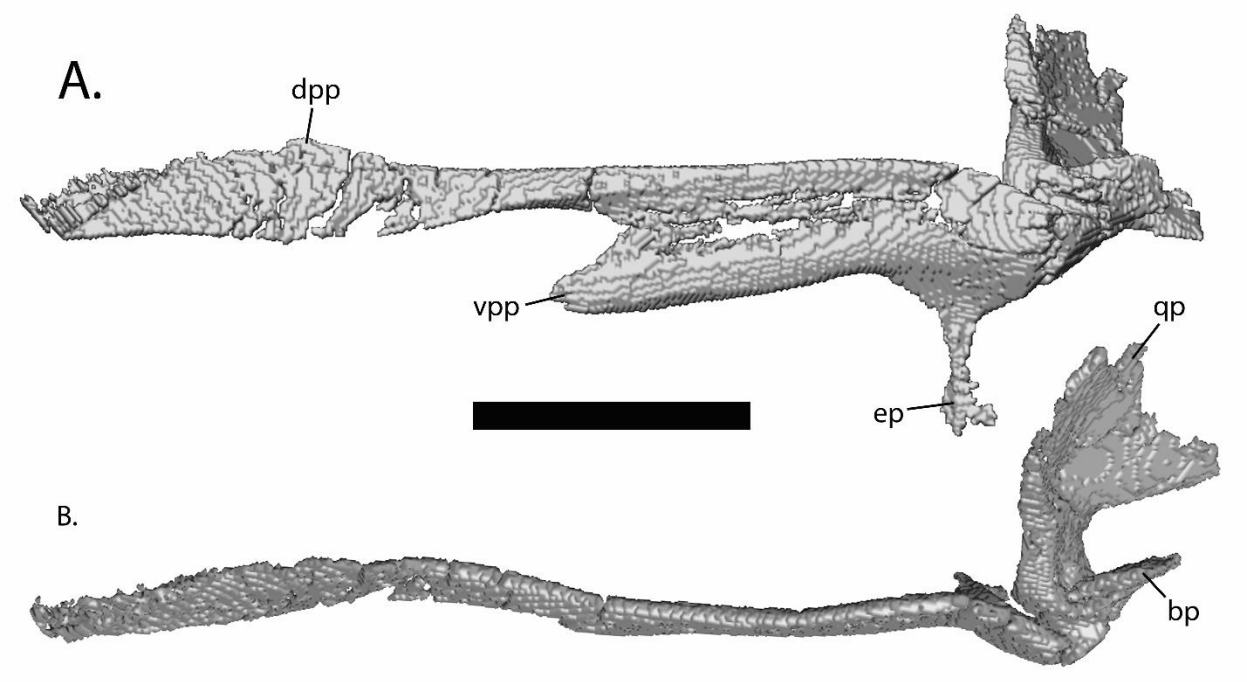

Figure 3.15. CT reconstructions of the right pterygoid of the juvenile *Gorgosaurus* individual TMP 2009.12.14 in (A) medial and (B) dorsal view. Abbreviations are as follows: bp, basipterygoid process; dpp, dorsal palatine process; ep, ectopterygoid process; qp, quadrate process; vpp, ventral palatine process. Scale bar equals 50 mm.

Figure 3.16. Comparison of *Gorgosaurus* mandibles in lateral view: (A) Juvenile individual TMP 2016.14.1 and (B) subadult individual ROM 1247. Abbreviations are as follows: adf, adductor fossa; an, angular; de, dentary; dg, dentary groove; sa, surangular; sf, surangular foramen; ss, surangular shelf. Scale bars equal 50 mm.

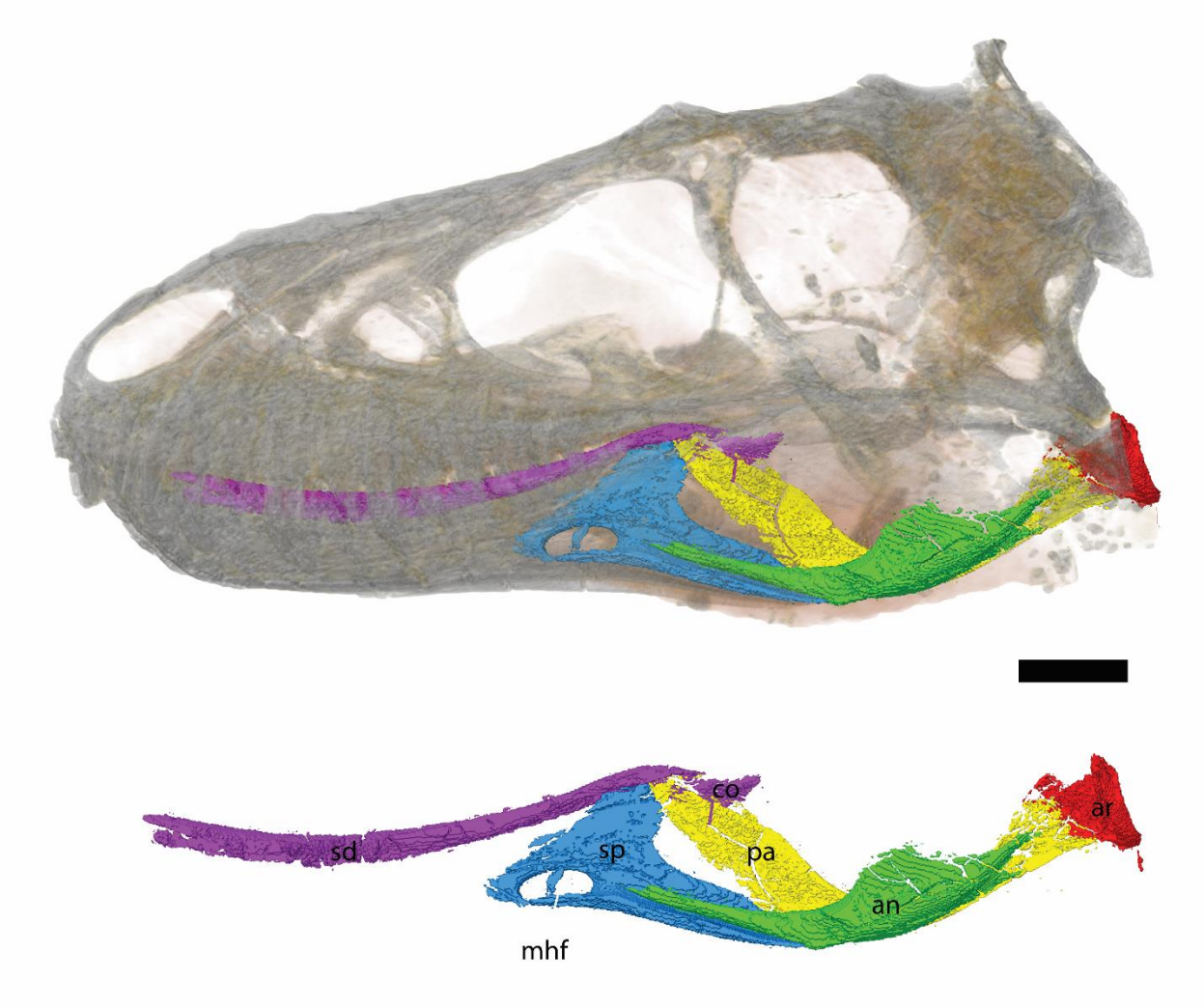

Figure 3.17. CT reconstructions of the medial mandibular bones of the juvenile *Gorgosaurus* individual TMP 2009.12.14. Abbreviations are as follows: an, angular; ar, articular; co, coronoid; mhf, mylohyoid foramen; pa, prearticular; sp, splenial. Scale bar equals 50 mm.

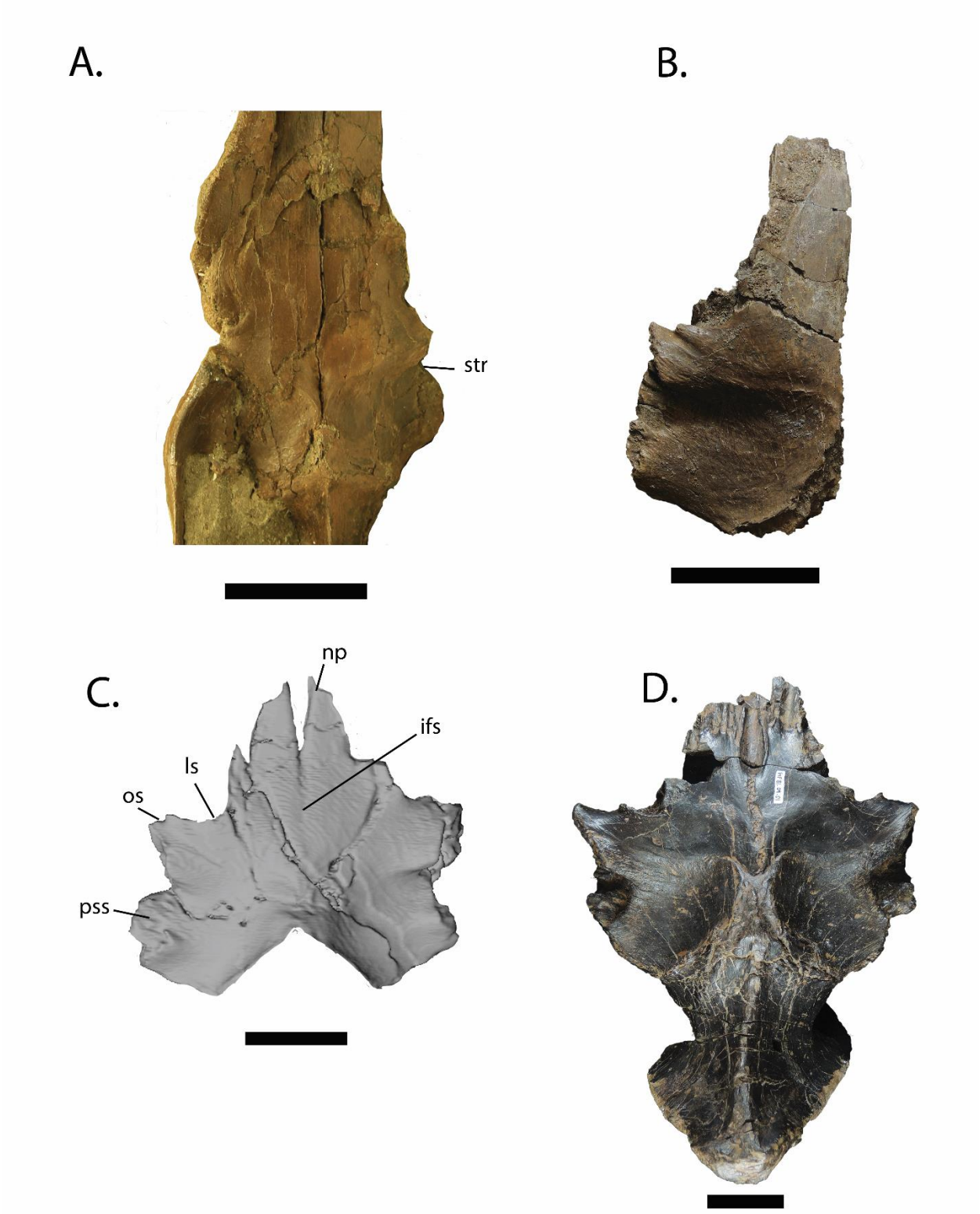
A.
str
B.
C.
np
ifs
ls
os
pss
D.

Figure 3.18. Albertosaurine frontals in dorsal view: (A) juvenile *Gorgosaurus* individuals, TMP 2009.12.14 and (B) TMP 1996.12.430, (C) adult *Gorgosaurus* individual, TMP 1994.12.602, and (D) large adult *Albertosaurus* individual, TMP 1981.9.1. Abbreviations are as follows: ifs, interfrontal suture; ls, lacrimal slot; np, nasal process; os, orbital slot; pas, postorbital articular surface; str, supratemporal ridge. Scale bars all equal 50 mm.

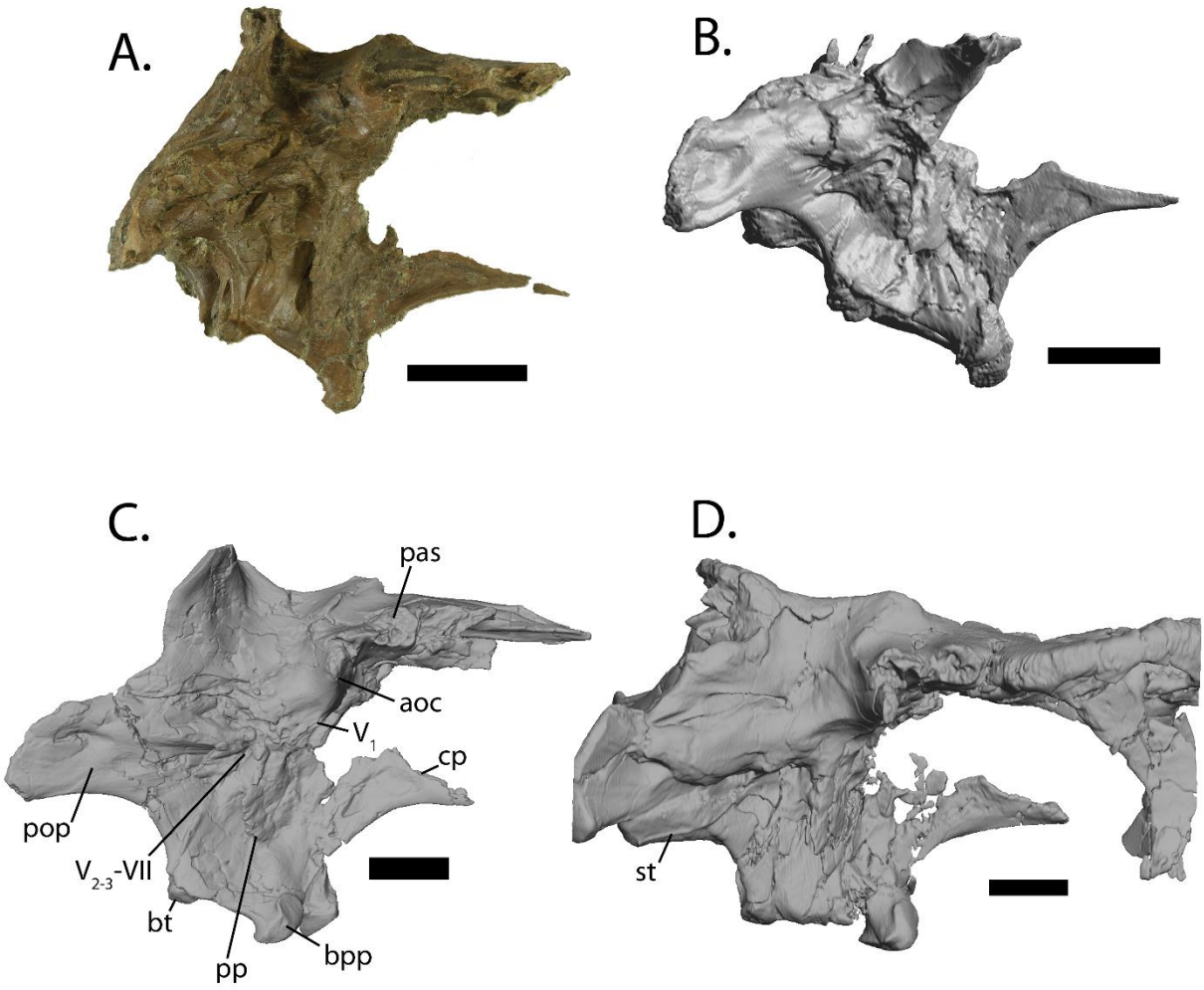

Figure 3.19. Comparison of *Gorgosaurus* braincases in lateral view: (A) juvenile individual, TMP 2009.12.14 and (B) juvenile individual, TMP 1994.143.1, (C) subadult individual, ROM 1247, and (D) adult individual, TMP 1994.12.602. Abbreviations are as follows: aoc, antotic crest; bpp, basipterygoid process; bt, basal tubera; cp, cultriform process; pas, postorbital articular surface; pop, paroccipital process; pp, preotic pendant; spop, swelling of paroccipital process (adult only); st, stapes; V_1, foramen for the ophthalmic nerve; V_{2-3}-VII, united fossa/foramen of the maxillomandibular and facial nerves. Scale bars all equal 50 mm.

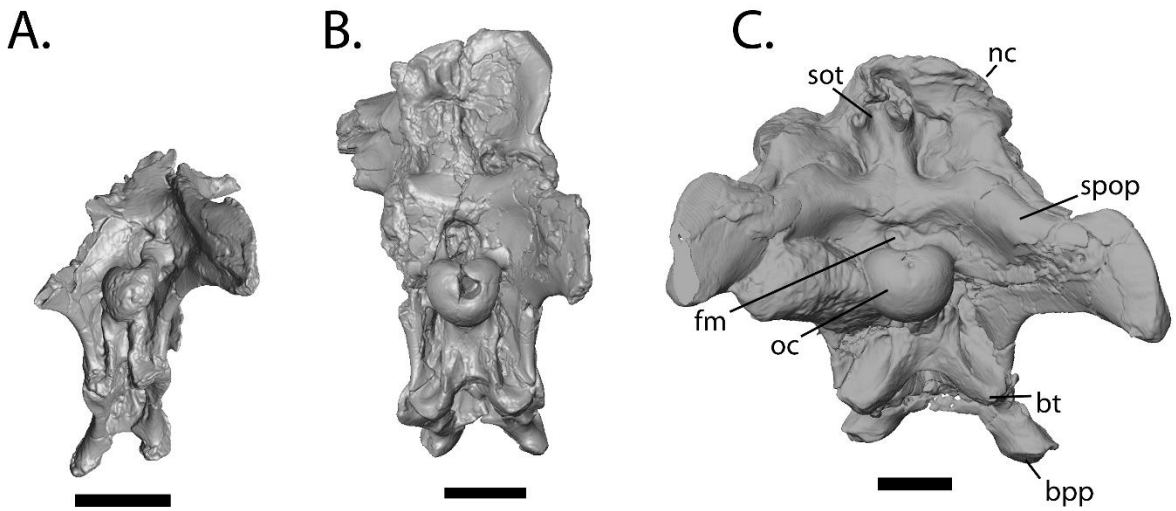

Figure 3.20. Comparison of *Gorgosaurus* braincases in caudal view: (A) juvenile individual, TMP 1994.143.1, (B) subadult individual, ROM 1247, and (C) adult individual, TMP 1994.12.602. Abbreviations are as follows: bpp, basipterygoid process; bt, basal tubera; fm, foramen magnum; nc, nuchal crest; oc, occipital condyle; sot, supraoccipital tabs; spop, swellings of paroccipital process (only in adult). Scale bars all equal 50 mm.

Table 3.1. Measurements of various cranial elements of TMP 2009.12.14. Centered measurements indicate either unpaired and fused midline bone (i.e. nasal and parietal). Blank spaces indicate bones that were unable to be measured either due to missing elements or accessibility.

	TMP 2009.12.14		TMP 2016.14.1	
	Left	Right	Left	Right
Skull, length from premaxilla to caudoventral corner of quadratojugal	497		515	
Premaxilla, body height	32	38		
Premaxilla, body length	32	36		
Nasal, rostrocaudal length	304		306	
Nasal, mediolateral width at caudal end of bony nares	35			
Nasal, mid-region minimum mediolateral width	29		33	
Nasal, frontal ramus mediolateral width at caudal end	36		~33	
Maxilla, maximum rostrocaudal length	320	>304	336	
Maxilla, dorsoventral height at rostral end of internal antorbital fenestra	113	116	109	
Maxilla, length of antorbital fossa rostral to the rostral end of internal antorbital fenestra	75	82	74	
Maxilla, length of bone rostral to rostral end of internal antorbital fenestra	151	167	162	
Maxilla, rostrocaudal length of tooth row	236	233	248	
Maxilla, length of maxillary fenestra	37	33	39	
Maxilla, depth of maxillary fenestra	25	25	24	
Lacrimal, length of dorsal bar	145		136	
Lacrimal, rostral ramus length	86		82	
Lacrimal, supraorbital process length	22		~26	
Lacrimal, maximum height (incl. cornual process)	116		129	
Lacrimal, cornual process height	12		13	
Postorbital, maximum length	117	111	121	
Postorbital, length of rostral ramus	36	37	42	
Postorbital, length of caudal ramus	37	35	46	
Postorbital, depth of ventral ramus	79	62	62	

Postorbital, maximum height	93	92	88	
Jugal, Maximum length	193		212	
Jugal, length of maxilla contact	86		83	
Jugal, maximum height of maxillary ramus	32		24	
Jugal, length of quadratojugal contact	64		78	
Jugal, height of quadratojugal ramus at rostroventral corner of laterotemporal fenestra	27		25	
Jugal, postorbital process dorsoventral height from rostroventral corner of laterotemporal fenestra	80		79	
Jugal, minimum suborbital height	33		23	
Quadratojugal, maximum length of ventral portion of bone	81		92	
Quadratojugal, length of dorsal process dorsal margin	45		57	
Quadratojugal, minimum length of dorsal process stem	16		19	
Quadratojugal, maximum depth	83		74	
Squamosal, maximum rostrodorsal length (oblique)	101		107	
Squamosal, rostrocaudal length of caudal process	18		18	
Squamosal, quadratojugal process length	44		65	
Squamosal, depth between dorsal and ventral postorbital processes	23		~18	
Quadrate, maximum length (rostrocaudal from cotylus to rostral edge of ala)	377			
Quadrate, mediolateral width between condyles	197			
Quadrate, dorsoventral height	500			
Dentary, maximum length	334	332	358	
Dentary, height through dentary chin	42	41	47	45
Dentary, length of tooth row	226	219	228	
Supradentary-coronoid, maximum length	285	289		
Supradentary-coronoid, maximum depth of alveolar margin	13	12		
Surangular, maximum length	232		264	
Surangular, maximum depth	58		66	
Surangular, depth at rostral margin of caudal surangular foramen	49		50	

Surangular, length of caudal surangular foramen	20		21	
Surangular, height of caudal surangular foramen	19		13	
Angular, rostrocaudal length	195			
Angular, depth at caudal end of dentary contact	18			
Splenial, maximum rostrocaudal length	158			
Splenial, maximum dorsoventral depth	64			
Frontal, rostrocaudal length of dorsal exposed portion	107	101	103	
Frontal, mediolateral width at rostral end of postorbital contact	37	43	44	
Frontal, dorsoventral depth at rostral end of postorbital contact	14	14	14	
Frontal, sagittal crest length	17	17	18	
Parietal, rostrocaudal length between rostral end of parietal wedge and caudal margin of nuchal crest on midline		64		~70
Parietal, mediolateral width of nuchal crest		71		
Parietal, mediolateral width at edge of frontal contact		~66		

Table 3.2. List of specimens that were CT scanned for this study.

Taxon	Specimen	Element	Voxel size
Gorgosaurus libratus	ROM 1247	braincase	0.49X0.49X0.63
	TMP 1991.36.500	cranium	0.59X0.59X0.32
	TMP 1991.153.1	braincase	
	TMP 1994.12.602	Nasal, lacrimals, braincase	0.98X0.98X1.25
	TMP 1994.12.602	braincase only	0.76X0.76X0.63
	TMP 1994.143.1	various skull elements	0.3X0.3X1.0
	TMP 1999.33.1	skull	0.93X0.93X0.63
	TMP 1997.12.223	maxilla	0.49X0.49X1.0
	TMP 2000.12.11	jugal	0.49X0.49X1.0
	TMP 2009.12.14	skull	0.60X0.60X0.50
	TMP 2015.12.70	ectopterygoid	0.49X0.49X1.0
	UALVP 10	cranium	0.98X0.98X0.3
Daspletosaurus	TMP 1996.12.151	lacrimal	0.49X0.49X1.0
	TMP 2001.36.1	Braincase roof	0.63X0.63X1.25
	TMP 2001.36.1	Maxilla, jugal	0.69X0.69X0.6

CHAPTER 4: CONCLUSIONS

In the context of recently discovered juvenile specimens of the tyrannosaurids *Gorgosaurus libratus* and *Daspletosaurus torosus*, the ontogeny of these taxa is revisited. A juvenile tyrannosaurid previously identified as *Daspletosaurus* sp., TMP 1994.143.1 (Currie, 2003a), is re-identified as *Gorgosaurus libratus*, based on the presence of several features shared with *Gorgosaurus libratus* and Albertosaurinae and the absence of features diagnostic of *Daspletosaurus* and Tyrannosaurinae. The taxonomic reassignment of TMP 1994.143.1, a specimen that has been used in several phylogenetic analyses, improves our understanding of albertosaurine ontogeny but may require a re-evaluation of phylogenetic character codings for *Daspletosaurus*. These findings reveal that many tyrannosaurid synapomorphies and autapomorphies are present in ontogenetically young individuals, but that some diagnostic characters (e.g., dorsal orientation of palatine vomeropterygoid neck, emargination at rostral end of DASS on postorbital) are gradually acquired, often asynchronously within and between individuals, through ontogeny. Furthermore, several previously unrecognized features of the postorbital that are useful in differentiating *Daspletosaurus* and *Gorgosaurus* have been discovered.

The cranial ontogeny of *Gorgosaurus libratus* is revised through the study of two of the smallest complete tyrannosaurid skulls (~500 mm skull length) known from North America. In general, *Gorgosaurus* and other tyrannosaurids exhibit similar ontogenetic trends, such as a dorsoventral deepening and mediolateral widening of the skull, development and expansion of cranial ornamentation, paranasal sinus inflation, transition from ziphodont to pachydont teeth, and inflation of the paroccipital processes by the tympanic recess. However, *Gorgosaurus*

undergoes at least one unique ontogenetic change among tyrannosaurids, namely the development of a caudally curling postorbital cornual process. *Gorgosaurus* also shares other ontogenetic changes with the closely related *Albertosaurus*, including the acquisition of a notch in the dorsal margin of the postorbital at the rostral end of the dorsal articular surface for the squamosal, transition from a rostrocaudally-oriented to a dorsally-oriented vomeropterygoid neck of the palatine, and transition from a horizontally-orientated to a rostrodorsally-oriented ventral quadratojugal-jugal contact. *Gorgosaurus* exhibits a mixture of unique (autapomorphic), subfamilial (i.e. albertosaurine), and familial (i.e. tyrannosaurid) trends in cranial ontogeny. The occurrence of exclusive ontogenetic patterns in *Gorgosaurus* suggests that other tyrannosaurid taxa may also undergo exclusive changes in cranial anatomy through ontogeny.

REFERENCES

Averianov, A. and H. D. Sues. 2012. Skeletal remains of Tyrannosauroidea (Dinosauria: Theropoda) from the Bissekty Formation (Upper Cretaceous: Turonian) of Uzbekistan. Cretaceous Research 34:284–297.

Bever, G. S., S. L. Brusatte, T. D. Carr, X. Xu, A. M. Balanoff, and M. a Norell. 2013. The braincase anatomy of the Late Cretaceous dinosaur *Alioramus* (Theropoda: Tyrannosauroidea). Bulletin of the American Museum of Natural History 376:1–72.

Bradley, G. J. 2015. Assessing social behaviour, ontogenetic change and taxonomic status in a juvenile *Gorgosaurus libratus* (Dinosauria; Theropoda; Tyrannosauridae): A multidisciplinary analysis M. Sc. Thesis, University of Alberta, Edmonton, Alberta, 208 pp.

Bradley, G. J., M. E. Burns, and P. J. Currie. 2015. Missing data estimation in tyrannosaurid dinosaurs: Can diameter take the place of circumference? Cretaceous Research 55:200-209.

Brochu, C. A. 2003. Osteology of *Tyrannosaurus rex*: Insights from a nearly complete skeleton and high-resolution computed tomographic analysis of the skull. Journal of Vertebrate Paleontology 22:1–138.

Brusatte, S. L., and T. D. Carr. 2016. The phylogeny and evolutionary history of tyrannosauroid dinosaurs. Scientific Reports 6:1–8.

Brusatte, S. L., T. D. Carr, and M. a. Norell. 2012. The osteology of *Alioramus*, a gracile and Long-Snouted Tyrannosaurid (Dinosauria: Theropoda) from the Late Cretaceous of Mongolia. Bulletin of the American Museum of Natural History 366:1–197.

Brusatte, S. L., T. D. Carr, G. M. Erickson, G. S. Bever, and M. A. Norell. 2009. A long-snouted, multihorned tyrannosaurid from the Late Cretaceous of Mongolia. Proceedings of the National Academy of Sciences pnas-0906911106.

Brusatte, S. L., T. D. Carr, T. E. Williamson, T. R. J. Holtz, D. W. E. Hone, and S. A. Williams. 2016. Dentary groove morphology does not distinguish "*Nanotyrannus*" as a valid taxon of tyrannosauroid dinosaur. Comment on: "Distribution of the dentary groove of theropod dinosaurs: Implications for theropod phylogeny and the validity of the genus *Nanotyrannus*. Cretaceous Research 65:232–237.

Brusatte, S.L., M. A. Norell, T. D. Carr, G. M. Erickson, J. R. Hutchinson, A. M. Balanoff, G. S. Bever, J. N. Choiniere, P. J. Makovicky, and X. Xing. 2010. Tyrannosaur paleobiology: new research on ancient exemplar organisms. Science 329:1481–1485.

Carpenter, K. 1992. Tyrannosaurids (Dinosauria) of Asia and North America; pp. 250–268 in N. J. Mateer and P. J. Chen (eds.), Aspects of Nonmarine Cretaceous Geology. China Ocean Press, Beijing.

Carr, T. D. 1999. Craniofacial ontogeny in Tyrannosauridae (Dinosauria, Coelurosauria). Journal of Vertebrate Paleontology 19:497–520.

Carr, T. D. 2010. A taxonomic assessment of the type series of *Albertosaurus sarcophagus* and the identity of Tyrannosauridae (Dinosauria, Coelurosauria) in the Albertosaurus bonebed from the Horseshoe Canyon Formation (Campanian–Maastrichtian, Late Cretaceous). Canadian Journal of Earth Sciences 47:1213–1226.

Carr, T. D., and T. E. Williamson. 2004. Diversity of Late Maastrichtian Tyrannosauridae (Dinosauridae: Theropoda) from western North America. Zoological Journal of the Linnean Society 142:479–523.

Carr, T. D., and T. E. Williamson. 2010. *Bistahieversor sealeyi*, gen. et sp. nov., a new tyrannosauroid from New Mexico and the origin of deep snouts in Tyrannosauroidea. Journal of Vertebrate Paleontology 30:1–16.

Carr, T. D., T. E. Williamson, and D. Schwimmer. 2005. A new genus and species of tyrannosauroid from the Late Cretaceous (Middle Campanian) Demopolis Formation of Alabama. Journal of Vertebrate Paleontology 25:119–143.

Carr, T. D., D. J. Varricchio, J. C. Sedlmayr, E. M. Roberts, and J. R. Moore. 2017. A new tyrannosaur with evidence for anagenesis and crocodile-like facial sensory system. Scientific Reports 7:1–11.

Currie, P. J. 1997. Braincase anatomy; pp. 81–85 in P. J. Currie and K. Padian (eds.), Encyclopedia of Dinosaurs. New York Academic Press, New York City, New York.

Currie, P. J. 2003a. Allometric growth in tyrannosaurids (Dinosauria: Theropoda) from the Upper Cretaceous of North America and Asia. Canadian Journal of Earth Sciences 40:651–665.

Currie, P. J. 2003b. Cranial anatomy of tyrannosaurid dinosaurs from the Late Cretaceous of Alberta, Canada. Acta Palaeontologica Polonica 48:191–226.

Currie, P. J., and D. Zhiming. 2001. New information on *Shanshanosaurus huoyanshanensis*, a juvenile tyrannosaurid (Theropoda, Dinosauria) from the Late Cretaceous of China. Canadian Journal of Earth Sciences 38:1729–1737.

Currie, P. J., J. H. Hurum, and K. Sabath. 2003. Skull structure and evolution in tyrannosaurid dinosaurs. Acta Palaeontologica Polonica 48:227–234.

Erickson, G. M., P. J. Makovicky, P. J. Currie, M. A. Norell, S. A. Yerby, and C. A. Brochu. 2004. Gigantism and comparative life-history parameters of tyrannosaurid dinosaurs. Nature 430:772–775.

Gold, M. E. L., S. L. Brusatte, and M. A. Norell. 2013. The Cranial pneumatic sinuses of the tyrannosaurid *Alioramus* (Dinosauria: Theropoda) and the evolution of cranial pneumaticity in theropod dinosaurs. American Museum Novitates 3790:1–46.

Fiorillo, A. R., and R. S. Tykoski. 2014. A diminutive new tyrannosaur from the top of the world. PLoS ONE 9:e91287. doi:10.1371/journal.pone.0091287. PMID: 24621577.

Holliday, C. M., and L. M. Witmer. 2008. Cranial kinesis in dinosaurs: intracranial joints, protractor muscles, and their significance for cranial evolution and function in diapsids. Journal of Vertebrate Paleontology 28:1073–1088.

Holtz Jr., T. R., 2001. The phylogeny and taxonomy of the Tyrannosauridae; pp. 64–83 in D. H. Tanke and K. Carpenter (eds.), Mesozoic vertebrate life. Indiana University Press, Bloomington, Indiana.

Hone, D. W. E., K. Wang, C. Sullivan, X. J. Zhao, S. Chen, D. Li, S. Ji, Q. Ji, X. Xu. 2011. A new, large tyrannosaurine theropod from the Upper Cretaceous of China. Cretaceous Research 32:495–503

Hone, D. W. E. and D. H. Tanke. 2015. Pre-and postmortem tyrannosaurid bite marks on the remains of *Daspletosaurus* (Tyrannosaurinae: Theropoda) from Dinosaur Provincial Park, Alberta, Canada. PeerJ 3:p.e885.

Hurum, J. H., and K. Sabath. 2003. Giant theropod dinosaurs from Asia and North America : Skulls of *Tarbosaurus bataar* and *Tyrannosaurus rex* compared. Acta Palaeontologica Polonica 48:161–190.

Kurzanov, S. M. 1976. A new Late Cretaceous carnosaur from Nogon-Tsav, Mongolia. Joint Soviet-Mongolian Paleontological Expedition Transactions 3:93–104, [in Russian, English summary].

Lambe, L. M. 1914. On a new genus and species of carnivorous dinosaur from the Belly River Formation of Alberta, with a descrip- tion of the skull of *Stephanosaurus marginatus* from the same horizon. The Ottawa Naturalist 28:158-164.

Larson, P. L. 2013. The case for *Nanotyrannus*; pp. 14–53, in J. M. Parrish, R. E. Molnar, P. J. Currie, and E. B. (Eva B. Koppelhus (eds.), Tyrannosaurid paleobiology. Indiana University Press.

Li, D., M. A. Norell, K.-Q. Gao, N. D. Smith, and P. J. Makovicky. 2010. A longirostrine tyrannosauroid from the Early Cretaceous of China. Proceedings of the Royal Society B: Biological Sciences 277:183–190.

Loewen, M. A., R. B. Irmis, J. J. W. Sertich, P. J. Currie, and S. D. Sampson. 2013. Tyrant dinosaur evolution tracks the rise and fall of Late Cretaceous oceans. PLoS ONE 8.

Lü, J., L. Yi, S. L. Brusatte, L. Yang, H. Li, and L. Chen. 2014. A new clade of Asian Late Cretaceous long-snouted tyrannosaurids. Nature Communications 5.

Miyashita, T., D. H. Tanke, and P. J. Currie. 2010. Variation in premaxillary tooth count and a developmental abnormality in a tyrannosaurid dinosaur. Acta Palaeontologica Polonica 55:635–643.

Osborn, H.F. 1905. Tyrannosaurus and other Cretaceous carnivorous dinosaurs. Bulletin of the American Museum of Natural History 21:259–265.

Rauhut, O. W. M., A. C. Milner, and S. Moore-Fay. 2010. Cranial osteology and phylogenetic position of the theropod dinosaur *Proceratosaurus bradleyi* (Woodward, 1910) from the Middle Jurassic of England. Zoological Journal of the Linnean Society 158:155–195.

Rayfield, E. J. 2004. Cranial mechanics and feeding in Tyrannosaurus rex. Proceedings of the Royal Society of London B 271: 1451–1459.

Rayfield, E. J. 2005. Aspects of comparative cranial mechanics in the theropod dinosaurs Coelophysis, Allosaurus and Tyrannosaurus. Zoological Journal of the Linnean Society 144:309–316.

Rothschild, B. M., and V. Naples. 2017. Apparent sixth sense in theropod evolution: The making of a Cretaceous weathervane. PLoS ONE 12:1–11.

Rozhdestvensky, A. K. 1965. Growth changes in Asian dinosaurs and some problems of their taxonomy. Paleontologičeskij žurnal 3:95–109.

Sereno, P. C. 2005. Stem Archosauria TaxonSearch http://www.taxonsearch.org/dev/file_home.php [version 1.0, 7 November 2005, linked to Sereno et al. 2005 reference below]

Sereno, P. C., S. McAllister, and S. L. Brusatte. 2005. TaxonSearch: a relational database for suprageneric taxa and phylogenetic definitions. Phyloinformatics 8:1–21.

Sereno, P.C., L. Tan, S.L. Brusatte, H.J. Kriegstein, X. Zhao, and K. Cloward. 2009. Tyrannosaurid skeletal design first evolved at small body size. Science 326:418-422.

Snively, E., Henderson, D. M. and Phillips, D. S. 2006. Fused and vaulted nasals of tyrannosaurid dinosaurs: implications for cranial strength and feeding mechanics. Acta Palaeontologica Polonica, 51: 435–454.

Snively, E., and A. P. Russell. 2007. Functional variation of neck muscles and their relation to feeding style in Tyrannosauridae and other large theropod dinosaurs. Anatomical Record 290:934–957.

Tsuihiji, T. 2010. Reconstructions of the axial muscle insertions in the occipital region of dinosaurs: Evaluations of past hypotheses on Marginocephalia and Tyrannosauridae using the extant phylogenetic bracket approach. Anatomical Record 293:1360–1386.

Tsuihiji, T., M. Watabe, K. Tsogtbaatar, T. Tsubamoto, R. Barsbold, S. Suzuki, A. H. Lee, R. C. Ridgely, Y. Kawahara, and L. M. Witmer. 2011. Cranial osteology of a juvenile specimen of *Tarbosaurus bataar (*Theropoda, Tyrannosauridae) from the Nemegt Formation (Upper Cretaceous) of Bugin Tsav, Mongolia. Journal of Vertebrate Paleontology 31:497–517.

Witmer, L. M. 1997. The evolution of the antorbital cavity of archosaurs: a study in soft-tissue reconstruction in the fossil record with an analysis of the function of pneumaticity. Society of Vertebrate Paleontology Memoir 3:1–73.

Witmer, L. M., and R. C. Ridgely. 2009. New insights into the brain, braincase, and ear region of tyrannosaurs (Dinosauria, Theropoda), with implications for sensory organization and behavior. Anatomical Record 292:1266–1296.

Witmer, L. M., and R. C. Ridgely. 2010. The Cleveland tyrannosaur skull (*Nanotyrannus* or *Tyrannosaurus*) - New findings based on CT scanning, with special reference to the braincase. Kirtlandia 57:61–81.

Xu, X., M. A. Norell, X. Kuang, X. Wang, Q. Zhao, and C. Jia. 2004. Basal tyrannosauroids from China and evidence for protofeathers in tyrannosauroids. Nature 431:680–684.

Xu, X., K. Wang, K. Zhang, Q. Ma, L. Xing, C. Sullivan, D. Hu, S. Cheng, and S. Wang. 2012. A gigantic feathered dinosaur from the Lower Cretaceous of China. Nature 484:92–95.

Zanno, L. E., J. P. Wiersma, M. A. Loewen, S. D. Sampson, and M. A. Getty. 2010. A preliminary report on the theropod dinosaur fauna of the Late Campanian Kaiparowits Formation, Grand-Staircase Escalante National Monument, Utah; pp. 173–186 in M. Eaton (ed.), Learning from the Land, Grand Staircase-Escalante National Monument Science Symposium Proceedings. Grand Staircase–Escalante Partners, Kanab, Utah.